Université d'Ottawa • University of Ottawa

Université d'Ottawa · University of Ottawa

FACULTÉ DES ÉTUDES SUPÉRIEURES ET POSTDOCTORALES

FACULTY OF GRADUATE AND POSTDOCTORAL STUDIES

Titus Y. TAO

AUTEUR DE LA THÈSE - AUTHOR OF THESIS

M. Sc. (Biology)

GRADE - DEGREE

Department of Biology

FACULTÉ, ÉCOLE, DÉPARTEMENT - FACULTY, SCHOOL, DEPARTMENT

TITRE DE LA THÈSE - TITLE OF THE THESIS

Functional Characterization of ZmGRP5, a Glycine-Rich Protein Specifically Expressed in the Cell Wall of Maize Silk

D.A. Johnson

DIRECTEUR DE LA THÈSE - THESIS SUPERVISOR

T. Ouellet

CO-DIRECTEUR DE LA THÈSE - THESIS CO-SUPERVISOR

EXAMINATEURS DE LA THÈSE - THESIS EXAMINERS

T.W. Moon

M. Paulin-Levasseur

J. Vierula

J.-M. De Koninck, Ph.D.

LE DOYEN DE LA FACULTÉ DES ÉTUDES SUPÉRIEURES ET POSTDOCTORALES

DEAN OF THE FACULTY OF GRADUATE AND POSTDOCTORAL STUDIES

Functional Characterization of ZmGRP5, a Glycine-Rich Protein Specifically Expressed in the Cell Wall of Maize Silk Tissue

Titus Tao

Thesis submitted to the Department of Biology in partial fulfullment
of the requirements for the degree of Master of Science.

University of Ottawa
Ottawa, Ontario, Canada
May, 2004

Your file Votre référence
ISBN: 0-494-01615-9
Our file Notre référence
ISBN: 0-494-01615-9

To my parents,
for encouraging me to dream.

To Evan Frank,
for helping me stay grounded in reality.

Abstract

Silk tissue is a specialized reproductive tissue of the maize plant, equivalent to the stigma and style portion of the female inflorescence. The moist and nutrient rich properties of maize silk tissue that facilitate pollen reception and the support of pollen tube growth also make maize silk a preferred site of infection by fungal pathogens such as *Fusarium graminearum*. The cDNA clone *zmgrp5* was isolated in a previous study to identify silk tissue-specific genes. ZmGRP5, the encoded protein, was predicted to be a cell wall glycine-rich protein (GRP) and was experimentally characterized in this study. Using polyclonal antiserum, immunoblot analysis confirmed the silk tissue specificity of the protein. Additionally, subcellular fractionation studies confirmed ZmGRP5 localization in the cell wall fraction, and not in any other subcellular fractions. Interaction of ZmGRP5 with the cell wall matrix was observed to be disrupted by the addition of the reducing agent ß-ME. The reversible nature of disulfide bond formation and disruption under different redox conditions suggest that ZmGRP5 could potentially be important in the regulation of cell wall structural properties such as elasticity and rigidity in accordance with environmental and developmental changes. The variable immobilization of ZmGRP5 to the cell wall matrix could also serve as a potential mechanism of activation or inactivation of any non-structural functions. The identification of potential post-translational modifications such as phosphorylation and glycosylation, which are rarely observed in other cell wall GRPs, suggest that the functional significance of these modifications in ZmGRP5 is worthy of further study.

Résumé

Chez le maïs, les soies constituent un tissu spécialisé dans la fonction reproductive. Correspondant au stigmate et au style de l'inflorescence, elles assurent la réception du pollen et la croissance du tube pollinique. Ce tissu bien hydraté et riche en nutriments est un site d'infection de choix pour le champignon pathogène *Fusarium graminearum*. Au cours d'une étude antérieure visant à identifier les gènes spécifiquement exprimés dans les soies, le clone d'ADNc *zmgrp5* (*zea maize glycine rich protein 5*) a été isolé. Le travail présenté ici a pour but de caractériser la protéine ZmGRP5 dont la structure prédite est celle d'une protéine riche en glycine de la paroi cellulaire végétale. Une technique de sous-fractionnement cellulaire combinée à l'immunodétection Western ont permis de confirmer la présence de la protéine ZmGRP5 dans la fraction pariétale, et son absence dans les autres fractions. Des interactions entre la protéine ZmGRP5 et la matrice pariétale ont été mises en évidence par la réduction des ponts disulfures à l'ajout d'un agent réducteur, le β-ME. La nature réversible de ces liens disulfures, en présence de conditions variables d'oxidoréduction, suggère que ZmGRP5 pourrait intervenir dans la régulation des processus régissant l'élasticité et la rigidité tissulaire en fonction des paramètres environnementaux et des différents stades de développement. L'immobilisation variable de ZmGRP5 à la matrice pariétale pourrait aussi servir de mécanisme d'activation ou d'inactivation de fonctions autres que structurales. L'identification de sites potentiels de modifications post-traductionnelles, (phosphorylation et glycosylation) lesquels sont rarement observés chez les autres protéines riche en glycine, suggère aussi d'autres rôles possibles pour la protéine ZmGRP5 justifiant ainsi des études plus approfondies.

Acknowledgements

I would like to thank Dr. Thérèse Ouellet for inspiring me to push the limits of my abilities, and her persistent and unwavering support and friendship throughout the pursuit of my M.Sc.

I thank Dr. Douglas A. Johnson for his guidance and helpful advice, which have made my return to academic life a pleasant one.

My gratitude goes to Dr. Jas Singh for introducing me to the fascinating world of plant science. Your sense of humour and love of life will always be remembered.

Many thanks to:

Dr. Steve Gleddie and Christine Gagnon for your advice and expertise in 2D SDS-PAGE;

Sahar Farah for your friendship and assistance with recombinant protein production;

Dr Shea Miller and Ann-Fook Yang for your help with microscopy;

Hélène Rocheleau et Anissa Lybaert pour votre assistance avec le résumé.

Finally, I would like to thank Dr. Johann Schernthaner and all my fellow co-workers from all the laboratories that I have worked in over the years during the pursuit of my degree for accommodating the atypical hours and high-strung nerves of a part-time student. I could not have done it without your support.

TABLE OF CONTENTS

List of Figures and Illustrations

List of Abbreviations

2D	two dimensional
ABA	abscissic acid
AGP	arabinogalactan protein
AtGRP	*Arabidopsis thaliana* glycine-rich protein
ß-ME	ß-mercaptoethanol
cDNA	copy deoxyribonucleic acid
CHAPS	3-[(3-Cholamidopropyl)dimethylamminio]-1-propanesulfonate
ConA	concanavalin-A
dpe	days post emergence
DTT	dithiothreitol
ECL	enhanced chemiluminescence
EDTA	ethylenediaminetetraacetic acid
ER	endoplasmic recticulum
GRP	glycine-rich protein
GST	glutathione S-transferase
hnRNPs	heterogeneous nuclear ribonucleoprotein
HPRG	hydroxyproline-rich glycoprotein
HRP	horseradish peroxidase
IHC	immunohistochemistry
IgG	immunoglobulin G
IP	immunoprecipitation
IEF	isoelectric focusing
IPG	immobilized pH gradient
IPTG	isopropyl ß-D-thiogalactopyranoside
KCl	potassium chloride
kD	kiloDalton
KH_2PO_4	potassium phosphate
LC-MS/MS	liquid chromatography-mass spectrometry/mass spectrometry
MALDI-ToF	matrix assisted laser desorption ionisation–time of flight

NaCl	sodium chloride
Na_2HPO_4	sodium phosphate
NR	non-reducing
ORF	open reading frame
OsGRP	*Oryza sativa* glycine-rich protein
PAGE	polyacrylamide gel electrophoresis
PBS	phosphate buffered saline
PCR	polymerase chain reaction
PhGRP1	*Petunia hybrida* glycine-rich protein 1
pI	isoelectric point
PMSF	phenylmethanesulfonyl fluoride
PNGaseF	peptide:N-glycosidase F
PR-1	pathogen response-1
PRP	proline-rich protein
PvGRP1.8	*Phaseolus vulgaris* glycine-rich protein 1.8
PVDF	polyvinylidene difluoride
RC/DC	reducing agent compatible/ detergent compatible
RIPA	radioactive immunoprecipitation assay
RNA	ribonucleic acid
SDS	sodium dodecyl sulphate
STE	saline Tris EDTA
siRNAs	small interfering ribonucleic acids
TBS	Tris buffered saline
WAK1	wall associated kinase 1
wGRP1	wheat glycine-rich protein 1
ZmGRP	*Zea mays* glycine-rich protein

1. INTRODUCTION

The focus of this thesis is the characterization of ZmGRP5, a putative cell wall protein encoded by a maize silk tissue-specific cDNA. The specialized morphology of maize silk tissue as a reproductive floral organ and the implications of silk tissue-specific protein expression on possible protein function(s) will be described. Plant cell wall GRPs (glycine-rich proteins) have been implicated in functions ranging from that of structural proteins to that of components of multi-protein complexes in pathogen response signaling pathways. Plant GRPs will be briefly reviewed as a modular protein "family" characterized by divergent protein domains and the implications of the modular domains on the functional characterization of ZmGRP5 will be explored. Furthermore, the plant cell wall will be reviewed as a dynamic extracellular matrix and the implications of *in muro* localization on ZmGRP5 function will be explored.

1.1 Maize as a Crop

Maize (*Zea mays spp. mays*) is a domesticated crop belonging to the grass family Poaceae. Unlike other cereal crops such as wheat and rice, maize was domesticated from the wild and developed as a crop by the Mesoamerican civilizations of the New World, with its closest living relative being the Mexican annual teosinte (*Zea mays spp. parviglumis*) (Doebley *et al.*, 1984). Noted for its high productivity due to the C4 pathway of photosynthesis, maize has spread rapidly to the rest of the world in the15th and 16th centuries since the Spanish conquest of Mexico to become the third most widely

grown crop in the world today (Salvador, 1997). Socially, maize grain is important as a staple food for human consumption in much of the developing world. Economically, maize is the most important crop grown in North America and is the basis of a multibillion dollar industry that supplies feed for the livestock industry and provides the raw material for an extensive array of industrial and pharmaceutical products such as ethanol, starch, dextrose, fibre, and plastics.

Maize production is limited by the cooler, shorter growning season found in Canada, and is mainly confined to regions of southwestern Ontario and southern Quebec that receive enough heat units (http://www.ontariocorn.org). Maize ear rot and the accompanying mycotoxin contamination and crop losses are of particular economic importance in eastern Canada, especially during wet growing seasons. Maize silk tissue is a targeted site of invasion by the infective agent, *Fusarium graminearum* (Reid *et al.*, 1992). Therefore, the identification of silk tissue-specific genes was initiated as part of a multidisciplinary study for the development of *Fusarium*-resistant maize at the Eastern Cereals and Oilseeds Research Centre, Agriculture and Agri-Foods Canada, Ottawa, ON, Canada.

1.2 Maize Silk as a Floral Tissue

Maize is distinguished from other members of the grass family, Poaceae, by the partitioning of the sexes into different flowers in the plant, a condition called monoecy. The male (staminate) inflorescence, the tassel, is found at the stem apex of the maize plant while the female (pistillate) inflorescence, the ear, protrudes from the main stem at

the tips of lateral branches that have become reduced and condensed (Dellaporta and Calderon-Urrea, 1993) (Fig. 1).

The maize ear is a composite fusion of individual female florets. Each kernel (ovary) in the maize ear is attached to a single strand of maize silk, which together constitute the pistil of a single maize floret (Miller, 1919). The maize silk is functionally equivalent to both the stigma and style portions of a typical pistil. The silk hairs that cover the length of the silk serve as pollen receptive surfaces that support pollen hydration and germination, a function typically associated with the stigma. Additionally, the main axis of the maize silk serves as a conductive path for pollen tube growth, a function typically attributed to the style, from the site of pollen germination at the silk hairs to the ultimate destination of the ovule, where fertilization takes place.

The duality of function of maize silk as a specialized reproductive tissue has resulted in conflicting designations of silk as either the stigma or the style in literature. According to one view, the maize silk is considered to be the stigma due to the distribution of silk hairs along the majority of its length, conforming to the Weatherwax definition of the stigma: the pollen-receptive part of the pistil (Heslop-Harrison *et al.*, 1984). Typical grass florets contain two feather-like pollen receptive branches called stigmas that both lead to a single ovary (Esau, 1984). In contrast, only a single maize silk emanates from each maize ovary (kernel). Each maize silk could thus be viewed as a composite fusion of the two feathery branches typical of other grass florets. Only a short portion of silk tissue, approximately 5mm near the entry point to the kernel, is free of the pollen receptive

Figure 1. Graphic representation of a maize plant showing the separation of the male (tassel) and female (ear) inflorescences.

From website of International Institute for Tropical Agriculture (IITA) http://www.iita.org/info/trn_mat/irg9/fig1.GIF

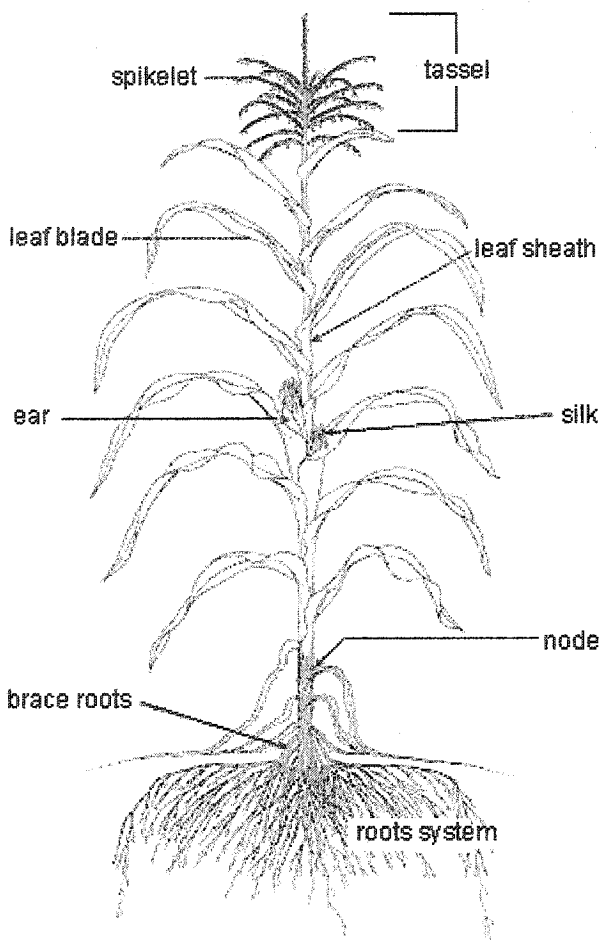
spikelet
tassel
leaf blade
leaf sheath
ear
silk
node
brace roots
roots system

hairs. This short portion is conceptualised as the style, the non-pollen-receptive part of the pistil.

According to a second view, the entire length of the silk can be viewed as the style of the maize pistil (Kroh *et al.*, 1979), while the individual pollen receptive silk hairs can be viewed as the stigma. Unlike typical styles, each maize silk contains not one, but two transmitting tracts that serve as pollen tube conductive pathways to the ovary. The transmitting tracts are associated with two vascular bundles that traverse the entire length of the silk from the kernel to the forked tip, where the two bundles separate (Miller, 1919).

The specific cell-types and tissue-types found within maize silk tissue perform distinctly specialized functions. These cell-types are best visualized in a cross-sectional view of silk tissue (Fig. 2). Such a cross-sectional view is representative of the entire length of the silk except at the base where silk hairs are not found, and at the forked tip where the two vascular "bundles" separate. Localization of ZmGRP5 expression to any specific cell-types within maize silk tissue will yield invaluable clues regarding possible related functions.

1.2.1 Silk Hairs

The pollen receptive silk "hairs" (Kroh *et al.*, 1979), or "trichomes" (Heslop-Harrison *et al.*, 1984) are multicellular outgrowths of epidermal origin specialized for pollen capture.

Figure 2. The cross-sectional view of 0 dpe silk tissue stained with toluidene blue. The cortex is roughly delineated between the perforated lines from the pith at the centre of the silk. Both are composed of round, undifferentiated parenchyma cells, which are visibly larger in diameter than the specialized sheath cells of the transmitting tract and the xylem vessels of associated vascular tissue.

X. xylem, TT. transmitting tract, C. cortex, Pi. pith, E. epidermis

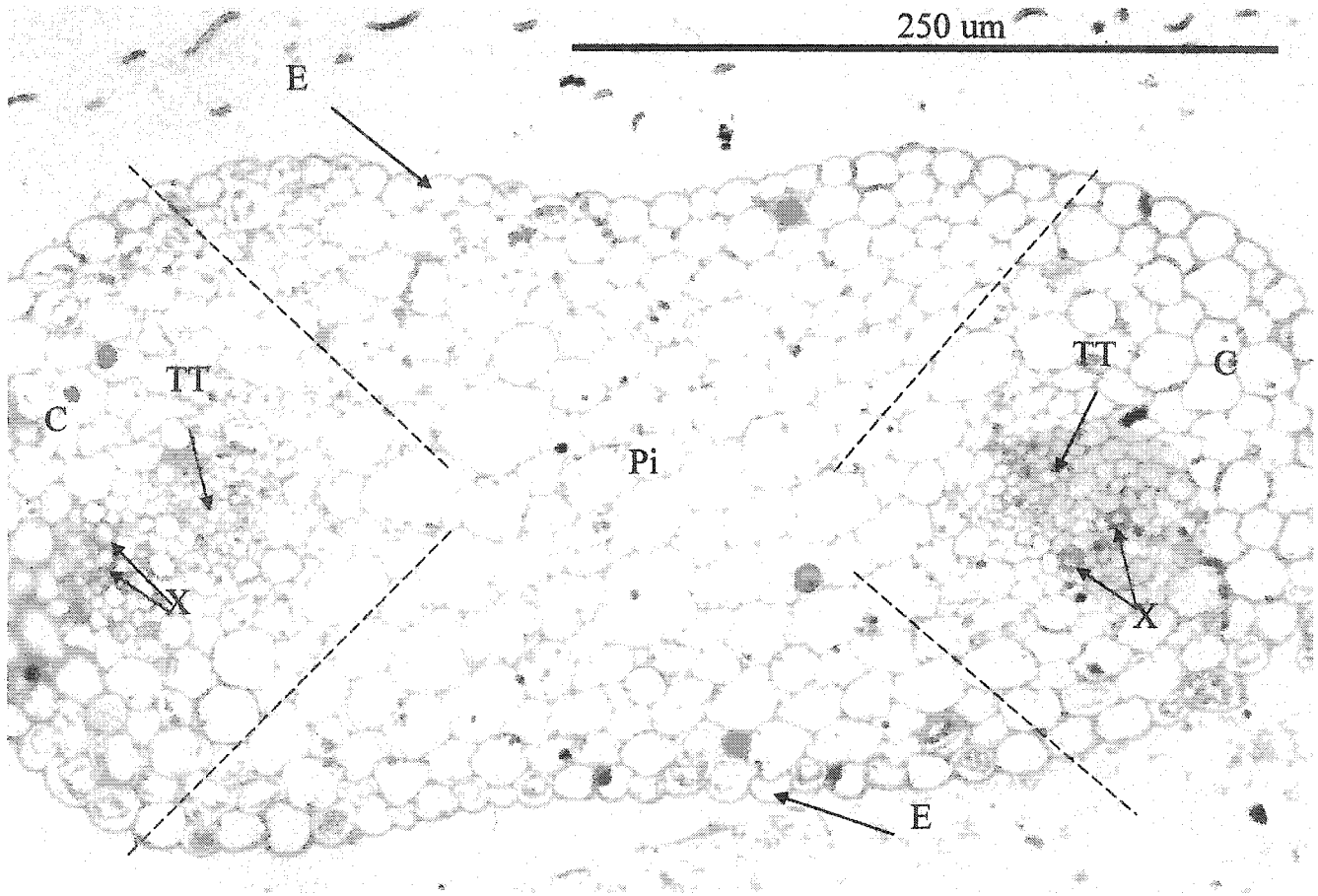
250 um
E
TT
C
Pi
TT
G
X
X
E

Surface secretions on the silk hairs are responsible for facilitating the events of pollen adhesion, hydration, and germination. The surface secretions are organized into a continuous pellicle composed of an outermost proteinaceous layer, an inner pectic polysaccharide layer, and an underlying discontinuous, highly permeable waxy cuticle. Wind dispersed pollen is initially only weakly held by the receptive silk hairs, possibly by the forces of electrostatic attraction. The adhesion becomes progressively more secure with the formation of a meniscus at the site of pollen contact with the silk hair. The proteinaceous surface layer on the silk hair interacts with the pectinaceous surface of the pollen, resulting in dispersal of the silk hair surface pellicle and initiation of water transfer from the silk hair to the hydrating pollen. Upon germination, a pollen tube penetrates the discontinuous cuticle of the silk hair and grows in the intercellular space of the silk hair, eventually entering the main axis of the maize silk.

1.2.2 Epidermis

The files of epidermal cells covering the main axis of the silk have heavily thickened outer walls and are covered by a continuous waxy cuticle that serves to reduce water loss to the environment. The maintenance of osmotic potential is an important factor in silk receptivity and kernel yield under water stressed conditions (Westgate and Boyer, 1985; Bassetti and Westgate, 1993c). Additionally, the epidermis of the silk and the overlying continuous cuticle could potentially be important as barriers against biotic stress such as pathogen infection.

1.2.3 Cortex and Pith

The cortex, located between the epidermis and the vascular bundles, is composed of undifferentiated parenchyma cells 4-5 cell layers thick. The tissue between the two vascular bundles at the centre of a cross-sectional view of the maize silk is referred to as the pith, and is also composed of undifferentiated parenchyma cells. The distinction between the cells of the pith and the cortex is not apparent, and the boundary between the two is not well defined.

The cortex is notable as a medium between the silk hairs and the transmitting tract during pollen tube growth (Heslop-Harrison *et al.*, 1984). The cells of the cortical parenchyma are especially elongated, with a length:width ratio of up to 30:1. As the pollen tube exits the basal cell complex of the silk hairs and grows into the main axis of the silk, it grows between the intercellular spaces of the cortical cells towards the transmitting tract in a stepwise manner across successive cell files. The cortical cells do not exhibit special structural adaptations directing the pollen tube to the transmitting tract associated with the vascular bundle, and pollen tube growth is suggested to be directed by chemotropic substances released from the transmitting tract.

1.2.4 Vascular Bundle

The two vascular bundles traversing the length of the silk are composed of the xylem vessels, phloem sieve tubes, and associated companion cells of the vascular system. The

xylem vessels are especially prominent in cross-sectional views of the silk as lignified tubes that supply the silk tissue with water. Given the extremely elongated nature of maize silk compared with more typical grass stigmas, the vascular system is especially developed to maintain the pollen receptivity and osmotic potential of the silk tissue throughout its whole length, which could vary from 2cm upwards to 70cm. While the phloem is less obvious and was not detected by Kroh *et al.* (1979), its sieve tubes were observed by Heslop-Harrison *et al.* (1984) to be located in the opposing side of the xylem vessels than the associated transmitting tract.

1.2.5 Transmitting Tract

The transmitting tract is a specialized tissue associated with the vascular bundle throughout most of the length of the maize silk, serving as a tract for pollen tube growth to the ovule. The tract is separated by one row of parenchyma cells from the vascular bundle in a cross-sectional view. The transmitting tract is composed of elongated, fusiform cells that appear circular and smaller in diameter than the cortical cells in cross-section. Copious amounts of pectinaceous polysaccharides and proteins are secreted from the cells into the large intercellular spaces to support pollen tub growth. The sperm cells inside the pollen tube move along inside the growing tip from the site of germination to the ultimate destination of the egg cell inside the ovary.

1.3 GRP "Family" Of Proteins

In plants, a constantly growing set of GRPs is being identified. However, very few GRPs have been characterized and the functions of most GRPs remain largely unknown. The GRP nomenclature is commonly used only for plant proteins containing the $(G\text{-}X)_n$ motif, where X is often glycine but other amino acids such as alanine, serine, valine, histidine, phenyalanine, tyrosine, and glutamic acid are also common. AtGRP1 to AtGRP8 from the model plant *Arabidopsis thaliana* were named in the order of discovery (de Oliveira *et al.*, 1990 and 1993). Two such proteins have been characterized in rice (*Oryza sativa*), OsGRP1 (Lei and Wu, 1991) and OsGRP2 (Fang *et al.*, 1991), while an abscissic acid inducible protein containing glycine-rich sequences was named RAB21 (Mundy and Chua, 1988). In maize, the above nomenclature was only adopted for the proteins ZmGRP3 (Goddemeier *et al.*, 1998) and ZmGRP4 (Matsuyama *et al.*, 1999), while the original names are retained for the first two GRPs identified (Gomez *et al.*, 1988; Didierjean *et al.*, 1992). In contrast, glycine-rich animal proteins, such as keratins, loricrins, nucleolins, fibrillarins, and hnRNPs (heterogeneous nuclear ribonucleoprotein) are named independently based on function and/or location (reviewed by Steinert *et al.*, 1991). Additionally, long stretches of glycine-rich sequences have also been found in spider dragline silk (Xu and Lewis, 1990), and the eggshell protein of the human parasite *Schistostoma mansoni* (Bobek *et al.*, 1986).

1.3.1 Diversity of GRPs

A survey of plant GRPs in literature reveals an incredible diversity of proteins with a seemingly unrelated array of functions. GRPs are involved in potential roles in plant defense, with transcriptional expression induced by stress stimuli such as viral infection and/or salicylic acid treatment (van Kan *et al.*, 1988; Fang *et al.*, 1991; Naqvi *et al.*, 1998), fungal infection or elicitor treatment (Brady *et al.*, 1993; Molina *et al.*, 1997), wounding and/or jasmonic acid treatment (Yasuda *et al.*, 1997; Richard *et al.*, 1999) and nematode infection (Potenza *et al.*, 2001). Other GRPs are environmentally induced by abscissic acid treatment and/or water stress (Mundy and Chua, 1988; Gomez *et al.*, 1988; Yu *et al.*, 1996; Nicolas *et al.*, 1997), cold stress (Ferullo *et al.*, 1997; Horvath and Olson., 1998; Karlson *et al.*, 2002), and circadian rhythm (Carpenter *et al.*, 1994; Heintzen *et al.*, 1997; Staiger *et al.*, 1999).

In addition to biotic and abiotic stress responsiveness, most GRPs are developmentally regulated with distinct temporal and spatial expression patterns. Examples include tissues associated with auxin-induced lateral root formation (Neuteboom *et al.*, 1999), early stage somatic embryogenesis (Sato *et al.*, 1995), *Phalaenopsis* orchid ovules 11 weeks after pollination (Nadeau *et al.*, 1996), seasonal accumulation in late wood of maritime pine (*Pinus pinaster* Ait) (Le Provost *et al.*, 2003), and vascular bundles of curved wood from bent loblolly pine (*Pinus taeda*) (Zhang *et al.*, 2000). GRPs are often specifically localized in distinct cell or tissue types, such as xylem sap and lignified metaxylem (Sakuta *et al.*, 1998; Sakuta and Satoh, 2000), unlignified primary walls of protoxylem

(Ryser and Keller, 1992), tapetum derived pollen exine surface (Koltunow *et al.*, 1990; Chen and Smith, 1993; Robert *et al.*, 1994;), root cap mucilage (Matsuyama *et al.*, 1999), flax fibres (Girault *et al.*, 2000), guard cells (Smart *et al.*, 2000), bundle sheath cells (Furumoto *et al.*, 2000), fruit (Santino *et al.*, 1997), nodules (Kevei *et al.*, 2002), anthers (de Oliveira *et al.*, 1993; Mousavi *et al.*, 2000), and ovules (Nadeau *et al.*, 1996).

With the exception of the RNA-binding GRPs, putative signal peptides are found in the majority of all other plant GRPs, which are often assumed to be structural proteins of cell walls without further experimental evidence in published literature. Very few predicted cell wall GRPs have been localized in specific cell types, and even fewer have known functions. GRP1.8 from French bean (*Phaseolus vulgaris)* is an extensively studied cell wall structural GRP (Keller *et al.*, 1988; Keller and Baumgartner, 1991; Ryser and Keller, 1992; Ryser *et al.*, 1997; Ringli *et al.*, 2001a and 2001b). Antibodies raised against GRP1.8 localized mainly in the unlignified primary cell walls of protoxylem cells in etiolating hypocotyls of French bean, and the protein has been proposed to play a role in the cell wall repair process during the elongation phase of xylem development. In addition, antibodies against the GRP1.8 has also identified "stress fibres" linking the secondary cell wall thickenings that form rings and helices in the protoxylem vessels of etiolating hypocotyls of soybean (*Glycine max*) and other dicots (Ryser, 2003; Ryser *et al.*, 2004). Another protein, PtGRP1, has been shown to be deposited at the cell wall/plasma membrane interface of phloem companion cells in the vascular bundles of the stem and young leaves of petunias (Condit and Meagher 1987; Condit, 1993).

While the few experimentally localized GRPs are mostly confined to cell walls, not all GRPs with signal peptides are necessarily structural. One such example, ZmGRP4, is secreted into the mucilage surrounding the root caps of maize, and may play possible roles as a lubricant during expansive growth of roots through soil, or play potential roles in signalling interactions with soil micro-organisms in the rhizosphere (Matsuyama *et al.*, 1999).

1.3.2 Modularity of GRPs

Upon closer inspection, it is evident that the classification of proteins as GRPs based on the presence of glycine-rich amino acid sequences is somewhat arbitrary and highly inconsistent. The $(G\text{-}X)_n$ motif could be highly irregular and variable in terms of higher order repeat patterns. The abundance of the $(G\text{-}X)_n$ motif repeats within these proteins is also highly variable. Some proteins are almost entirely glycine-rich, while others have glycine-rich motifs along with other non-glycine-rich motifs. Some other proteins, such as the GRPs found specifically in the nodules of *Vicia faba* (Schroder *et al.*, 1997) and *Alnus glutinosa* (Pawlowski *et al.*, 1997), do not contain particular glycine-rich repetitive motifs at all, but simply have generally increased glycine content.

It has been suggested that GRPs could perhaps be best viewed simply as proteins with a common motif rather than a protein family of related function (Sachetto-Martins *et al.*, 2000). GRP can thus be conceptualised as modular proteins with glycine-rich regions for structural flexibility and other divergent properties derived from the non-glycine rich

domains such as N-terminal secretory signal peptides, RNA-binding domains, oleosin lipid binding domains, and cysteine-rich domains (Fig. 3).

1.3.2.1 Glycine-Rich Domains

The unifying feature of GRPs is the presence of quasi-repetitive, glycine-rich peptide sequences. The regions of homology between GRPs are often confined to the glycine residues, and the patterns of glycine-rich repeats are highly irregular and variable.

Two models of secondary structural motifs have been proposed for the glycine-rich repeats: the glycine loop and the ß-sheet (Fig. 4). According to the ß-sheet model, GRPs containing higher order glycine-rich repeats are arranged in anti-parallel strands joined by intervening turns of lower glycine content. The charged side chains of intervening non-glycine residues all project out of the plane of the sheet on the same side, generating a ß-sheet that is hydrophilic on one side and hydrophobic on the other despite the low number of hydrophobic amino acid residues. This model has been proposed for the structure of PhGRP1 (Condit, 1993). The projection of hydrophilic residue side-chains from one side of the ß-sheet and the projection of hydrophobic residue side-chains from the opposite plane allow the possible formation of directionally oriented hydrophobic surfaces. The ß-sheet model was proposed to allow PhGRP1 to engage in hydrophobic interactions with other structures of the cell wall or plasma membrane. The same model has been proposed to explain the observed hydrophobic interactions of PvGRP1.8 (Ringli *et al.*, 2001a).

Figure 3. Schematic representation of characterized plant GRPs containing various sub-domains. Adapted from Fig. 2, Sachetto-Martins *et al.* (2000)

Legend:

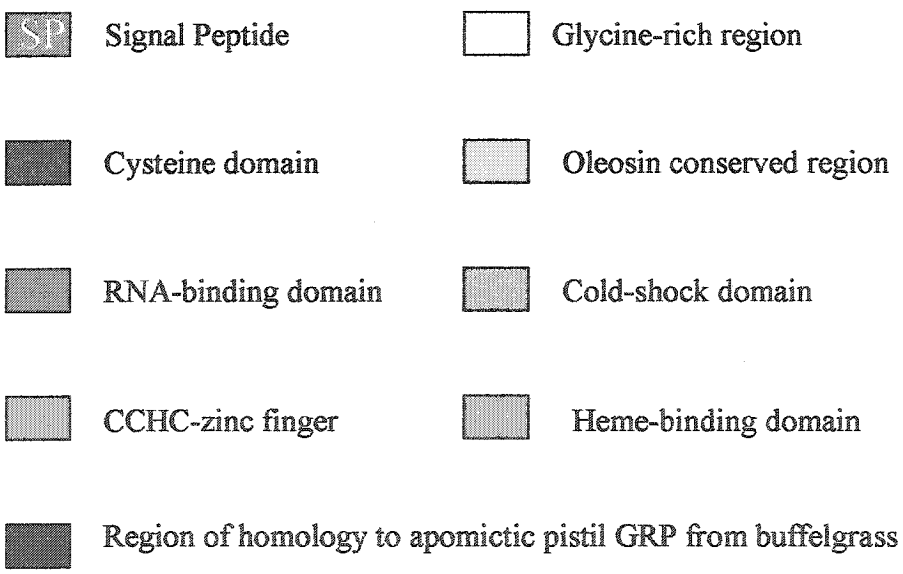

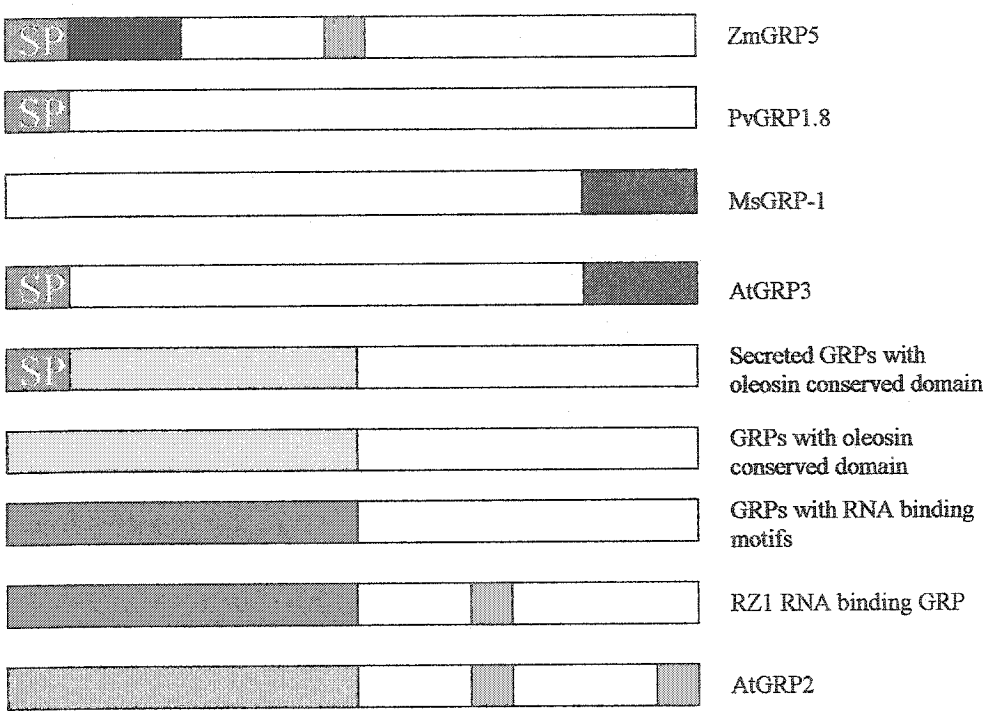
SP
ZmGRP5
SP
PvGRP1.8
MsGRP-1
SP
AtGRP3
SP
Secreted GRPs with oleosin conserved domain
GRPs with oleosin conserved domain
GRPs with RNA binding motifs
RZ1 RNA binding GRP
AtGRP2

Figure 4. Secondary structure prediction for GRPs. Copied directly from Fig. 1, Sachetto-Martins *et al.*, 2000.

A Glycine loop model applied to sequence of AtGRP5

B Beta pleated sheet model applied to sequence of PvGRP1.

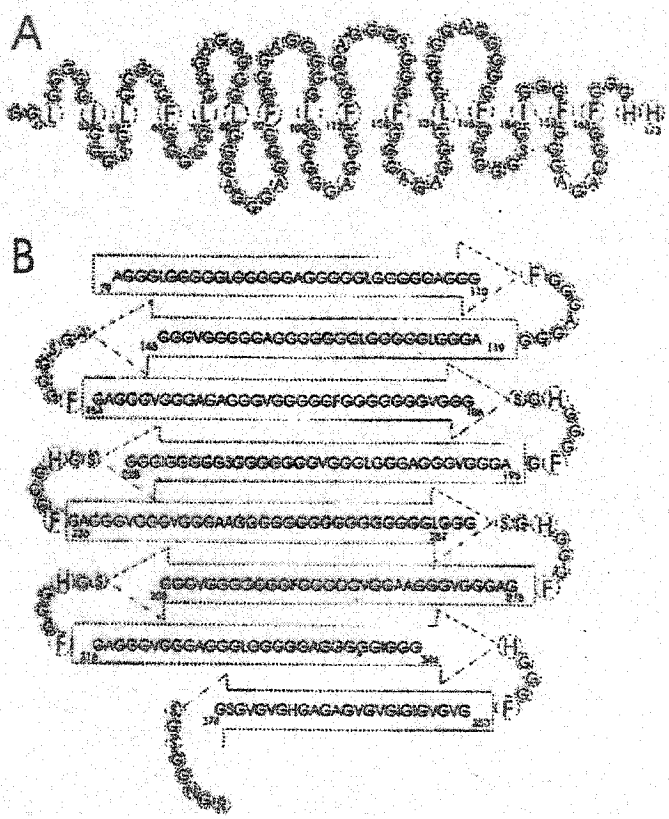
A
B

In the glycine loop model (Steinert *et al.*, 1991), the glycine-rich sequences are forced into loop-like configurations anchored around intervening aromatic residues such as tyrosine or phenylalanine, which are stacked in an ordered array by hydrophobic interactions between the aromatic rings. The glycine loop structure is predicted to be highly flexible and devoid of any necessarily unique conformation or higher order repeat pattern. The non-glycine residues interspersed within the glycine loops are often hydrophilic (serines, threonines, and asparagines) or charged (arginines, histidines), and are usually located at or near the "apex" of the glycine loops. These residues are proposed to engage in hydrogen bonding interactions and could be responsible for the stress bearing tensile strength and elasticity of animal keratin intermediate filaments.

In addition to the above two models, which have not been experimentally confirmed, structural studies of spider dragline silks suggest that glycine-rich repeats adopt structural conformations called ß-turns (Lewis, 1992). In addition, the intervening blocks of poly alanine repeats that alternate with the glycine-rich repeats in dragline silk were found to be responsible for the formation of crystalline ß-sheets. Dragline silks are noted for extremely high tensile strength as well as limited elasticity (35% resilient). The crystalline ß-sheets are suspected to be responsible for tensile strength by cross-linking and reinforcing the polymer network (Gosline *et al.*, 1999), while the glycine-rich ß-turns are suspected to be responsible for elasticity due to a lack of complex side chain interactions from the glycine residues, which have a single hydrogen as their R group. In contrast to the dragline silks, which form the web frame and radii of spider webs, flagelliform silks compose the capture spiral of spider webs and are composed almost

almost exclusively of glycine-rich repeats (Hayashi and Lewis, 1998). The series of tandem ß-turns resulting from the glycine-rich repeats have been proposed to form a spring-like helix structure called a ß-spiral, which forms the basis for the elasticity of silk. Interestingly, the almost exclusively glycine-rich primary sequence of flagelliform silks coincides with its higher elasticity and lower tensile strength compared to dragline silks.

1.3.2.2 Non-Glycine-Rich Domains

While the structural flexibility of GRPs may be due to the presence of glycine-rich repeats, other divergent functions can be attributed to the presence of non-glycine-rich domains (Fig. 3). The most ubiquitous non-glycine-rich domain found in GRPs is the N-terminal secretory signal peptide, the presence upon which the predicted extracellular localization of most plant cell wall GRPs is based. The hydrophobic signal peptide is predicted to insert the protein across the membrane of the ER (endoplasmic recticulum), whereupon it is cleaved specifically by ER localized proteases and the mature protein is released into the ER lumen and is transported down the secretory pathway into the Golgi apparatus, vesicles, and eventually targeted outside the plasma membrane by exocytosis (Nielsen *et al.*, 1997; Lippincott-Schwartz *et al.*, 2000).

RNA binding GRPs are characterized by the presence of RNA binding domains in the N-terminus, which is implicated in transcriptional regulation in the nucleus. Examples of RNA binding GRPs in plant include MA16 (Gomez *et al.*, 1988), an abscissic acid and water stress inducible protein that accumulate in mature embryos of maize, and its

homologues in tobacco (Hirose *et al.*, 1993), sorghum (Cretin and Puigdomenech, 1990), beechnut (Nicolas *et al.*, 1997), and *Arabidopsis* (de Oliveira *et al.*, 1990).

GRPs containing conserved oleosin domains in the N-terminus and glycine rich repeats in the C-terminus include AtGRP6, AtGRP7, and AtGRP8 from *Arabidopsis* (de Oliveira *et al.*, 1993), and oleosin-GRP homolgues from tobacco (Koltunow *et al.*, 1990), tomato (Chen and Smith, 1993) and *Brassica napus* (Robert *et al.*, 1994). All are derived from the inner tapetum layer of the anthers and form components of the outer pollen wall, where potential roles in pollen-pistil interactions during fertilization are possible. While the function of oleosin GRPs have not been proven, the oleosin domain is responsible for the lipid-binding properties of this class of proteins.

Cysteine-rich domains have been implicated in protein binding through the formation of disulfide bonds. AtGRP3 has been shown to interact with WAK1 (wall-associated receptor kinase 1) of *Arabidopsis* by binding to the extracellular domain of WAK1 and initiating a pathogen responsive signalling pathway (Park *et al.*, 2001; Yang *et al.*, 2003). It is proposed that the cysteine domain in the C-terminal tail of AtGRP3 is bound to an equivalent conserved cysteine domain in WAK1.

1.4 The Cell Wall

Contrary to the traditional view of the cell wall as a static rigid box giving structural support to the plant cell, a new understanding of the cell wall as a dynamic extracellular

matrix has emerged from more recent studies in cell wall biology. Far from being static, the cell wall should instead be viewed as a responsive, virtual extension of the cytoplasm complete with roles in defense, signalling, intercellular communication, cell expansion, adhesion, separation, translocation, differentiation, and morphogenesis (Showalter, 1993; Carpita and Gibeaut, 1993).

The cell wall is composed of a fibre composite network of cross-linked carbohydrate polymers in which an ordered array of cellulose microfibrils coated with hemicelluloses such as xyloglucans are embedded in a gel of cross-linked pectins (Carpita and Gibeaut, 1993). Proteins, phenolics such as lignin and varying amounts of other linked carbohydrates are embedded within this matrix. The cell wall properties of different cell types are highly variable, determined by the differing composition of the matrix components (Pennell, 1998). Many extracellular enzymes have been identified that restructure and modify the polymer composition of the matrix, which is constantly adjusted with developmental and environmental changes (Roberts, 2001). Additionally, polymer interactions between existing matrix components also regulate this dynamic change. Cell wall loosening results from the disruption of bonds linking cell wall polymers (Cosgrove, 2000), while the formation of new cross-linkages increases cell wall rigidity (Bradley *et al.*, 1992)

Several classes of structural proteins have been identified in the cell wall matrix. The most abundant are HPRGs (hydroxyproline-rich glycoproteins), structural proteins that account for as much as 10-20% of the dry weight of growing cell walls (Kieliszewski and

Shpak, 2001). The HPRG superfamily contains three major sub-groups, all distinguished by post-translational modifications such as the hydroxylation of proline residues, and the glycosylation of hydroxyproline and serine residues by various sugar moieties. The first major group, extensins, contain repeating units of the signature pentapeptide serine-$(hydroxyproline)_4$ and are important in cell wall cross-linking and extensive growth (Kieliszewski and Lamport, 1994). PRPs (proline-rich proteins) are highly repetitive, less glycosylated, tend to be shorter in length than the extensins, and several have been implicated in plant defense via the formation of covalent oxidative cross-links that harden the cell wall (Bradley *et al.*, 1992; Waffenschmidt *et al.*, 1993). AGPs (arabinogalactan-proteins) are the least repetitive and are extremely soluble and heavily arabinosylated. AGPs are especially abundant in the intercellular space and are proposed to be importantly signalling molecules (Majewska-Sawka and Nothnagel, 2000).

The other major group of cell wall proteins are the GRPs, which are distinguished by the abundance of glycine instead of proline residues have been suspected to function as structural proteins that contribute to the flexibility and elasticity of growing tissue (Ringli *et al.*, 2001b). However, exceptions to this role include AtGRP3, which is implicated in a pathogen-response signalling pathway (Park *et al.*, 2001). The key to the understanding the function of each GRP lies in the identification of interaction partners and the nature of such associations in the dynamic cell wall matrix.

1.5 Statement of Objectives

Maize silk is a specialized floral tissue that serves as a receptive surface for pollen adhesion, and as a nutrient rich and moist conductive medium for pollen tube growth. These same properties also make maize silk tissue a target of foraging by insect pests (Hoffmann *et al.,* 2000; Hazzard *et al.,* 2003) and a targeted site of invasion by fungal pathogens such as *Fusarium graminearum,* the infective agent of maize ear rot (Reid *et al.*, 1992).

A silk-tissue specific gene, *zmgrp5* (*Zea mays* glycine-rich protein 5), and its promoter were previously isolated (Ouellet *et al.,* 2003). The promoter was intended to drive resistance gene expression at the targeted site of infection as part of a multi-team effort to produce *Fusarium* resistant maize. The silk tissue-specific cDNA clone was initially isolated by subtractive suppressive hybridization (PCR-Select DNA Subtraction Kit, BD-Biosciences). Northern hybridization experiments had confirmed the mRNA expression of the gene to be silk tissue-specific and developmentally regulated (Fig. 5).

The ultimate goal of this study is to characterize the function of ZmGRP5, the predicted protein product encoded by the *zmgrp5* gene. Given the importance of maize silk tissue in both fertility and pathogenicity, the discovery of the function(s) of ZmGRP5, the first GRP with silk tissue-specific expression, would be of major importance. ZmGRP5 differs significantly from other GRPs previously isolated from maize such as MA16 (Gomez et al., 1988) and CHEM2 (Didierjean et al., 1992), found in immature embryos, or

Figure 5. Silk tissue specificity of ZmGRP5. Total RNA extracted from various maize tissues (10 μg /lane) was hybridized with radio-labelled ZmGRP5 cDNA probe.

dpe, days post emergence.

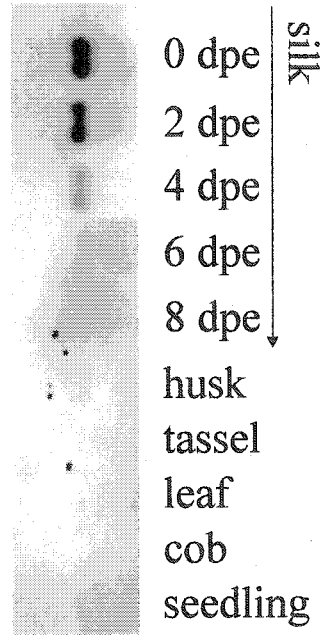
silk
0 dpe
2 dpe
4 dpe
6 dpe
8 dpe
husk
tassel
leaf
cob
seedling

ZmGRP3 (Goddemeier et al., 1998) and ZmGRP4 (Matsuyama et al., 1999), which are expressed in the extracellular matrix of roots. Due to the lack of clarity regarding function that can be concluded from existing characterized plant GRPs, this study intends to experimentally verify some properties of the native ZmGRP5 protein regarding localization, extractability, and protein complex formation as predicted by.some of its putative protein domains. The experiments will be carried out using an immunological approach with a ZmGRP5 antiserum.

Hypothesis 1: The expression of ZmGRP5 is silk tissue specific. This is to be confirmed at the translational level by probing immunoblots of various maize tissue extracts with the antiserum.

Hypothesis 2: ZmGRP5 is a secretory protein targeted to the cell wall matrix. This is to be tested by fractionation of maize silk tissue extracts into cell wall and cytosolic components followed by immunoblotting. Cell wall interactions with matrix components will be tested in protein extractability studies where maize silk tissue will be extracted with different buffers containing ionic and non-ionic detergents, salts, and reducing agents.

Hypothesis 3: ZmGRP5 is associated in multimeric protein complexes via disulphide bond formation mediated by cysteine residues. This is to be tested using SDS-PAGE separation of maize silk extracts using different concentrations of reducing agents in extraction and loading buffers. The disruption of multi-protein complexes into individual

subcomponents and monomers will be monitored with immunoblot detection. Additionally, the identification of potential interacting proteins will be attempted by co-immunoprecipitation.

Hypothesis 4: ZmGRP5 is the target of post-translational modifications. Bioinformatic analysis of the predicted protein sequence suggests possible modifications such as phosphorylation and glycosylation. This would result in isoforms of differing mass and charge than the polypeptide backbone, which has a predicted molecular weight of 14.7 kD and pI (isoelectric point) of 8.71. The status of ZmGRP5 post-translational modifications is to be monitored by immunoblot analysis of silk extracts separated by 2D (2-dimensional) SDS-PAGE.

Experimental results from the testing of the above four hypothesis should verify putative properties of ZmGRP5 that could contribute to ultimate function.The confirmation of silk tissue specificity is important to establish possible fertility-related functions. The sub-cellular localization and identification of possible interactions with the cell wall matrix are important to allow comparison of ZmGRP5 with other cell wall GRPs that could contribute to cell wall elasticity during expansive growth.The identification of potential interacting protein partners that associate with ZmGRP5 in multi-protein complexes is especially significant. The identities of the potential interacting partners would suggest associated functions for ZmGRP5. Finally, the confirmation of post-translational modifications such as phosphorylation or glycosylation would also suggest associated protein interactions

MATERIALS AND METHODS

2.1 Plant Material

Maize plants were field grown at the Central Experimental Farm, Eastern Cereals and Oilseeds Research Centre, Agriculture and Agri-Foods Canada, Ottawa, ON, Canada. Maize ears were bagged to prevent pollination and monitored daily for silk emergence, the developmental stage at which the first silk tissue begins to emerge from the enveloping husk tissue in the maize ear. Maize silk tissue was sampled at 0 dpe (days post emergence), the developmental stage at which the first maize silk tissue emerges from the surrounding husk tissue at the tip of a maize ear. This was the developmental stage at which the expression of the zmgrp5 mRNA was the highest in previous Northern Blot analaysis, and at which the ZmGRP5 protein is expected to be expressed. The silk tissue sampled was cut from an area in the maize ear referred to as the silk-channel: the area just above the tip of the maize cob, and just below the point of actual silk emergence from the surrounding husk. The enveloping husk tissue was removed, and the silk tissue was submerged immediately in liquid nitrogen and stored at –80 °C.

2.2 Recombinant ZmGRP5 Protein

2.2.1 Plasmid Construction

A SacI-BstXI fragment of the *zmgrp5* cDNA encoding amino acid residues 31-101 blunted with the Klenow fragment of *E. coli* DNA Polymerase-I was sub-cloned into the SmaI site of pGEX 4T-3 (Amersham Biosciences). The resultant plasmid, pB1, would code for a fusion protein consisting of an N-terminal GST (glutathione S-transferase) tag followed by the truncated version of ZmGRP5 cloned in the C-terminal region.

A SacI-NdeI fragment of the *zmgrp5* cDNA encoding amino acid residues 31-187 blunted with the Klenow fragment of *E. coli* DNA Polymerase-I was also subcloned into the SmaI site of pGEX 4T-3. The resultant plasmid, pN1, would express a fusion protein consisting of an N-terminal GST tag followed by the full-length version of ZmGRP5 cloned in the C-terminal region.

The following DNA methods used for plasmid construction were performed as described in Current Protocols in Molecular Biology (Ausubel *et al.*, 1994): plasmid DNA preparation, restriction enzyme digestion of DNA, vector DNA dephosphorylation, DNA purification from agarose gels, plasmid ligation, transformation of *E. coli*, and PCR screening of *E. coli* transformants.

2.2.2 Protein Expression and Purification

The GST-ZmGRP5 fusion plasmids were used to transform *Escherischia coli* cells of the BL21 strain (Amersham Biosciences). Overnight cultures of transformed *E. coli* were diluted 1:100 in 1 litre of fresh 2X YT medium, supplemented with ampicillin (100 μg mL^{-1}), and grown for approximately 4 hours at 37 °C until the beginning of log phase growth (OD_{600nm} reading of 0.5-0.7). Expression of the recombinant GST-fusion protein was induced with the addition of IPTG (isopropyl ß-D-thiogalactopyranoside) at 0.1 mM final concentration. After 2 hours growth at 37 °C, the culture was centrifuged for 10 minutes (5000 *g* at 4 °C). The bacterial pellet was resuspended in 1:50 original culture volume of STE buffer (50 mM Tris pH 8.0, 1 mM EDTA, 10 mM DTT, and 150 mM NaCl). The bacterial pellet was resuspended in 1:10 original culture volume of STE buffer (50 mM Tris pH 8.0, 1 mM EDTA, 10 mM DTT, and 150 mM NaCl) and re-centrifuged to remove residual media. The rinsed cell pellet was resuspended in 1:50 original culture volume of STE.

Solubilization of inclusion bodies and subsequent purification of the fusion protein was adapted from the method of Frangioni and Neel (1993). After freezing, the bacteria pellet was thawed and incubated on ice for 20 minutes with the addition of lysozyme (1 mg mL^{-1}). *N*-lauroylsarcosine was then added at 1.5% (w/v) final concentration, and the resulting cell suspension was vortex-mixed for 5 seconds and sonicated on ice using a Fisher Vibratec sonicator at 40% duty cycle and microtip limit of 4.2. Sonication was performed using 7x10 second pulses, cooling on ice for 1 minute intervals between each pulse. The

cell lysate was clarified by centrifugation for 30 minutes at 20,000*g* and then incubated at 4 °C on a rotating platform with Triton X-100 (final concentration of 4% [v/v]) and 2 mL of glutathione–Sepharose 4B (AP Biosciences) beads prewashed and swollen in PBS (150 mM NaCl, 3 mM KCl, 10 mM Na_2HPO_4, and 2 mM KH_2PO_4, pH 7.4). After incubation for 2 hours, the beads were packed into a gravity drip column, and washed in 10 volumes of ice-cold PBS. The fusion protein was eluted from the column in 1 mL fractions with 10 mM reduced glutathione in 50 mM Tris pH 8.0. A portion was used to immunize rabbits for the production of polyclonal antiserum (see **2.3**).

An aliquot of the purified GST-ZmGRP5 fusion protein was analyzed by denaturing SDS-PAGE (sodium dodecyl sulfate – polyacrylamide gel electrophoresis: see **2.6**), stained in Coomassie Blue R-250 in 40% methanol, 10% acetic acid, destained in 40% methanol, 10% acetic acid, and the protein bands were excised in gel slices and submitted for sequence confirmation by LC-MS/MS (liquid chromatography-mass spectrometry/mass spectrometry) as recommended by the Eastern Quebec Proteomics Centre (http://www.crchul.ulaval.ca/crchul/en/serv/Default.htm).

2.2.3 Thrombin Digestion of Fusion Protein

A portion of the GST-ZmGRP5 fusion protein was captured on a mini-column packed with 150 µL of glutathione–Sepharose 4B beads and digested with thrombin protease to generate recombinant ZmGRP5 protein without the GST tag. Two bed volumes of PBS containing 50 units thrombin protease (Amersham Biosciences) was added to the column

and allowed to flow through by gravity drip. The column was capped and sealed with paraffin to retain moisture in the Sepharose beads. On-column digestion of the fusion protein was conducted overnight at room temperature. Five 100 µL fractions of the cleaved ZmGRP5 component of the original fusion protein were eluted from the column upon addition of PBS. The GST tag component that remained captured on the beads was eluted subsequently with Glutathione Elution Buffer (10 mM reduced glutathione in 50 mM Tris pH 8.0) and collected in 5 x 100 µL fractions.

Aliquots of the respective thrombin digest and glutathione elution from above were analyzed by SDS-PAGE (see **2.6**), stained and protein bands were excised in gel slices and submitted for sequence confirmation by LC-MS/MS as above.

2.3 Polyclonal Antiserum

Immunization of rabbits and antiserum production was performed at the animal care facilities at the Canadian Food Inspection Agency, Ottawa, ON, Canada. Pre-immune antiserum was collected from two New Zealand rabbits prior to immunization. Two hundred microgram of purified GST-ZmGRP5 fusion protein was injected into each rabbit with an equal volume of Freund's complete adjuvant (Sigma-Aldrich). A booster inoculation containing 100 µg of purified GST-ZmGRP5 mixed with equal volume of Freund's incomplete adjuvant (Sigma-Aldrich) was performed at day 28 post immunization. Blood was collected from the rabbits at day 42 for verification of the presence of antibodies against GST-ZmGRP5 in the sera. A final bleed of the rabbits was

conducted at day 49, and the blood was incubated for 1 hour at 37 °C to allow coagulation of the blood clot and inactivation of the complement in the serum. Clarified antisera was separated from the coagulant by low speed centrifugation at 500 *g* and used directly in immunological studies.

2.4 Protein Extraction and Cell Wall Fractionation

All tissues were ground in a mortar and pestle in liquid nitrogen into a fine powder before extraction with two volumes of the appropriate buffers by incubation at 4 °C for 30 minutes on a rotator.

2.4.1 Direct Extraction

Tissue samples were directly extracted with a single extraction buffer. The soluble extract was clarified from the insoluble cell wall debris by centrifugation at 15000 *g* for 5 minutes at 4 °C. The clarified supernatant was transferred to new tubes before subsequent protein quantification and immunoblot analysis.

2.4.1.1 Tissue Series

Laemmli Buffer (20% glycerol, 4% SDS, 0.005% bromophenol blue, 125 mM Tris, and 10% ß-mercaptoethanol [ß-ME: CH_3CH_2SH]) was used to directly extract proteins from the following maize tissues: silk, husk, cob, leaf, and tassel, all collected at the

developmental stage of 0 dpe silk from the enveloping husk of maize ears. In addition, field grown seedlings were collected at 7 days post germination, as well as pollen directly shed from tassels at anthesis. Each tissue sample was pooled using tissue collected from at least two maize plants to equalize sampling bias.

2.4.1.2 pH and Reducing Agent Series

Silk tissue sampled at 0 dpe was directly extracted with the following buffers to test the effect of pH and the reducing agent ß-ME on protein solubility/extractability:

Buffer 1: 50 mM Tris pH 4.6, 1% SDS.

Buffer 2: 50 mM Tris pH 5.5, 1% SDS.

Buffer 3: 50 mM Tris pH 6.8, 1% SDS.

Buffer 4: 50 mM Tris pH 8.0, 1% SDS.

Buffer 5 (Laemmli Buffer-NR [Non-reducing]): 20% glycerol, 4% SDS, 0.005% bromophenol blue, 125 mM Tris pH 6.8.

Buffer 6 (Laemmli Buffer): 20% glycerol, 4% SDS, 0.005% bromophenol blue, 125 mM Tris pH 6.8, and 10% ß-ME.

Buffer 7: 50 mM sodium citrate pH 5.5, 1% SDS.

Buffer 8: 50 mM potassium acetate pH 4.6, 1% SDS.

In addition to pH, the impact of heat on protein solubility and extractability was also investigated. Each buffer was used for two separate extraction treatments, the first by incubation at 4 °C for 30 minutes, while the second was boiled at 95 °C for 15 minutes.

2.4.2 Cell Wall Fractionation

2.4.2.1 Crude Centrifugation

Tissue samples were first extracted using the method of Matsuyama *et al.* (1999). Silk tissue was first extracted with Matsuyama Aqueous Buffer (50 mM Tris pH 6.8, 3 mM EDTA, 3 mM DTT, and 3 mM PMSF), then centrifuged as for direct extraction and the supernatant was transferred to a new tube and referred to as fraction A (aqueous soluble). The pellet, containing mostly cell wall associated material, was re-extracted with Matsuyama SDS Buffer (125 mM Tris pH 6.8, 1% SDS) and centrifuged as above. The resulting supernatant was removed and referred to as fraction B (SDS soluble).

2.4.2.2 Ultracentrifugation with Sucrose Cushion

Tissue was first extracted with Aqueous Buffer (50 mM Tris pH 8.0, 3 mM EDTA, 3 mM DTT, and 3 mM PMSF). The suspension was overlayed on 2 mL of a 40% (w/v) sucrose cushion for ultracentrifugation at 100,000 *g*, 4 °C for 1 hour. The resulting phases are a top aqueous layer, a middle sucrose cushion layer, and a cell wall pellet at the bottom of the tube. The aqueous surface layer containing the plasma membrane and cytosolic fraction (Ringli *et al.*, 2001a) was transferred to a new tube for further analysis. The sucrose cushion was discarded, and the purified cell wall pellet was washed in more Aqueous buffer before sequential extraction with subsequent extraction buffers.

Sequential extraction of the cell wall pellet was performed with different buffers to investigate the impact on protein extraction of the ionic detergent SDS, non-ionic detergent Triton X-100, and high salt conditions without detergents. The cell wall pellet was divided into two samples. The first was sequentially extracted with 1 M NaCl Buffer (125 mM Tris pH 8.0, 1 M NaCl), followed by SDS Buffer (125 mM Tris pH 8.0, 1% SDS), and then Laemmli Buffer. The second was sequentially extracted with Triton Buffer (125 mM Tris pH 8.0, 1% Triton X-100), followed by SDS Buffer (125 mM Tris pH 8.0, 1% SDS), and then Laemmli Buffer.

2.4.2.3 Miracloth Filtration

Tissue was first extracted with Aqueous Buffer (50 mM Tris pH 8.0, 3 mM EDTA, 3 mM DTT, and 3 mM PMSF). The suspension was filtered over a single layer of Miracloth (Calbiochem) by gravity flow at 4 °C. An aliquot of the flow-through was collected and referred to as the Aqueous fraction. The cell wall slurry collected by the filter was washed in 12 volumes of aqueous buffer. An aliquot of the final flow-through was collected and referred to as the Wash fraction. The cell wall debris on the filter was gently squeezed to remove all remaining buffer before being divided into equal portions and transferred with a spatula into microcentrifuge tubes.

The cell wall fractions were subsequently extracted with the following buffers with downstream immunoprecipitation experiments in mind:

Buffer 1: 1% SDS, 50 mM Tris pH 8.0, 2 mM EDTA

Buffer 2: 1% Triton, 50 mM Tris pH 8.0, 2 mM EDTA

Buffer 3: 0.15 M NaCl, 50 mM Tris pH 8.0, 2 mM EDTA

Buffer 4 (RIPA Buffer): 1% Triton, 0.1% SDS, 1% deoxycholate, 0.15 M NaCl, 50 mM Tris pH 8.0, 2 mM EDTA

Buffer 5 (modified RIPA buffer: 1% Triton, 0.1% SDS, 0.1% deoxycholate, 0.15 M NaCl, 50 mM Tris pH 8.0, 2 mM EDTA

Additionally, all cell wall pellets extracted with above buffers were also re-extracted with Laemmli Buffer.

2.5 Protein Quantification

The RC/DC Protein Assay Kit (Bio-Rad Laboratories) was used to quantify tissue extracts in this study. Many extraction buffers used in this study contain detergents and reducing agents at concentrations that are incompatible with the Bradford and Lowry Assays. The total proteins in the extracts were separated from interfering components in solution by precipitation followed by centrifugation into a pellet. The detergents and reducing agents in the original extracts were eliminated by removal of the supernatant and subsequent washing of the protein pellet. Final protein quantification was performed by resuspension of the protein pellet followed by addition of colorimetric detection reagents as in a typical Lowry Assay.

2.6 Denaturing SDS-PAGE

Before loading on SDS-PAGE, all protein extracts were mixed with an equal volume of Laemmli Buffer (20% glycerol, 4% SDS, 0.005% bromophenol blue, 125 mM Tris pH 6.8, and 10% ß-ME) and incubated in a heat block at 95 °C for 5 minutes. Initially, protein extracts were mixed with 5 volumes of Ausubel Buffer (36% glycerol, 12% SDS, 0.005% bromophenol blue, 125 mM Tris pH6.8, and 0.6 M DTT; from Current Protocols in Molecular Biology, Ausubel *et al.*, 1994) for SDS-PAGE analysis. However, the DTT (dithiothreitol) used in the preparation of the buffer exhibited degraded reducing agent activity. All protein samples separated by SDS-PAGE in this study are loaded with Laemmli Buffer, and not the degraded Ausubel Buffer unless specifically stated otherwise.

Plant tissue extracts from direct extraction with Laemmli Buffer are not diluted further and are heated directly before loading on gels for separation by SDS-PAGE. Heated samples are resolved in a 4% acrylamide stacking gel, 15% acrylamide separation gel in Running Buffer (25 mM Tris, 250 mM glycine, 0.1 % SDS) at 150 V for approximately 1 hour until the bromophenol blue gel front migrates to the bottom of the gel.

2.7 Immuno-blot Analysis

Denaturing SDS-PAGE gels were electro-transferred in Transfer Buffer (25 mM Tris, 192 mM glycine, and 20% methanol) at 100 V for 1 hour using a tank transfer apparatus

(Bio-Rad Laboratories) onto Immuno-Blot PVDF membranes (Bio-Rad Laboratories) pre-wetted with methanol. PVDF blots were blocked overnight at 4 °C with 5% skim milk in TBS (Tris buffered saline: 10 mM Tris pH 8.0, 150 mM NaCl). Primary rabbit antiserum (1:5000 dilution), or purified anti-GST IgG (Sigma-Aldrich; 1:500 dilution) incubation was performed at room temperature for 2 hours with 5% Blocking Reagent (Roche Diagnostics) in TBS. Blots were subsequently washed for 2 x 15 minutes in TBS with 0.1% Tween-20 and re-blocked for 20 minutes in 5% Blocking Reagent in TBS. The secondary antibody, HRP (horseradish peroxidase) goat anti-rabbit IgG conjugate (Bio-Rad Laboratories), was used at 1:20,000 dilution in 5% Blocking Reagent in TBS for 1 hour at room temperature. Blots were washed again for 4 x 15 minutes in TBS and incubated with BM Chemiluminescence Western Blotting Substrate (Roche Diagnostics). Blots are put between two sheets of cellophane and detected by chemiluminsecence with Kodak X-OMAT AR film.

2.8 Two Dimensional SDS-PAGE

Frozen silk tissue was powdered and extracted in Rehydration Buffer (8 M urea/ 2 M thiourea, 2% CHAPS, 50 mM DTT, 0.2% ampholytes [pH 3-10, Bio-Rad Laboratories], and 0.0005% bromophenol blue) at room temperature for 1 hour on a rotator. Extractions were conducted in triplicate, using 65 mg, 125 mg, and 250 mg amounts of powdered silk tissue in 250 µL of Rehydration Buffer (respectively 1:4, 1:2, and 1:1 [w/v] ratios of tissue to buffer). Insoluble cell wall debris was removed by centrifugation at 13000 rpm

for 10 minutes, and the supernatant was transferred to a new tube as the protein extract to be quantified and separated by electrophoresis.

The Non-Interfering Protein Assay (Geno Technology Inc.) was used to quantify protein extracts used in 2D SDS-PAGE. Interfering components were removed by protein precipitation as in the RC/DC Protein Assay, while the final colorimetric detection step is based on the binding of copper ions to the peptide backbone. This method is not affected by the amino acid composition bias of proteins as was observed with Bradford and Lowry based detection methods.

Silk protein extracts containing 250 µg of total protein were loaded on 7 cm IPG (immobilized pH gradient) strips (pH 3-10 range, Bio-Rad Laboratories) by passive rehydration overnight at room temperature. Proteins on the IPG strips were focused according to isoelectric point using a PROTEAN IEF cell (Bio-Rad Laboratories) programmed to 8,000 volt-hours.

IPG strips resolved by IEF were incubated for 10 minutes in DTT Equilibration Buffer (6 M urea, 2% SDS, 0.05 M Tris pH 8.8; 20% glycerol, and 2% [256 mM] DTT), followed by 10 minutes in Iodoacetamide Equilibration Buffer (6 M urea, 2% SDS, 0.05 M Tris pH 8.8; 20% glycerol, and 2.5% iodoacetamide). The IPG strips were then embedded directly on top of second dimension gels with 0.5% agarose prepared in SDS-PAGE Running Buffer. The second dimension gels are composed of a 4% acrylamide stacking

gel, 15% acrylamide separation gel, and the proteins are separated by mass under the same conditions as for standard SDS-PAGE.

2.9 Immunoprecipitation (IP)

Tissue extracts in SDS Buffer (1% SDS, 50 mM Tris pH 8.0, 2 mM EDTA) were diluted 1:10 in IP Dilution Buffer (0.01% SDS, 1.1% Triton X-100, 1.2 mM EDTA, 16.7 mM Tris pH 8.0, and 167 mM NaCl), resulting in final IP compatible conditions of 0.1% SDS, 1.0% Triton X-100, 2 mM EDTA, 20 mM Tris pH 8.0, and 150 mM NaCl. Tissue extracts in RIPA Buffer (1% Triton, 0.1% SDS, 1% deoxycholate, 0.15 M NaCl, 50 mM Tris pH 8.0, 2 mM EDTA) were used directly for IP.

Rabbit antiserum against the GST-ZmGRP5 fusion protein was added to the IP ready protein extracts at 1:100 to1:200 dilutions and incubated overnight on a rotator at 4 °C. ProteinA-Sepharose was added (50 µL per 1 mL IP reaction) and incubated for 2 hours on a rotator at 4 °C. The IP reactions were subsequently centrifuged at 15000 rpm for 10 minutes. The supernatant was removed and the ProteinA-Sepharose pellet was washed in 3 x 1 mL of RIPA buffer. An equal volume of Laemmli Buffer was added to the washed ProteinA-Sepharose beads (bound fraction) and the negative control supernatant (unbound fraction) for analysis by SDS-PAGE and immunoblots.

3. RESULTS

The objective of this study is the preliminary characterization of ZmGRP5, a protein encoded by a previously isolated maize silk tissue specific cDNA. A specific function for ZmGRP5 could not be readily deduced based on the existing literature of characterized GRPs, a diverse yet poorly understood 'family' of plant proteins. However, bioinformatic analysis of the primary amino acid sequence of ZmGRP5 identified several putative domains that suggest certain protein properties that could contribute to ultimate function.

An immunological approach was employed to characterize properties of the ZmGRP5 in maize silk tissue and to verify some of the putative domains. Recombinant GST-ZmGRP5 fusion protein produced in *E. coli* was used to immunize rabbits. The resulting antiserum was used for analysis of maize silk extracts on immunoblots. The silk tissue specificity of ZmGRP5 was tested at the protein level by immunoblotting extracts from various maize tissues. Subcellular fractionation of the cell wall matrix from the cytosol, organelles, and plasma membranes was performed on maize silk extracts to test the subcellular localization of ZmGRP5. Differential extraction procedures using buffers varying in composition or concentration of detergents, salts, pH, reducing agents, in addition to differential heat treatments, were performed to characterize the nature of the association of ZmGRP5 within the cell wall matrix. 2D SDS-PAGE was used to separate potential isoforms of ZmGRP5 resulting from post-translational modifications.

3.1 Bioinformatic Analysis of ZmGRP5

Bioinformatic analysis suggests that our protein of interest is a GRP that is targeted to the secretory pathway by an N-terminal signal peptide. Additional distinguishing characteristics include a putative heme-binding domain, and a non-glycine-rich area of homology to an uncharacterized GRP differentially expressed in the apomictic pistil of buffelgrass. The above information was used as a starting point in the experimental design toward the characterization of ZmGRP5 protein localization and function in this study.

3.1.1 Primary Sequence Analysis

Amino acid sequence prediction based on translation of the longest ORF (open reading frame) of the mRNA sequence of ZmGRP5 yielded a protein of 187 amino acids with a mass of 17445.53 Daltons (Fig. 6). The protein sequence is notable for a high glycine content of 40.6%, and a high tyrosine content of 8.0% (Appendix 1). The high glycine content is indicative of its identity as a plant GRP. The high tyrosine content is a characteristic shared by several other characterized GRPs such as PvGRP1.8, in which the tyrosine is suggested to play a role in protein immobilization to the cell wall via the formation of isodityrosine covalent bonds (Ringli *et al.*, 2001a). Additionally, the presence of two cysteine residues suggest disulfide bond forming potential and possible covalent association of ZmGRP5 with other polypeptides in a multi-subunit protein complex.

Figure 6. Nucleotide sequence and translated ORF (open reading frame) of isolated cDNA clone coding for ZmGRP5. Note position of restriction enzyme sites SacI, BstXI, and NdeI used in subsequent cloning into pGEX-3T4 recombinant protein expression plasmids (Fig. 8, 9).


GTCCTACGTAGTCGAGGACTACCGCAAGAAATGGGGGTCAACAAGTCTGCAGTTCTGCTTGGTGTGGTTTTGGTC 75
M G V N K S A V L L G V V L V
SacI
TCAGTCCTTCTCGGCTTCCTGGACGTTGTGTACGCAAGGGAGCTCACTGAAGCCAATGGCTCTGGACTGAAGAAT 150
S V L L G F L D V V Y A R E L T E A N G S G L K N
AATGTGAAGCCTGCAGGAGAGCCTGGGCTCAAGGATGAGAAGTGGTTTGGTGGTAGATACAAGCATGGTGGAGGG 225
N V K P A G E P G L K D E K W F G G R Y K H G G G
TATGGAAACAACCAGCCCGGATACGGCGGCGGAGGAAACAGCCAACCTGGATACGGCGGCGGAGGAAACAGCCAG 300
Y G N N Q P G Y G G G G N S Q P G Y G G G G N S Q
BstXI
CCCGGATACGGTGGAGGATACAAGCGCCATCACCCTGGTGGCGGCTACGGGTCTGGACAAGGAGGGCCTGGATGT 375
P G Y G G G Y K R H H P G G G Y G S G Q G G P G C
GGATGTGGAGGAGGGTATGGAGGTGGCAATGGTAGTCCTGGGTACGGCGATGACAATGGTGGTGGCAGTGGCACT 450
G C G G G Y G G G N G S P G Y G D D N G G G S G T
GGCGGTGGAAATGGCAATGCTGGTGGGTACGGAGGAGGAGGAGGCGGCGGTTATGGAGGCGGCTACGGCAGTGGT 525
G G G N G N A G G Y G G G G G G Y G G G Y G S G
AGTGGTACAGCACCAGGAGGCGGATATCATGGCGGCGGTGGTGCACAACGCTACGCTGGGCAGAACTAGCAAGAA 600
S G T A P G G G Y H G G G A Q R Y A G Q N .
CAACCCCTTATGCTAGTTTATGTTAAATAAACGATCCATTGTTCATGTGACTGAGCAATTTAAGCAGTGAAGGAT 675
NdeI
CTTGACTCGTGTTATTTGTGTTACCATATGTATTGGTTGTTTTATGTTTAAGATGAATGTACACCGCTATTTGTA 750
TGTCGAACTCGTTGCATGGAGATGAAAAAAAAAAGGCACAAAAACATCAGCAAAAAAAAAAAAAAAA 816

Other amino acid residues worth noting are serine and threonine residues, which are potential targets for post-translational modifications such as phosphorylation and glycosylation. Serine and threonine residues as well as tyrosine residues are targets for phosphorylation, during which a hydroxyl group is replaced by a phosphate group. Prediction with NetPhos 2.0 (http://www.cbs.dtu.dk) suggests that phosphorylation is likely to occur at residues S127, S138, S164, T31, Y66, Y73, Y83, Y93, Y97, and Y130 (Appendix 2). Another form of post-translational modification, glycosylation, occurs via the addition of oligosaccharide side chains to targeted amino acid residues on the polypeptide backbone. Serine and threonine residues are target sites for O-linked glycosylation, but none of the residues in ZmGRP5 was predicted to be glycosylated based on mammalian (NetOGlyc 3.0-Appendix 3) or fungal (DictyOGlyc 1.1-Appendix 4) prediction matrices. Arginine residues within the context of the consensus sequence (N-X-S/T) are target sites for N-linked glycosylation. ZmGRP5 was predicted to have two potential N-linked glycosylation sites at amino acid positions N4 and N34 (NetNGlyc 1.0-Appendix5).

3.1.2 Protein Domains and Structural Predictions (Fig. 7)

ZmGRP5 contains a putative N-terminal signal peptide of 27 hydrophobic amino acids, which targets the protein into the secretory pathway of the plant cell according to the subcellular localization prediction program TargetP V1.0 (http://www.cbs.dtu.dk) (Appendix 6). The ZmGRP5 pre-protein is predicted to insert across the membrane of the ER (endoplasmic reticulum) from the site of translation at the ribosome (Emanuelsson

Figure 7.

A Amino acid sequence representation of ZmGRP5

B Diagramatic representation of putative domains within Z-mGRP5

Legend:

Signal Peptide: **MGVNKSAVLLGVVLVSVLLGFLDVVYA**

Region of homology to buffelgrass apomictic pistil GRP:
YARELTEANGSGLKNNVKPAGEPGLKDEKW

Glycine-rich region

Putative heme-binding domain: *YKRHPGC*

Tyrosine residues

Cysteine residues

A

MGVNKSAVLLGVVLVSVLLGFLDVVYAREL
TEANGSGLKNNVKPAGEPGLKDEKWFGGRY
KHGGGYGNNQPGYGGGGNSQPGYGGGGNSQ
PGYGGGYKRHKPGGGYGSGQGGPGCGCGGG
YGGGNGSPGYGDDNGGGSGTGGGNGNAGGY
GGGGGGGYGGGYGSGSGTAPGGGYHGGGGA
QRYAGQN

B

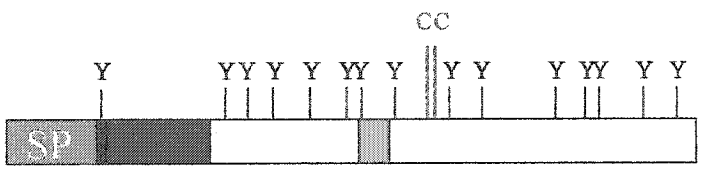

et al., 2000). The mature protein is predicted to be cleaved from the hydrophobic signal peptide between the amino acids A27 and R28, and to be released into the lumen of the ER (Nielsen *et al.*, 1997). The absence of ER anchoring sequences such as KDEL or HDEL in ZmGRP5 suggests that the mature protein is most likely transported out of the ER into the Golgi apparatus. The absence of Golgi, vesicle, or vacuole retention sequences would suggest that ZmGRP5 is ultimately secreted to the extracellular matrix. This is supported by protein target prediction using the PSORT prediction program (http://psort.ims.u-tokyo.ac.jp/) (Appendix 7), which suggests high probabilities of extracellular localization, but also high probabilities for vacuole targeting, as well as lower probabilities for peroxisome and plasma membrane targeting. The experimental verification of the actual subcellular target of ZmGRP5 would be a significant indicator of possible protein function.

The mature protein of 160 amino acids (14687.12 Daltons) has an even higher glycine content of 45.6% (Appendix 8). Protein structural prediction using the 'Protean' feature of the Lasergene Expert Sequence Analysis Software (DNAStar -Appendix 9) suggests that ZmGRP5 is arranged mainly in random turns and coils, and beta regions. The bulk of the mature protein, especially the glycine-rich regions, is expected to be hydrophilic and highly flexible, qualities that suggest that ZmGRP5 is a cell wall protein. The mature protein is also predicted to be highly antigenic, a quality that is especially relevant for the production of ZmGRP5 antibodies in this study.

Submission of the ZmGRP5 amino acid sequence to PROSITE (http://us.expasy.org/cgi-bin/scanprosite) uncovered the presence of two potential protein domains (Appendix 10). The profile of a glycine-rich domain typical of GRPs was found between amino acid position 35–179 of ZmGRP5. The glycine-rich domain found in ZmGRP5 can be subdivided into two distinct regions separated by the heme-binding domain. The higher order glycine-rich pattern of $N(N/S)QPGYG_4$ was found in three tandem repeats upstream from the heme-binding domain. The remaining downstream glycine-rich region is made up of mostly glycine residues interspersed with a few non-glycine residues in a highly random and variable fashion. The distinctions between the glycine-rich repeat patterns were noted in previously characterized GRPs such as PvGRP1.8, which is composed of 6 tandem repeats of the amino acid pattern $G_3AG_3QG_3AG_3YGQG_2EH$ in the middle region of the protein between the randomly patterned glycine-rich regions in the amino-terminal and carboxyl-terminal (Ringli, 2001a). The significance of glycine-rich repeat patterns on protein structure and function has not been well characterized to date, but is worthy of further investigation in this study.

A heme-binding domain signature, [FY]-[LIVMK]-x(2)-H-P-[GA]-G, was found at amino acid position 97–104 (YKrhHPGG). The signature sequence was derived from proteins of the cytochrome b5 family: membrane-bound hemoproteins that act as electron carriers for several membrane-bound oxygenases (Ozols, 1989). The presence of this signature sequence suggests a possible enzyme associated function in ZmGRP5. However, the accuracy of prediction of the heme-binding consensus pattern is

questionable, and the electron carrier feature has not been found in any GRPs characterized to date.

3.1.3 Protein Sequence Homology

A homology search was performed using the translated ZmGRP5 protein sequence against a non-redundant protein database using BLASTP-2.2.8 (Altschul *et al.*, 1997) (http://www.ncbi.nlm.nih.gov/BLAST/) (Appendix11). The above homology search yielded only one significant match with an E-value of 0.017: a GRP that is differentially expressed in the pistils of apomictic buffelgrass (*Pennisetum ciliare*) (Appendix12). The area of homology resided within amino acid position 26-55. The glycine-rich portion of the sequence did not show any homology. However, when the same sequence was submitted for homology search using FASTA3.4t21 (Pearson and Lipman., 1988) (http://www.ebi.ac.uk/fasta33/index.html) (Appendix 13), additional matches were found with a diverse group of other glycine-rich proteins including PvGRP1.8, HvGRP, BnGRP22, OsGRP1, OsGRP2, AtGRP5, PtGRP1, loricrin, keratin, and fluke eggshell protein. However, homology was limited to irregular stretches of glycine residues, and not to any specific motifs.

The apomictic GRP identified in the homology search was differentially expressed in the apomictic (asexual) pistils of buffelgrass, a warm season perennial forage grass widely cultivated throughout the semi-arid tropics (Vielle-Calzada *et al.*, 1996). Buffelgrass is a model plant especially noted for the study of reproduction by apomixis, an asexual

method of generating viable embryo without fertilization (Burson *et al.*, 1990). Apomixis within the grass family Poaceae is predominantly by apospory, a form of apomixis in which somatic, non-germinal cells in the ovule give rise to unreduced (diploid) female egg cells that give rise to embryos without fertilization. Buffelgrass reproduces mostly by obligate apospory, but rare sexual plants have been recovered.

The expression of the buffelgrass GRP in the apomictic pistils of asexual plants, but not in the pistils of sexual plants, suggested that the above protein is possibly implicated in functions related to asexual reproduction. However, the location of the protein within the apomictic pistil, ie., the stigma, the style, or the ovary is not known and the protein has not been characterized beyond the differential expression pattern of the cDNA. Therefore, reproductive functions could not be automatically assumed for the buffelgrass GRP, or by implication for ZmGRP5.

3.2 Antibody Production

Antibody based immunological methods such as immunoblotting, immunohistochemistry, and immunoprecipitation are commonly used in the characterization of protein function. It is the aim of this study to produce polyclonal antisera to localize native ZmGRP expression to specific cell-type(s) at the silk tissue level, and to the cell wall at the sub-cellular level.

3.2.1 Recombinant GST-ZmGRP5 Fusion Protein

Recombinant GST-ZmGRP5 fusion protein was produced and purified from *E. coli* transformed with protein expression plasmids. Both a truncated version (pB1) encoding amino acids 31-101 of ZmGRP5 and a long version (pN1) encoding amino acids 31-187 of ZmGRP5 were cloned in frame into the pGEX-4T3 downstream of the GST tag (Fig. 8 and 9). Only cDNA coding for the mature peptide was included in both constructs, with the N-terminal region encoding the signal peptide removed by digestion at the conveniently located SacI site (Fig. 6).

The truncated ZmGRP5 plasmid (pB1) included the region of homology to the apomictic buffelgrass GRP, as well as the portion of the glycine-rich region containing the glycine-rich triple tandem repeat of $N(N/S)QPGYG_4$. These regions were studied independently of the randomly repeated glycine-rich C-terminal contained in pN1 by digestion with the conveniently located BstXI restriction digest site. Additionally, the putative heme-binding domain was bisected by the restriction enzyme BstXI. This would also allow comparison with antisera produced against an intact heme-binding domain in the plasmid containing the long version of ZmGRP5 (pN1).

Nucleotide sequencing of the GST-ZmGRP5 cDNA insert junctions of the plasmids showed the fusion protein to be in frame at the DNA level. Production of recombinant fusion protein was attempted in *E. coli* cultures transformed with the pB1 and pN1 plasmids. SDS-PAGE followed by Coomassie Blue staining revealed the production of

Figure 8.

A Amino acid sequence representation of portion of GST-ZmGRP5 fusion plasmid: **pB1** (SacI/BstXI)

B Diagramatic representation of GST-ZmGRP5 fusion plasmid: **pB1** (SacI/BstXI)

Legend:

Schistostoma japonicum GST fusion protein tag

Region of homology to buffelgrass apomictic pistil GRP:
TEANGSGLKNNVKPAGEPGLKDEKW

Glycine-rich region:
FGGRYKHGGGYGNNQPGYGGGGNSQPGYGGGGNSQPGYGGG

Part of putative heme-binding domain: *YKRHH*

Y
|
Tyrosine residues

A

TEANGSGLKNNVKPAGEPGLKDEKWFGGRY
KHGGGYGNNQPGYGGGGNSQPGYGGGGNSQ
PGYGGGYKRHH

B

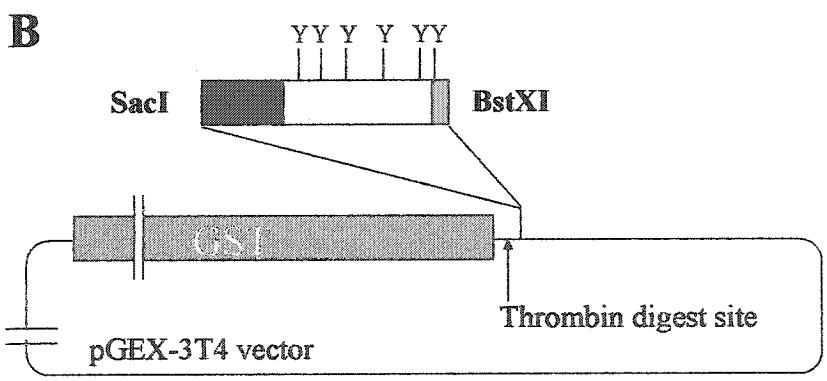

Figure 9.

A Sequence representation of GST-ZmGRP5 fusion plasmid: **pN1**(SacI/NdeI)

B Diagramatic representation of GST-ZmGRP5 fusion plasmid: **pN1**(SacI/NdeI)

Legend:

Schistostoma japonicum GST fusion protein tag

Region of homology to buffelgrass apomictic pistil GRP:
TEANGSGLKNNVKPAGEPGLKDEKW

Glycine-rich regions

Putative heme-binding domain: YKRHHPGG

Y Tyrosine residues

C Cysteine residues

A

TEANGSGLKNNVKPAGEPGLKDEKWFGGRY

KHGGGYGNNQPGYGGGGNSQPGYGGGGNSQ

PGYGGGYKRHHPGGGYGSGQGGPGCGCGGG

YGGGNGSPGYGDDNGGGSGTGGGNGNAGGY

GGGGGGGYGGGYGSGSGTAPGGGYHGGGGA

QRYAGQN

B

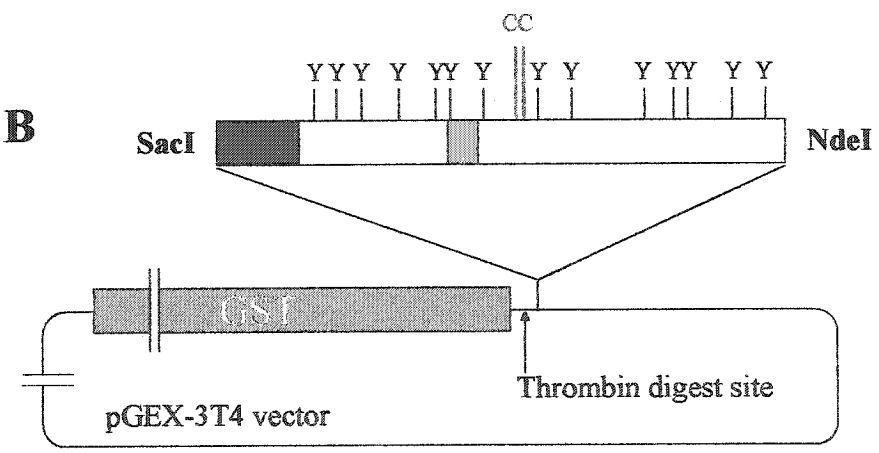

recombinant fusion protein only in pB1 but not in pN1 transformed *E. coli* extracts (Fig. 10A). An over-expressed 35.3 kD protein band corresponding to the GST-ZmGRP5 fusion protein encoded by pB1 (Appendix 14) was observed in the clarified bacterial sonicate. The same protein band was also successfully captured on the glutathione resin while other *E. coli* proteins were washed off in the flow-through. The purified GST-ZmGRP5 fusion protein from pB1 was eluted from the glutathione resin column and used in the subsequent immunization of rabbits.

In contrast, the fusion protein encoded by pN1 was not detected in the bacterial sonicate nor captured on the glutathione resin. The failure of expression of the full-length version of ZmGRP5, but not the truncated version, in *E. coli* may relate to the different sequences cloned. In addition to the larger coding region, the full-length version includes the 3' UTR (untranslated region) of ZmGRP5 which may affect expression. Additionally, the full-length version of ZmGRP5 could be unstable and subject to protease degradation in *E. coli*.

The clarified bacterial sonicate for the pGEX-3T4 vector control contained a highly over-expressed 27.8 kD protein band corresponding to the *Schistostoma japonicum* GST tag. The presence of the same band in the bacterial pellet fraction showed that the inclusion body solubilization step performed in this study was only partially effective, but enough protein was solubilized nonetheless in the clarified sonicate fraction for downstream purification steps.

Figure 10. Coomassie Blue stained SDS-PAGE. 10 μL of each protein sample was loaded in the presence of Laemmli Buffer (1:1 dilution).

A Preliminary verification of the production and purification of recombinant GST-ZmGRP5 fusion protein in *E. coli*.

1. Prestained Protein MW Marker (MBI #SM0431), 2. clarified sonicate (pB1), 3. resin captured fusion protein (pB1), 4. clarified sonicate (pN1), 5. resin captured fusion protein (pN1), 6. sonicate pellet (pGEX-3T4 GST control), 7. clarified sonicate (pGEX-3T4 GST control).

B Final verification of purified and eluted GST-zmGRP fusion protein.

1. GST-ZmGRP5 (pN1), 2. GST-ZmGRP5 (pB1), 3. Unstained Low Range SDS-PAGE Standards (BioRad #161-0304)

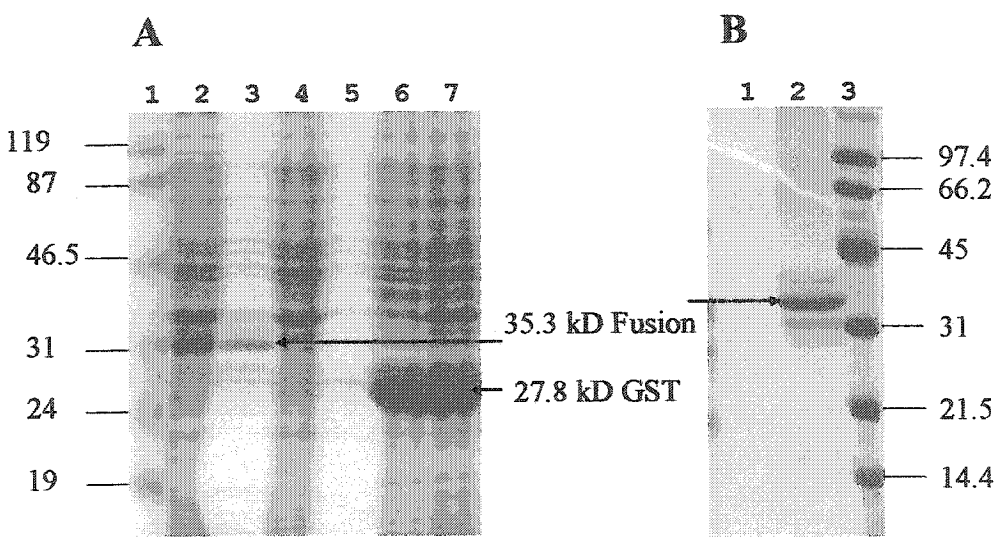
A
1 2 3 4 5 6 7
119
87
46.5
31
24
19
35.3 kD Fusion
27.8 kD GST
B
1 2 3
97.4
66.2
45
31
21.5
14.4

3.2.2 Confirmation of Identity of Purified GST-ZmGRP5

Gel slices containing the fusion protein band cut from Coomassie blue stained SDS-PAGE gels (Fig. 10B) were submitted to the Eastern Quebec Proteomics Centre at the University of Laval for protein sequence confirmation by LC-MS/MS (Liquid chromatography-mass spectrometry/mass spectrometry). The predicted mass and charge of individual peptides after trypsin digest (Appendix 15) of the fusion protein corresponded well to the actual LC-MS/MS data (Appendix 16). While amino acid sequences obtained from most of the trypsin-digested peptides corresponded to the GST tag portion of the fusion protein, 3 peptides (GSIPEFPTEANGSGLK, NNVKPAGEPGLK, and NNVKPAGEPGLKDEK) matched that of ZmGRP5. The amino acid stretch GSIPEFP was derived from the region of the fusion protein encoded by the multiple cloning sites between the GST tag and the ZmGRP5 insert. It is also noteworthy that the peptide NNVKPAGEPGLKDEK resulted from incomplete trypsin digest between the K and D residues.

The remaining region of the fusion protein encoding for ZmGRP5 was mostly composed of trypsin digested peptides of 6 amino acids or less and were thus too small in mass to be detected by MS (mass spectrometry) technology. The only predicted trypsin digested peptide of a significant mass that was not detected was a comparatively large peptide of 37 amino acids in the glycine-rich region (HGGGYGNNQ..QPGYGGGYK). This could possibly be attributed to the uncharged state of glycine residues, which dominate the composition of the above peptide. As the assignment of peptide identity using MS is

determined by the ratio of mass to charge, it was not surprising that the extremely low charged state of the above peptide could be beyond the limit of detection by MS technology.

In summary, the LC-MS/MS data confirmed to a high degree of certainty that the amino acids encoded by the truncated ZmGRP5 cDNA insert was in frame and was properly translated in the GST-ZmGRP5 fusion protein.

3.2.3 Confirmation of Identity of Thrombin Digested GST-ZmGRP5

In addition to the sequence confirmation of the GST-ZmGRP5 fusion protein, attempts were also made to isolate the truncated ZmGRP5 encoding portion of the fusion protein from Coomassie Blue stained SDS-PAGE gels for additional sequence confirmation by LC-MS/MS. Thrombin digestion of GST-ZmGRP5 was performed, in which the fusion protein was expected to be cleaved into a 26.2 kD GST tag component (Appendix 17) and a 9.1 kD protein band encoding for the truncated ZmGRP5 portion of the fusion protein (Appendix 18). On-column thrombin protease digest was followed by elution by PBS, whereupon the GST tag remains bound to the column while the cleaved truncated ZmGRP5 was eluted (Appendix 19). The resin bound GST tag was subsequently eluted with glutathione. Fractions collected from the thrombin digest elution and the glutathione elution were separated by SDS-PAGE and detected by Coomassie Blue staining.

The 9.1 kD protein band expected for the truncated ZmGRP5 in the thrombin digest elution was not detected in the Coomassie blue stained gel (Fig. 11). Instead, an unexpected protein band of approximately 14 kD was detected. The 14 kD protein band of questionable identity was also submitted for LC-MS/MS protein sequence analysis for clarification. LC-MS/MS detected four trypsin digest peptides with overlapping sequences matching a stretch of 32 amino acids near the C-terminal region of prothrombin (Appendix 20). The 14 kD protein band could thus be identified as a possible breakdown product resulting from the thrombin protease that was initially added to the column for cleavage of the fusion protein.

The failure to detect the 9.1 kD band was contrary to expected results. Thrombin digestion was shown to be complete, as the glutathione elution yielded only the 26.3 kD cleaved GST band, while no traces of the 35.3 kD GST-ZmGRP5 fusion protein band was detected. Therefore, there was no reason not to expect the detection of a 9.1 kD band corresponding to the cleaved ZmGRP5 portion of the fusion protein. The smallest band in the protein standard used in the gel was 14.4 kD, therefore no reference band in the size range of 9.1 kD was available to pinpoint the exact position of the cleaved ZmGRP5. However, the gel was run until the bromophenol blue tracking dye had migrated to the bottom edge of the gel. Bromophenol blue is expected to migrate just behind the chloride ion front at the bottom of the gel, and ahead of most protein molecules based on migration size. Therefore, it was highly unlikely for the 9.1 kD band to have run off the gel and other reasons must account for the failure to detect the band with Coomassie Blue staining.

Figure 11. Coomassie Blue stained SDS-PAGE analysis of thrombin protease digest of resin captured GST-ZmGRP5 fusion protein (pB1). 10 μL of each protein sample was loaded in the presence of Laemmli Buffer (1:1 dilution).

M: Unstained SDS-PAGE Standard, Low Range (BioRad); Thrombin digest elution #1, 2, 3, 4, 5; Glutathione elution #1, 2, 3, 4.

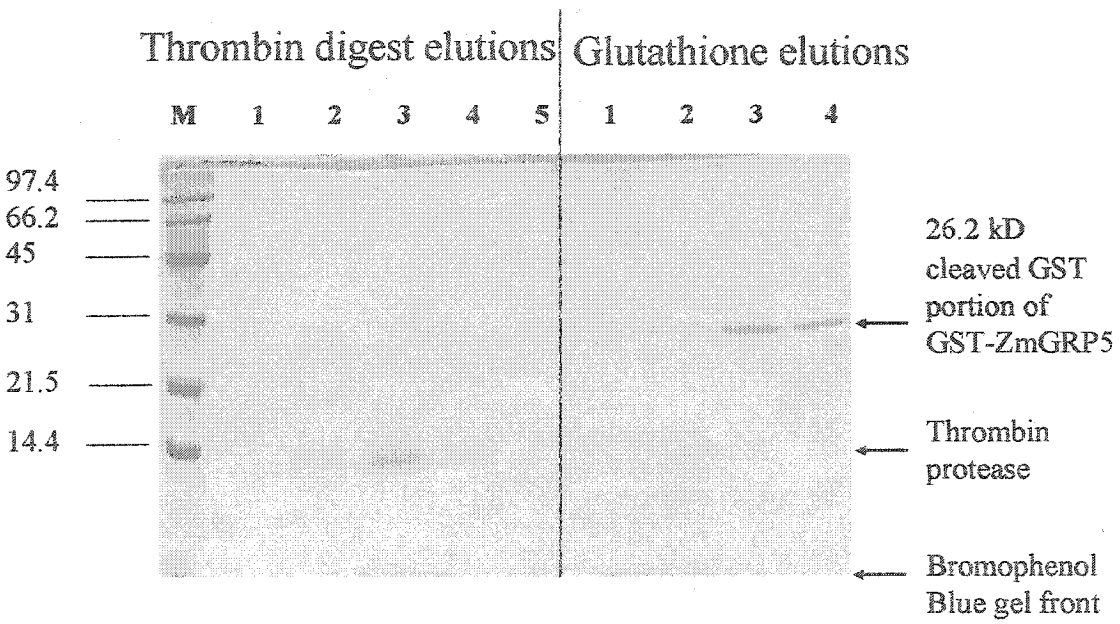
Thrombin digest elutions
Glutathione elutions
M
1
2
3
4
5
1
2
3
4
97.4
66.2
45
31
21.5
14.4
26.2 kD cleaved GST portion of GST-ZmGRP5
Thrombin protease
Bromophenol Blue gel front

A closer inspection of the methodology of Coomassie Blue staining revealed a highly likely explanation for the failure to detect the 9.1 kD band for the cleaved ZmGRP5 portion of the fusion protein. According to the website for Amersham Biosciences (http://www.electrophoresis.apbiotech.com/aptrix/upp00919.nsf/Content/Elpho_1D_Detection_Gel+Staining_2_Staining+gels+with+Coomassie+Brilliant+Blue), Coomassie blue staining of peptides smaller than 10 kD in SDS-PAGE gels must be preceded by fixation in glutaraldehyde to cross-link the peptides to the gel matrix. This extra fixation step prevents peptide diffusion out of the gel in the subsequent Coomassie blue staining steps. The methanol and acetic acid present in the Coomassie blue staining solution is not effective for fixing peptides below10 kD. As a result, the 9.1 kD band is highly likely to have diffused out of the gel during the Coomassie blue staining steps performed in this experiment.

In summary, additional LC-MS/MS sequence confirmation from the truncated ZmGRP5 encoding portion of the fusion protein was not possible in this study. The thrombin cleaved 9.1 kD truncated ZmGRP5 peptide was not detected by Coomassie blue stained SDS-PAGE and was likely to have diffused out of the gel matrix during the staining process. Given the positive protein sequence confirmation already obtained from the GST-ZmGRP5 fusion protein band, attempts were not made to repeat the isolation of the 9.1 kD cleaved ZmGRP5 peptide band. The extra glutaraldehyde fixation step necessary to cross-link the 9.1 kD band to the SDS-PAGE gel matrix was also not compatible with downstream trypsin digest and LC-MS/MS analysis.

3.2.4 Confirmation of Antiserum Specificity

Polyclonal antiserum was produced using rabbits immunized with the purified recombinant GST-ZmGRP5 fusion protein. The resulting antiserum was tested for specificity to the GST-ZmGRP5 immunogen (Fig. 12). Positive detection by the antiserum was observed with both the fusion protein (35.3 kD) and the truncated ZmGRP5 (9.1 kD) component after on-column thrombin digest and elution.

The antiserum did not react with the cleaved GST tag (26.2 kD) that remained immobilized on the resin column after thrombin digest and elution of ZmGRP5 with PBS. The antiserum also tested negative for the GST tag in the glutathione elution. However, a very weak signal was observable in the 9.1 kD region in the glutathione elution. This could be attributed to trace amounts of truncated ZmGRP5 (9.1 kD) that had escaped initial elution in PBS after thrombin digest. The trace amounts of truncated ZmGRP5 remaining in the resin had co-eluted with the GST tag in the glutathione elution.

In summary, the antiserum produced in this study was specific for the truncated ZmGRP5 portion of the fusion protein used in the immunization process, and not the GST tag portion. The antiserum could thus be assumed to be free of anti-GST antibodies. The antisera could be used directly in downstream immuno-detection experiments to characterize ZmGRP5 without further purification.

Figure 12. Immunoblot testing of rabbit antiserum specificity against recombinant GST-ZmGRP5 fusion protein. 10 μL of each protein sample was loaded in the presence of Laemmli Buffer (1:1 dilution).

A 1. Resin captured GST-ZmGRP fusion protein

2. Resin captured GST tag after thrombin digest and elution of ZmGRP5.

B 1. Thrombin digest elution #3, of Fig.11

2. Glutathione elution #3, of Fig.11

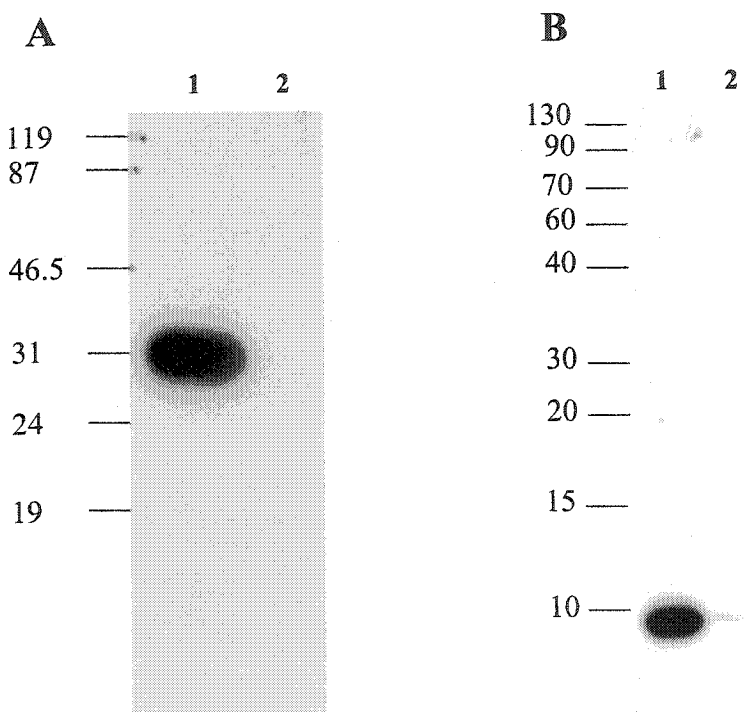
A
1
2
119
87
46.5
31
24
19
B
1
2
130
90
70
60
40
30
20
15
10

3.3 Characterization of Native ZmGRP5 from Maize Silk

3.3.1 ZmGRP5 is Silk Tissue Specific

ZmGRP5 had previously been shown to be silk tissue specific at the RNA level (Fig. 5). To test the tissue specificity of ZmGRP5 at the protein level, a panel of various maize tissues directly extracted with Laemmli Buffer was quantified. Aliquots each containing 20 μg of total protein of varying volumes were heated and directly loaded on SDS-PAGE without further dilution. Equal loading was confirmed by staining with Coomassie Brilliant Blue (results not shown). Duplicate gels were transferred and subjected to immunoblot analysis with the GST-ZmGRP5 antisera (Fig. 13A). The Laemmli Buffer component SDS unfolds protein secondary and tertiary structure by disrupting all non-covalent interactions, while the reducing agent ß-ME breaks disulfide bonds linking multi-protein complexes into monomeric subunits.

The rabbit antiserum produced against the recombinant GST-ZmGRP5 fusion protein reacted with only one detectable band of approximately 15 kD in the silk extract, close to the predicted mass of the mature ZmGRP5 monomer. The 15 kD band was not detected in any other tissue. Assuming the identity of the 15 kD band in silk is indeed ZmGRP5, the detection of this protein in silk tissue extract but not in any other tissue extracts supports the predicted silk tissue specificity of ZmGRP5.

Figure 13. Immunoblot analysis of maize tissue extracts separated by denaturing SDS-PAGE. All tissues were sampled at 0 dpe for silk development except for pollen, which was collected at anthesis. Differing volumes equivalent to 20 ug total protein was loaded for each tissue extract sample: 1. silk, 2. leaf, 3. pollen, 4. tassel, 5. husk, 6. cob, 7. seedling

A Probed with GST-ZmGRP5 antiserum,
1:5000 dilution

B Probed with anti-GST IgG (Sigma-Aldrich, #G7781),
1:500 dilution.

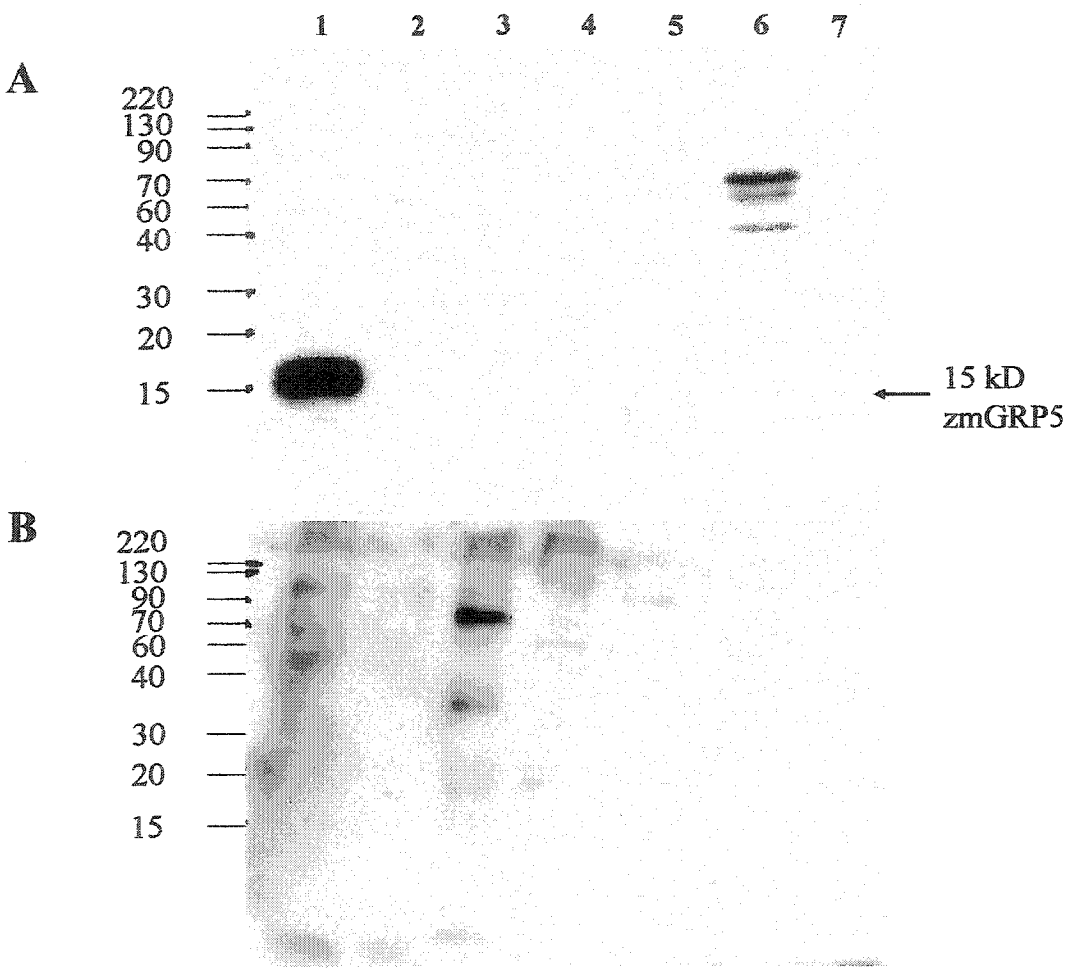
1
2
3
4
5
6
7
A
220
130
90
70
60
40
30
20
15
15 kD
zmGRP5
B
220
130
90
70
60
40
30
20
15

However, in maize cob tissue, bands of approximately 40, 60, and 70 kD were also detected. The identity of the higher molecular weight bands, and the possible reasons for their detection with this antiserum will be investigated further in the Discussion.

An identical blot probed with pre-immune antiserum detected no bands at all (results not shown), eliminating the possibility of the 15 kD band in silk tissue as an artifact band detected by pre-existing antibodies found in the rabbit serum prior to immunization. Purified anti-GST IgG (Immunoglobulin G, Sigma-Aldrich, #G7781) was also used to probe an identical maize tissue blot (Fig. 13B). The anti-GST was raised against GST immunogen from *Schistostoma japonicum*, the same source as the GST tag from the pGEX-3T4 vector. No band was detected in silk tissue extract at the 15 kD region with the anti-GST IgG, even at 1/500 dilution, at which background "noise" is observed on the blot. While previous antiserum characterization results suggested that the GST-ZmGRP5 antiserum did not contain an anti-GST component, the additional results using anti-GST IgG suggested that even if this assumption was false, the 15 kD band detected by the GST-ZmGRP5 antiserum was not a cross-reacting native maize GST.

The identities of the approximately 70 kD and 35 kD protein bands that were detected in pollen extract by the anti-GST in this study (Fig. 13B) are uncertain, but did not appear to be native maize GST. In maize, native zmGST had been characterized to 42 isoforms in the Genebank protein database, all of which were found as homo- or hetero-dimers composed of monomers of 25 to 27 kD (Jepson *et al.*, 1994). This does not seem to match the band size detected in pollen by anti-GST.

In summary, the antisera against the recombinant GST-ZmGRP5 fusion reacted with only one detectable band of approximately 15 kD in maize silk extract. The identity of the band was highly likely to be that of ZmGRP5 based on molecular weight prediction. In addition, the band was not detected with pre-immune antiserum or purified anti-GST. These results suggested that the band was specific to the anti-ZmGRP5 component of the antiserum and was not an artifact band cross-reacting to other antibodies in the antiserum. Therefore, the silk tissue specificity of ZmGRP5 could be reasonably confirmed at the protein level, as the 15 kD band was detected only in silk tissue extract and not in any other tissue extracts.

3.3.2 ZmGRP5 is a Cell Wall Protein

An extracellular localization of ZmGRP5 was predicted based on the presence of an N-terminal secretory signal peptide and the absence of any ER or Golgi anchoring sequences. This study attempted to confirm this extracellular localization, in particular the cell wall matrix, using three different cell wall fractionation methods.

3.3.2.1 Crude Cell Wall Fractionation

ZmGRP4 was previously characterized to be an extracellular matrix protein found in the root cap mucilage of maize (Matsuyama *et al.*, 1999) using both immunoblotting and immunocytochemistry methods. For the immunoblot, a crude cell wall fractionation

method was used in which powdered root caps were extracted with an aqueous buffer and centrifuged into a crude cell wall pellet and a crude aqueous cytosolic fraction. The crude cell wall pellet was re-extracted with an SDS based buffer, re-centrifuged, and the SDS-soluble supernatant was removed and referred to as the cell wall extract (Fig. 14A).

Given the similarities of ZmGRP4 to ZmGRP5 in terms of glycine content and presence of signal peptides, this method was applied directly without any modifications to the cell wall fractionation and SDS extraction of silk tissue samples in this study. Crude fractionated extracts were separated by SDS-PAGE and subjected to immunoblot analysis using the GST-ZmGRP5 antiserum (Fig. 14).

A protein band of approximately 15 kD corresponding to the predicted molecular weight of the ZmGRP5 mature protein was detected in the SDS-soluble cell wall fraction, but not in the aqueous cytosolic fraction of maize silk protein extracts. This experimental result supported the predicted cell wall localization of ZmGRP5. In addition, ZmGRP5 was shown to be extractable by the ionic detergent SDS from the cell wall matrix. The crude cell wall fractionation method, however, could not guarantee a cell wall pellet fraction free from contaminants such as chloroplasts, mitochondria, nuclei, and possibly vacuoles and plasma membrane. As a result, cell wall localization for ZmGRP5 could not be proven with certainty.

Figure 14. Crude centrifugation fractionation of silk tissue extracts. Silk was sampled at developmental stage of 0 dpe.

A. Schematic representation of crude cell wall fractionation

B. Immunoblot analysis of crude centrifugation fractionated silk tissue extracts with GST-ZmGRP5 antiserum. 10 µL of each protein sample was loaded in the presence of Laemmli Buffer (1:1 dilution).

1. Cell Wall fraction extracted with Matsuyama SDS Buffer
2. Cytosolic fraction extracted with Matsuyama Aqueous Buffer

A

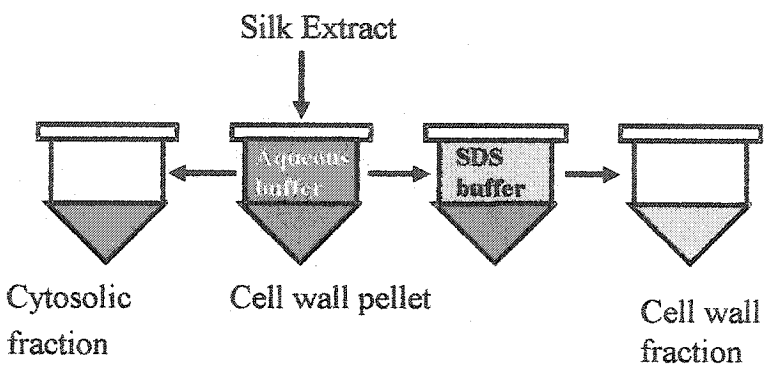
Silk Extract
Aqueous buffer
SDS buffer
Cytosolic fraction
Cell wall pellet
Cell wall fraction

B

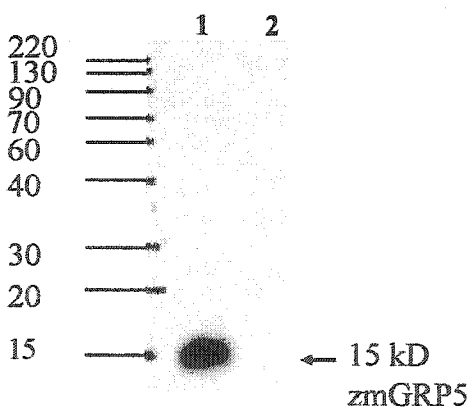
1
2
220
130
90
70
60
40
30
20
15
15 kD
zmGRP5

3.3.2.2 Cell Wall Fractionation with Sucrose Cushion

Cell wall fractionation was repeated using methods that better separate the sub-cellular components with greater certainty. Centrifugation of aqueous silk extract over a sucrose cushion (Ringli *et al.*, 2001a) was used for improved separation of cell wall from other cellular components, especially plasma membranes (Fig. 15). The impact of salts and different detergents on the extractability of the target protein was also investigated, using sequential extraction of the cell wall fraction with buffers containing progressively more solubilizing reagents (modified from Robertson *et al.*, 1997). Namely, the sucrose cushion fractionated cell wall pellet was recovered and divided into two samples. The first sample was sequentially extracted with 1 M NaCl Buffer, SDS Buffer, and then Laemmli Buffer. The second sample was sequentially extracted with Triton Buffer, SDS Buffer, and then Laemmli Buffer. After the sequential addition of each buffer, centrifugation was used to separate the cell wall pellet from the supernatant. The supernatant was removed and the cell wall pellet was re-extracted with the next buffer. The microtubes containing the cell wall pellets in the final Laemmli Buffer were directly heated at 95 °C without centrifugation for direct separation by SDS-PAGE.

Immunoblot analysis was performed on the sequential extracts (Fig. 16). As expected, the target ZmGRP5 protein band of 15kD was not detected in the aqueous cytosolic fraction. Extraction of the cell wall pellet with Triton Buffer did not yield the target band, suggesting that ZmGRP5 could not be extracted with a purely non-ionic detergent such as Triton X-100. Extraction of the cell wall pellet with 1 M NaCl Buffer also did not yield

Figure 15. Schematic representation of cell wall fractionation using a sucrose cushion followed by serial extraction of cell wall with buffers containing different detergents and salt concentrations. #1, #5: Aqueous Buffer. #2: 1M NaCl Buffer. #3,#7: SDS Buffer. #4, #8: Laemmli Buffer. #6: Triton Buffer.

CW. Cell Wall

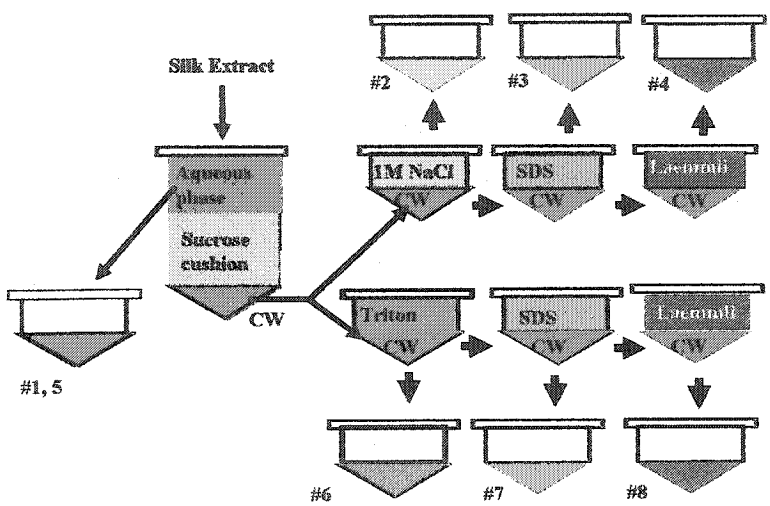
Silk Extract
Aqueous phase
Sucrose cushion
CW
#1, 5
1M NaCl
CW
SDS
CW
Lacunah
CW
#2
#3
#4
Triton
CW
SDS
CW
Lacunah
CW
#6
#7
#8

Figure 16. Immunoblot analysis of sucrose cushion fractionated silk tissue extracts with GST-ZmGRP5 antiserum. Silk was sampled at developmental stage of 0 dpe. 10 µL of each protein sample was loaded in the presence of Laemmli Buffer (1:1 dilution). 10 µL of samples directly extracted in Laemmli Buffer was loaded without further dilution.

1. Aqueous Buffer, 2. 1 M NaCl Buffer, 3. SDS Buffer, 4. Laemmli Buffer,

5. Aqueous Buffer, 6. Triton Buffer, 7. SDS Buffer, 8. Laemmli Buffer

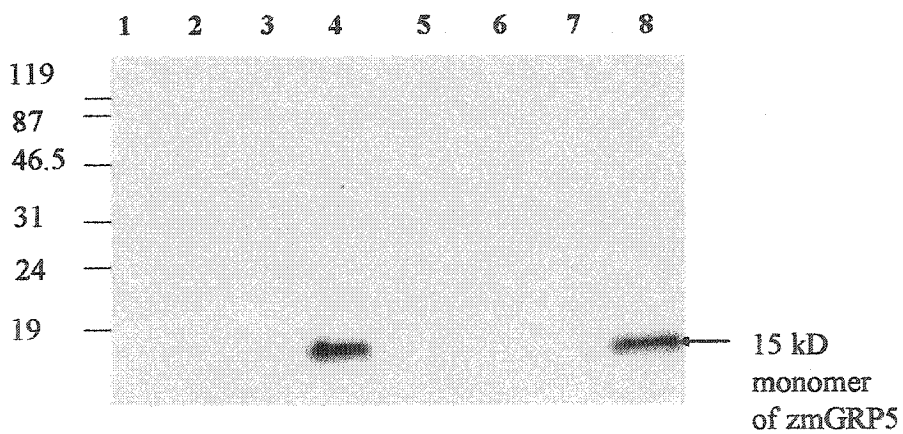
1 2 3 4 5 6 7 8
119
87
46.5
31
24
19
15 kD
monomer
of zmGRP5

the target 15 kD band, suggesting that ZmGRP5 could not be dissociated from the cell wall by disruption of ionic bonds under high salt conditions.

SDS, an ionic detergent, had previously been used to successfully extract the 15 kD target band from silk cell wall fractions (Fig. 14B). Additionally, SDS had also been widely used in extracting other GRPs such as ZmGRP4 (Matsuyama, *et al.*, 1999) from plant cell walls and extracellular matrices. However, in this particular experiment, no target band was detected in the SDS cell wall extract, while subsequent sequential extraction with Laemmli Buffer yielded a strong 15 kD band as expected. This result indicated that the target protein was present in the cell wall pellet, but was not extracted by the SDS buffer in this particular experiment. The observed change in extractability of ZmGRP5 by SDS buffer could possibly be attributed to interference from components in the Triton buffer and 1 M NaCl buffer that were used in the sequential serial extraction method in this experiment before SDS buffer was introduced. This was investigated further in downstream experiments.

In summary, the detection of the 15 kD target band in the cell wall pellet after extensive washing and sequential extraction with different buffers confirmed the predicted cell wall localization of ZmGRP5. The use of a sucrose cushion in this particular fractionation experiment was an improvement upon the crude cell wall pellet fractionated in previous extractions. The interphase directly on top of the sucrose cushion, thought to contain the plasma membrane by Ringli et al. (2001), was removed and was not included in either the aqueous cytosolic fraction or the cell wall pellet at the bottom of the tube. However, the

high gravitational force used during ultracentrifugation and a pale greenish colour in the pellet suggested that chloroplasts and possibly other organelles were still present in the pellet and better cell wall fractionation methods were still necessary to definitively show the cell wall localization of ZmGRP5.

3.3.2.3 Cell Wall Fractionation using Miracloth Filtration

Cell wall fractionation was further improved upon by using an extraction method adapted from the isolation of the cell wall expansin from cucumber seedlings (McQueen-Mason *et al.*, 1992) that employs Miracloth (Calbiochem), a rayon polyester mesh with an acrylic binder used to filter the cell wall fraction from the total silk tissue extract. Miracloth was originally designed for protoplast isolation. With a pore size of 22-25 μm, filtration with Miracloth should result in a more complete removal of organelles as well as intact protoplasts, which should filter through the Miracloth filter along with the aqueous soluble cytosolic fraction. The cell wall debris fraction that is retained by the Miracloth filter was washed and re-filtered to remove any remaining soluble components. Cell walls were recovered and divided into separate aliquots, each treated with a different extraction buffer (Fig. 17). The impact of salts and different detergents on the extractability of the target protein was re-examined, and extraction buffers were designed to ensure compatibility with buffers used with downstream IP (immunoprecipitation) experiments (**3.3.6**).

Figure 17. Schematic representation of cell wall fractionation using Miracloth filters followed by extraction of cell wall with immunoprecipitation compatible buffers at room temperature. Each cell wall pellet following extraction with original buffers was divided into two samples and subjected to re-extraction with Laemmli Buffer.

CW. Cell Wall

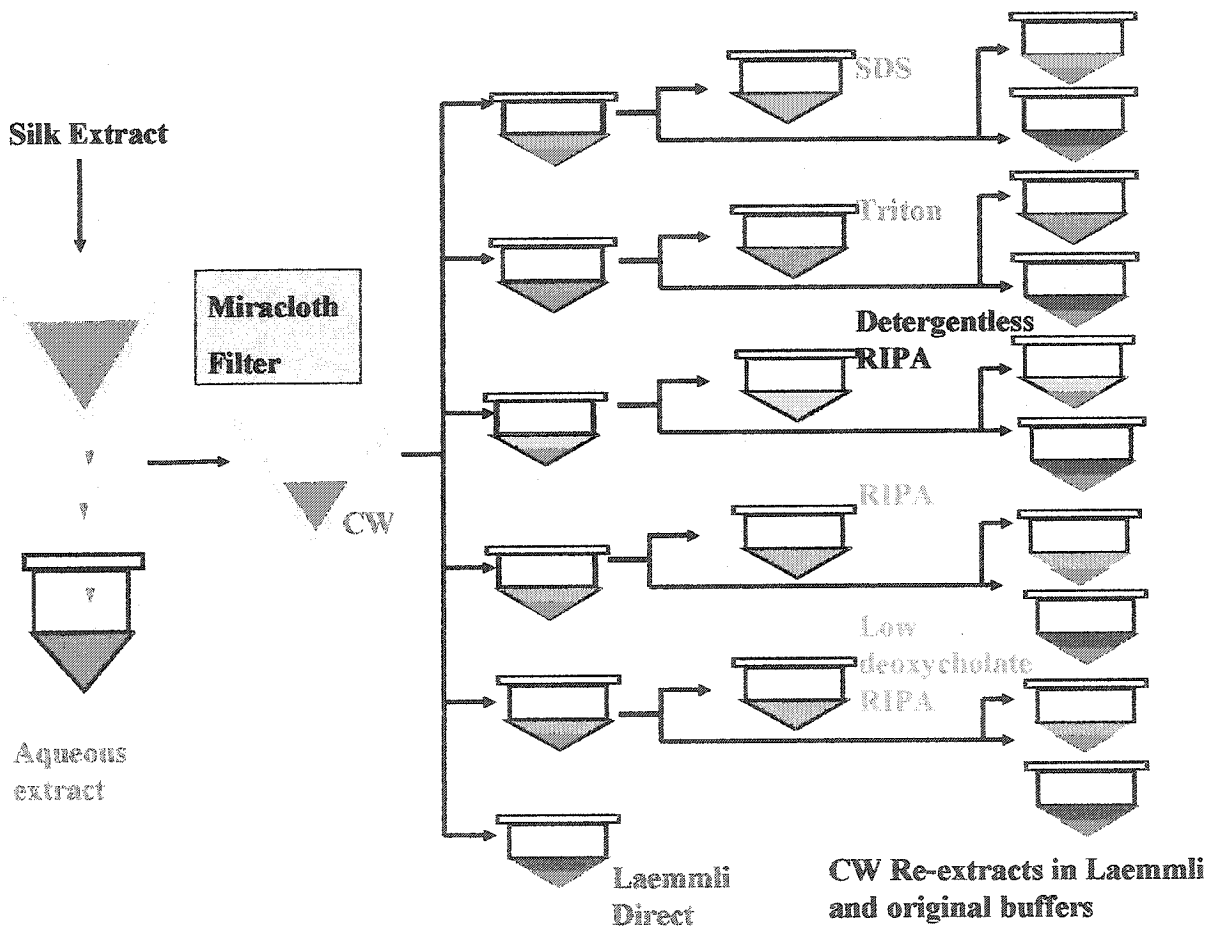
Silk Extract
Miracloth Filter
CW
Aqueous extract
SDS
Triton
Detergentless RIPA
RIPA
Low deoxycholate RIPA
Laemmli Direct
CW Re-extracts in Laemmli and original buffers

Immunoblot analysis revealed that the target 15 kD ZmGRP5 protein band was in the cell wall fraction, and not present in the cytosolic Aqueous Buffer fraction. However, the target protein was only extracted from the cell wall directly with Laemmli Buffer, but not with SDS Buffer, Triton Buffer, Detergentless RIPA Buffer, RIPA Buffer, or Low deoxycholate RIPA Buffer (Fig. 18A). While the latter four buffers were not expected to solubilize ZmGRP5 from the cell wall given the lack of or low concentration of SDS, the failure of SDS buffer to extract the target protein was contradictory to the experimental results previously observed with the crude cell wall fraction (Fig. 14B). Additionally, because the cell wall fractions were divided and extracted directly with the respective buffers, the failure once again of SDS buffer to extract ZmGRP5 from the cell wall could not be attributed to possible interference from Triton and other buffer components during sequential extraction strategies such as was suggested for the sucrose cushion fractioned cell wall samples (Fig. 16).

Portions of the cell wall samples that were previously extracted with SDS Buffer, Triton Buffer, Detergentless RIPA Buffer, RIPA Buffer, and Low Deoxycholate RIPA Buffer were re-extracted with Laemmli Buffer. The microtubes containing the cell wall pellets and added Laemmli Buffer were directly heated at 95 °C without centrifugation for direct separation by SDS-PAGE. Immunoblot analysis revealed the presence of the target 15 kD band in all the cell wall samples. This confirmed that the negative results from the original buffer extracts could be attributed to a failure of extraction rather than the absence of the target protein in the cell wall samples (Fig. 18B).

Figure 18. Immunoblot analysis of Miracloth fractionated silk tissue extracts with GST-ZmGRP5 antiserum. Silk was sampled at developmental stage of 0 dpe. 10 μL of each protein sample was loaded in the presence of Laemmli Buffer (1:1 dilution). 10 μL of samples directly extracted in Laemmli Buffer was loaded without further dilution.

A. Original extraction at room temperature: *A* (Aqueous Buffer), *W* (Wash), #1 (SDS Buffer), #2 (Triton Buffer), #3 (Detergentless RIPA Buffer), #4 (RIPA Buffer), #5 (Low Deoxycholate RIPA Buffer), *D* (Direct extraction in Laemmli Buffer).

B. Re-extraction of cell wall pellets from A with Laemmli Buffer: #1, 2, 3, 4, 5.

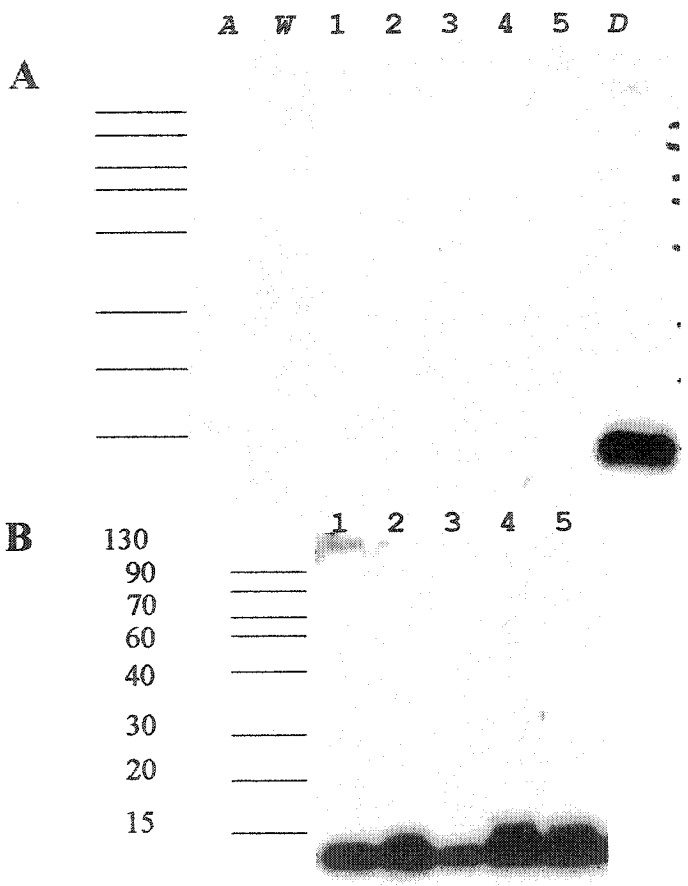
A
A W 1 2 3 4 5 D
B
130
90
70
60
40
30
20
15
1 2 3 4 5

In summary, the predicted cell wall localization of ZmGRP5 was confirmed by all three cell wall fractionation methods: crude centrifugation, centrifugation with sucrose cushion, and Miracloth filtration. In the last method, the Miracloth pore size of 22-25 μm insures the filtration of intact protoplasts and organelles, as well as structures associated with the secretory pathway such as the ER, Golgi, vacuole, vesicles, and plasma membrane, while the cell wall matrix was retained. The target 15 kD band was not soluble in the various aqueous buffers used, and remains bound to the cell wall fraction using all three methods. However, ZmGRP5 from the crude cell wall fraction was extracted with SDS buffer, while ZmGRP5 remained immobilized in the cell walls isolated using the sucrose cushion and Miracloth filtration methods.

3.3.3 Extractability of ZmGRP5 from the Cell Wall

3.3.3.1 Effect of pH

Variability in the extraction of ZmGRP5 from the cell wall preparations was observed in the previous experiments with buffers containing the ionic detergent SDS. Assuming the starting silk tissue material had not changed during the intervening storage time at –80 °C between the different experiments, the difference in pH between the Matsuyama SDS buffer (pH 6.8) used in the crude cell wall fractionation method and the SDS buffer (pH 8.0) used in the sucrose cushion and Miracloth filtration cell wall fractionation methods could be a possible reason for variation in extraction of ZmGRP5.

SDS buffer (pH 8.0) had been used to extract ZmGRP5 from cell walls fractionated with the sucrose cushion and Miracloth filtration methods with downstream IP experiment compatibility in mind. However, a closer examination of literature pertaining to extraction of protein from cell walls suggested that a more acidic extraction buffer would more closely match native cell wall conditions. Cell walls in plant tissues that are actively undergoing extensive growth by cellular elongation have been observed to exhibit a phenomenon called "acid-growth" (Rayle and Cleland., 1992). Cell wall fibre cross-links are disrupted by acidic conditions induced in growing tissue at pH values lower than 5.5, allowing "slippage" of the fibres and elongation by extension of the cell wall (Cosgrove, 2001). It is reasonable to predict that the cell walls of maize silk would also be acidic given the rapid growth via cell elongation associated with silk emergence (Bassetti and Westgate, 1993a).

The pH 5.5 Citrate Buffer containing 1% SDS had been used successfully to extract PvGRP1.8 from the cell walls of etiolating French bean hypocotyls (Ringli *et al.*, 2001a). The pH 4.6 Acetate Buffer was used to extract beta-expansin from the extracellular matrix of maize pollen (Li *et al.*, 2003) and alpha-expansin from the cell walls of cucumber seedlings (McQueen-Mason *et al.*, 1992). In this experiment (Fig. 19), the above two buffers was included in the attempt to extract ZmGRP5 from silk tissue in the presence of 1% SDS. Tris buffers at pH 4.6, 5.5, 6.8, and 8.0, all containing1% SDS, were also used in comparison. In addition, Laemmli buffers, both reducing and non-reducing, were also included as extraction buffers, not only as positive controls for ZmGRP5 solubilization, but also because both are SDS-based Tris buffers at pH 6.8.

Figure 19. Schematic representation of the investigation of silk tissue extractability. Powdered silk tissue was extracted with buffers differing in pH and reducing agent content. All silk tisssue extractions were conducted in duplicate (not shown) with heating (95 °C), and without (4 °C). Each cell wall pellet following extraction with original buffer was subjected to re-extraction with Laemmli buffer.

CW. Cell Wall

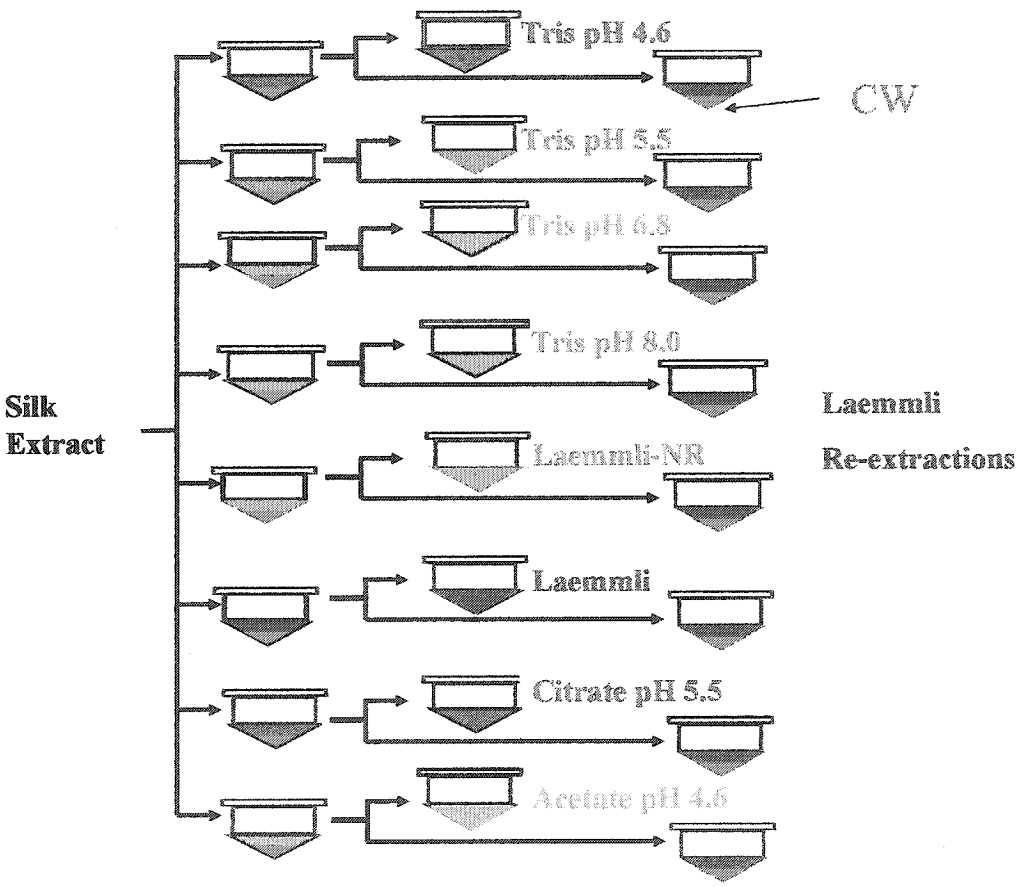
Tris pH 4.6
CW
Tris pH 5.5
Tris pH 6.8
Tris pH 8.0
Silk
Extract
Laemmli
Re-extractions
Laemmli-NR
Laemmli
Citrate pH 5.5
Acetate pH 4.6

Interestingly, with the exception of the pH 8.0 Tris Buffer, aliquots of silk extracts from all other buffers spotted on colorpHast Indicator Strips pH 0-14 (EM Science) exhibited an acidic pH in the range of pH 4-5 (results not shown). Only the pH 8.0 Tris Buffer maintained buffering capacity after silk tissue extraction. Given that Tris has a pKa of 8.1 at 25 °C (Sigma-Aldrich Canada, 2002-2003, p.2034), it is not surprising that the other Tris 'buffers' did not maintain buffering capacity. The pH of the silk extracts is also a good indicator that rapidly elongating silk tissue is naturally acidic, although differentiation between cytosolic versus cell wall pH could not be deduced.

Immunoblot analysis of the silk tissue extracts revealed no difference between the above buffers. All buffers failed to extract ZmGRP5, except in the case of the Laemmli buffer extract, where the 15 kD band was once again detected (Fig. 20A). Re-extraction of all cell wall samples with Laemmli buffer once again proved the presence of the ZmGRP5 target in the samples that initially failed to be extracted by the buffers of the pH series (Fig. 20B). The experimental results seemed to suggest that pH was not a factor in the extractability of ZmGRP5. The positive extraction results observed with Laemmli buffer must have been dependant on some other property of the buffer besides pH.

3.3.3.2 Effect of the reducing agent ß-ME

Laemmli Buffer had consistently extracted the 15 kD protein band in all experiments attempted. This particular experiment attempted to identify the exact buffer components responsible. The most likely candidate is the reducing agent ß-ME, which was not found

Figure 20. Immunoblot analysis of the re-extraction of cell wall pellets with Laemmli Buffer. Blots are probed with GST-ZmGRP5 antiserum. Silk was sampled at developmental stage of 0 dpe. 10 µL of each protein sample was loaded in the presence of Laemmli Buffer (1:1 dilution). 10 µL of samples directly extracted in Laemmli Buffer (#5, #6) was loaded without further dilution. ß-ME was added to extract #5 (10% final concentration) before separating on SDS-PAGE.

A Extraction with following buffers at 4 °C, 30 minutes: #1 (Tris, pH 4.6), #2 (Tris, pH 5.5), #3 (Tris, p H6.8), #4 (Tris, pH 8.0), #5 (Laemmli Buffer-NR), #6 (Laemmli Buffer), #7 (citrate, pH 5.5), #8 (acetate, pH 4.6).

B Re-extraction with Laemmli buffer at 95 °C, 15 minutes of the cell wall pellets previously extracted with the following original buffers: #1 (Tris, pH 4.6), #2 (Tris, pH 5.5), #3 (Tris, pH 6.8), #4 (Tris, pH 8.0), #5 (Laemmli Buffer-NR), #6 (Laemmli Buffer), #7 (citrate, pH 5.5), #8 (acetate, pH 4.6)

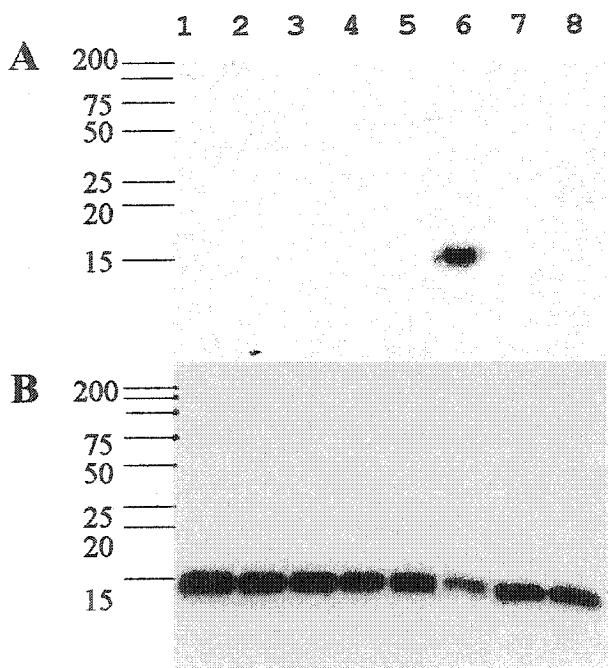
1 2 3 4 5 6 7 8
A
200
75
50
25
20
15
B
200
75
50
25
20
15

in any other buffers used in the previous experiments. Silk tissue extraction was compared between Laemmli Buffer and Laemmli-NR (Non-Reducing) Buffer, which had identical buffer components with the exception of the absence of any ß-ME in the Laemmli-NR Buffer.

Immunoblot analysis revealed that the 15 kD band was once again detected in the Laemmli Buffer control extract. Laemmli-NR Buffer failed to exhibit the presence of the 15 kD band (Fig 20A), which suggested that the presence or absence of a reducing agent such as ß-ME was the determining factor in the extraction of ZmGRP5.

Cell wall pellets from the above extractions were subjected to re-extraction with Laemmli Buffer. Immunoblot analysis revealed the detection of the 15 kD band in all cell wall samples that had previously tested negative with their original buffers (Fig. 20B). Interestingly, the re-extraction sample obtained from the cell wall that was also originally extracted with Laemmli Buffer (#6) exhibited a lower band intensity compared to the re-extracted samples obtained from cell walls that had been originally extracted with other buffers. This result was consistent with the depletion of ZmGRP5 from the cell wall by the first round of extraction with Laemmli Buffer, while the remaining samples had not lost any ZmGRP5 from the cell wall during the first round of extraction with their respective original buffers.

3.3.3.3 Effect of Heat

Previous studies have shown that a soybean seed coat aleurone layer GRP was extracted with hot water (Matsui *et al.*, 1994). It is possible that heat would also play a role in the solubilization of ZmGRP5 from the cell wall. All buffer extractions from above experiments were performed in duplicate, one at 4 °C, and the other at 95 °C. All buffer extracts (supernatants) were transferred to new microfuge tubes after centrifugation and separated from the cell wall pellets, including samples extracted with Laemmli buffer. Immunoblot analysis results detected a stronger signal for the 15 kD band from the heated Laemmli extract compared to the unheated Laemmli extract (Fig. 21). All other buffer extracts remained negative for ZmGRP5 with or without heat treatment. These results appeared to suggest heat to be only a minor contributing factor, but not the determining factor, in the extractability of ZmGRP5 from maize silk tissue. This is not surprising, considering that the role of heat in denaturing SDS-PAGE is to speed the disruption of non-covalent bonds by SDS by increasing molecular kinetics (http//:www.ruf.rice.edu/~bioslabs/studies/sds-page/denature.html). Similarly, the thiol reduction of disulfide bonds by ß-ME is not dependent on heat itself.

In summary, pH was not a factor in the extractability of ZmGRP5 from maize silk cell walls in this particular experiment. The presence or absence of the reducing agent ß-ME appeared to be the determining factor in terms of ZmGRP5 extractability. Heating increases the yield of ZmGRP5 in Laemmli Buffer extracts, but did not alter the differences in extractability observed between the different buffers. The previously

Figure 21. Immunoblot analysis of the impact of reducing agent, pH, and heat on the extraction of native ZmGRP5 from maize silk tissue with SDS based buffers. Silk was sampled at developmental stage of 0 dpe. Blots are probed with GST-ZmGRP5 antiserum. 10 µL of each protein sample was loaded in the presence of Laemmli Buffer (1:1 dilution). 10 µL of samples directly extracted in Laemmli Buffer (#6) was loaded without further dilution. 10% final ß-ME was added to the Laemmli-NR extract (#5) before separating on SDS-PAGE.

A Extraction at 4 °C, 30 minutes with following buffers (same silk extracts as used for Fig. 20A): #1 (Tris, pH 4.6), #2 (Tris, pH 5.5), #3 (Tris, pH 6.8), #4 (Tris, pH 8.0), #5 (Laemmli-NR), #6 (Laemmli), #7 (citrate, pH 5.5), #8 (acetate, pH 4.6)

B Extraction at 95 °C, 15 minutes with following buffers: #1 (Tris, pH 4.6), #2 (Tris, pH 5.5), #3 (Tris, pH 6.8), #4 (Tris, pH 8.0), #5 (Laemmli-NR), #6 (Laemmli), #7 (citrate, pH 5.5), #8 (acetate, pH 4.6)

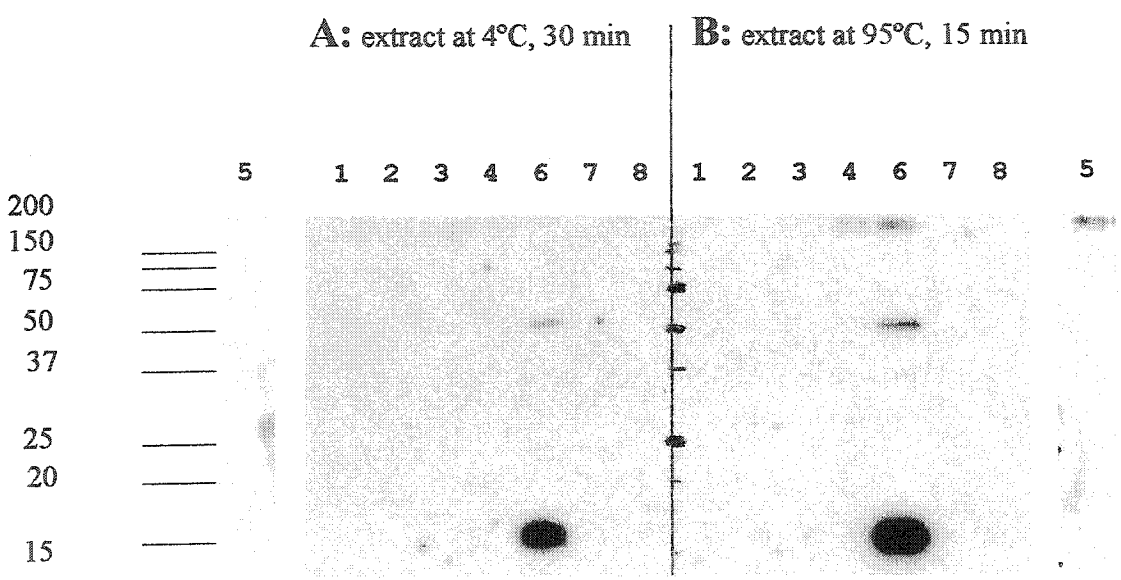
A: extract at 4°C, 30 min
B: extract at 95°C, 15 min
5
1
2
3
4
6
7
8
1
2
3
4
6
7
8
5
200
150
75
50
37
25
20
15

observed extractability of ZmGRP5 with Matsuyama SDS Buffer was not duplicated with any of the buffers. The possible reasons for such changes in extractability with SDS will be examined in the Discussion section.

3.3.4 Two Dimensional SDS-PAGE

2D SDS-PAGE involves the separation of protein mixtures based on charge using IEF (isoelectric focusing) in the horizontal dimension followed by separation based on mass in the vertical dimension using conventional SDS-PAGE. The resulting separation of proteins over a greater gel surface area allows for an increase in the resolution of individual protein spots. The increased resolution has the potential to separate isoforms of the native ZmGRP5 that could exist due to post-translational modifications provided that they result in differences in mass and/or charge that would not be resolved by standard SDS-PAGE. In addition, the increased protein spot resolution of 2D SDS-PAGE could also be exploited to isolate the native ZmGRP5 protein for amino acid sequence confirmation.

Proteins extracted with 2D SDS-PAGE compatible Rehydration Buffer were passively diffused into IPG (immobilized pH gradient) strips. IEF was then performed to separate the proteins by the application of an electric field through a medium with a pH gradient. The IPG strips were then equilibrated in DTT Equilibration Buffer to disrupt disulfide bonds, followed by Iodoacetamide Equilibration Buffer, which alkylates the reduced cysteines to prevent reshuffling of disulfide bonds. Both buffers contain SDS to coat the

proteins for standard separation by mass using second-dimension SDS-PAGE (analogous to boiling samples in Laemmli Buffer prior to standard SDS-PAGE, see Bio-Rad Laboratories Bulletin #2651). The equilibrated IPG strips are embedded on top of the second-dimension SDS-PAGE gel and separated by SDS-PAGE.

3.3.4.1 Post-translational Modifications

Sixty five milligram of frozen silk tissue was extracted with 250 µL Rehydration Buffer. 150 µg of total silk tissue proteins was separated by 2D SDS-PAGE and subjected to immunoblot analysis with the GST-ZmGRP antiserum. Several protein spots were detected in the region of the blot corresponding to the predicted mass of 14.7 kD and pI of 8.71 (Fig. 22B). The detection of more than one protein spot suggests that post-translational modifications of the protein have occured, which would create ZmGRP5 isoforms of varying mass and charge. Three of these spots *(x1, x2, x3)* appear to be of identical mass, but of slightly varying pI. All three putative isoforms of ZmGRP5 would have appeared as a single protein band in standard SDS-PAGE. Additionally, a fourth protein spot *(x4)* had a slightly higher mass as well as higher pI. The differences in mass between *x4* and the other spots *(x1, x2, x3)* was also too slight to be detected as separate protein bands in immunoblots previously separated by standard SDS-PAGE.

ZmGRP5 is predicted to have ten potential phosphorylation sites. Phosphorylation is likely responsible for the three distinct protein spots *(x1, x2, x3)* of slightly differing pI but no detectable differences in mass. Glycosylation, which involves the addition of

Figure 22. Attempted isolation of ZmGRP5 from silk extracts by 2D SDS-PAGE. Silk was sampled at developmental stage of 0 dpe. A rectangle is drawn around area containing ZmGRP5 isoforms on immunoblot and is superimposed on other blot treatments and SDS-PAGE gel (150 μg of total protein in Resuspension Buffer).

A. SDS-PAGE gel directly stained with Coomassie Blue:

Replicate SDS-PAGE gel is transferred to a PVDF blot, which is sequentially treated with the following:

B. Immunoblot probed with GST-ZmGRP5 antiserum

C. Colloidal Gold stained blot

D. Coomassie Blue stained blot

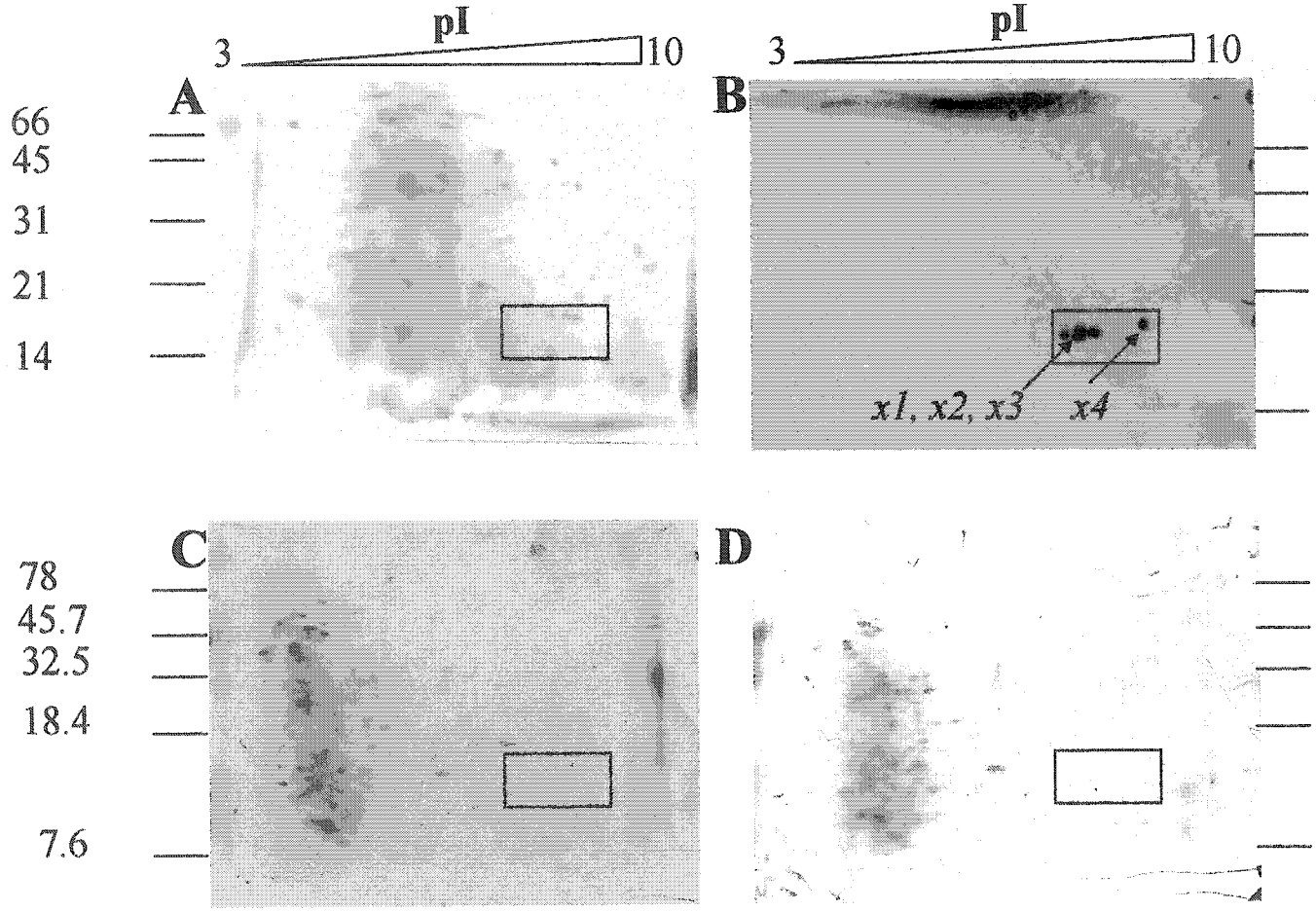
pI
3
10
A
66
45
31
21
14
pI
3
10
B
x1, x2, x3
x4
C
78
45.7
32.5
18.4
7.6
D

oligosaccharides, could be responsible for the increased mass and increased pI observed for protein spot *x4*. ZmGRP5 was predicted to have two potential N-linked glycosylation sites at amino acid positions N4 and N34. However, multiple combinations of phosphorylation and glycosylation events are possible and the resulting heterogeneity of protein mass and charge makes assignment of protein spot identity between the isoforms impossible without more targeted experimental approaches which will be investigated in the Discussion section.

3.3.4.2 Attempted Isolation of Native ZmGRP5

In an effort to verify the identity of the approximately 15 kD protein band detected in previous immunoblots as ZmGRP5, attempts were made to pick protein spots corresponding to the expected ZmGRP5 protein directly from Coomassie Blue stained 2D SDS-PAGE gels for amino acid sequence confirmation. Many protein spots were detected in the gel, including the area of the gel corresponding to the predicted mass and charge of ZmGRP5 (Fig. 22A). Attempts were made to identify and "map" the immunoblot positive protein spots corresponding to the ZmGRP5 protein in the context of the total protein spot pattern on a 2D gel. Blots were stained with colloidal gold (Fig. 22C) after immunodetection (Fig. 22B). The spots from immunodetection did not appear as strong, distinct spots with colloidal gold staining. The same could be observed when the blot was stained with Coomassie Blue (Fig. 22D). As a result, it was not possible to identify a protein spot from a replicate 2D SDS-PAGE gel stained directly with Coomassie Blue that corresponds to the same spots detected on the immunoblot

3.3.5 ZmGRP5 as a Subunit in a Multimeric Complex

The cysteine residues in the amino acid sequence of ZmGRP5 may serve as potential sites for disulfide bond formation under oxidizing conditions. Covalent disulfide bonds stabilize the tertiary and quaternary structures of proteins and usually are formed during the folding of proteins in the ER. The majority of secretory proteins contain disulfide bonds, while most cytosolic proteins do not (Lodish *et al.*, 2000). Given the predicted secretory nature of ZmGRP5, it is highly likely that disulfide bonds are formed with at least one of the two cysteine residues of ZmGRP5. Disulfide bonding could be intramolecular or intermolecular. Intramolecular disulfide bond formation between the cysteine residues C115 and C117 could be possible, but the close proximity of the cysteine residues may cause unfavorable steric hindrance. Intermolecular disulfide bonding between cysteine residues on different copies of the ZmGRP5 monomer could create covalently bonded homo-multimers. Alternatively, ZmGRP5 could exist as (a) subunit(s) of a hetero-multimer protein complex covalently linked to other protein subunits of completely different amino acid sequence.

If any of the above hypothetical complexes were formed by ZmGRP5 in its native state, reducing agents in the extraction buffer or the loading buffer would be necessary to disrupt such disulfide bonds before the respective protein monomers could migrate individually as distinct linear protein bands separated by SDS-PAGE. In contrast, under non-reducing conditions, the multimeric complexes joined by intermolecular disulfide

bonds would remain intact and migrate as a single unit with a molecular weight much higher than that of the ZmGRP5 monomer. Intramolecular disulfide bonding within ZmGRP5 monomers, if they were to occur, would prevent the protein from unfolding into a linear rod. The partially folded ZmGRP5 monomer would be expected to migrate more quickly under non-reducing SDS-PAGE conditions and appear slightly lower in mass than a completely unfolded linear monomer run under reducing conditions (Campbell and Braam, 1998).

3.3.5.1 Partially Reducing SDS-PAGE

ZmGRP5 was extracted from silk tissue with Matsuyama SDS Buffer without the presence of any reducing agents. A gel loading buffer containing a reducing agent was added to the SDS extract to disrupt disulfide bonds and break down multi-protein complexes as was standard before separation by denaturing SDS-PAGE. At the beginning of this study, a gel-loading buffer henceforth named Ausubel Buffer was prepared using DTT as the reducing agent. Silk extract samples separated by SDS-PAGE after heating with Ausubel Buffer resulted in the immuno-detection of two protein bands by the GST-ZmGRP5 antiserum: an approximately 15 kD band that corresponded to the predicted molecular weight for the mature protein of ZmGRP5 of 14687.12 Daltons, as well as an additional band of approximately 60 kD of unknown identity (results not shown). The above experiment was repeated several times, with the same results each time.

To clarify the status of the 60 kD band in case of potential contamination, the above experiment was repeated using fresh silk extracts as well as new gel running buffers and immunoblot reagents. In addition, Laemmli Buffer was used as an alternative gel-loading buffer to Ausubel Buffer, and each was added to different aliquots of the same silk extract. Laemmli Buffer was added to the Matsuyama SDS Buffer at 1:1 (v/v) ratio, resulting in a final ß-ME concentration of 5% (700 mM). Ausubel Buffer was added to the Matsuyama SDS Buffer at 1:5 (v/v), resulting in a final DTT concentration of 100 mM. DTT is a stronger reducing agent than ß-ME, and the above final concentrations were considered equivalent for use in denaturing SDS-PAGE (see Sigma-Aldrich Canada, 2002-2003, p.706).

Immunoblot analysis of above samples containing approximately 10 µg each of total protein revealed the presence of a strong band of 15 kD and a very weak band 60 kD in the sample containing Laemmli Buffer. In contrast, both the 15 kD band as well as the 60kD band appeared strong in the sample containing Ausubel Buffer (Fig. 23). As the initial silk tissue extract was the same, the differences observed between the two samples could be directly attributed to the differences in the loading buffers. While the final concentration of individual chemical components such as glycerol and Tris in Laemmli Buffer and Ausubel Buffer after dilution in silk extract was slightly different, the major difference between the two was the reducing agent used: 700 mM ß-ME in Laemmli Buffer and 100 mM DTT in Ausubel Buffer.

Figure 23. Immunoblot analysis of effect of reducing agents on the size mobility of native ZmGRP5 separated by denaturing SDS-PAGE. Silk was sampled at developmental stage of 0 dpe. Maize silk tissue directly extracted with Matsuyama SDS buffer containing approximately 20 μg total protein was loaded in the presence of the following gel loading buffers:

1. Laemmli Buffer: final concentration of 5% (700 mM) ß-ME
2. Ausubel Buffer: final theoretical concentration of 100 mM DTT

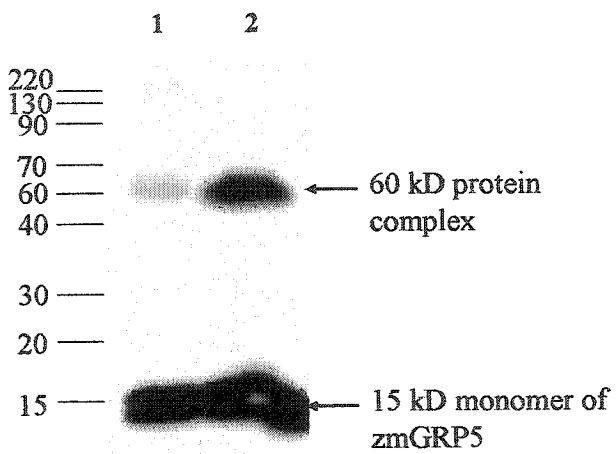
1
2
220
130
90
70
60
40
30
20
15
60 kD protein complex
15 kD monomer of zmGRP5

While the 15 kD band is the monomeric form of the ZmGRP5 mature protein, the 60 kD band could be a multimeric form of ZmGRP5. It is possible that the 60 kD band is a tetramer formed by the joining of four individual 15 kD ZmGRP5 monomers by disulfide bonds. Alternatively, the identity of the band could be a multimeric complex composed of at least a single 15 kD ZmGRP5 monomer joined to other protein subunits by disulfide bond(s) that add up to an apparent mass of 60 kD.

Given the above assumptions, the experimental results appeared to suggest that the DTT in Ausubel Buffer was not as effective as the ß-ME in Laemmli Buffer at disrupting the disulfide bonds that connect the multi-protein complex (60 kD). While the 60 kD band was also detected in the sample containing Laemmli Buffer, the band was weak, suggesting that the disruption of disulfide bonds was close to completion. Upon closer examination, it was noted that while the Laemmli Buffer was made freshly with ß-ME before use, the Ausubel Buffer was made with DTT that had been stored at –20 °C for over 5 years. In addition, the Ausubel Buffer was stored at 4 °C for over a month prior to use, and was not stored at –20 °C as was recommended (Ausubel *et al.*, 1994). While partially reducing conditions were suspected to be responsible for the appearance of both the multimeric (60 kD) and monomeric (15 kD) forms of ZmGRP5, the actual reducing activity of DTT in the Ausubel Buffer was not quantified.

The serendipitous creation of partially reducing conditions due to improper storage of DTT in the Ausubel Buffer was suggested by the immunoblot results above using silk

extracted with Matsuyama SDS Buffer. To clarify the above observations, attempts were made at a later date to repeat the experiment by substituting Ausubel Buffer with a series of gel loading buffers containing decreasing concentrations of ß-ME to produce SDS-PAGE conditions that range from completely reducing, to partially reducing, to non-reducing. The original silk extract in Matsuyama SDS Buffer had not been retained, however, and several attempts to extract the 15 kD protein band from silk tissue that had been stored at –80 °C for over a year with various versions of SDS buffers were unsuccessful as was previously observed in section **3.3.2**. As a result, no equivalent input silk extract sample was available to duplicate the experiment.

3.3.5.2 Removal or Dilution of ß-ME from Laemmli Extracts

Attempts were made to repeat the above experiment using the Laemmli Buffer silk extracts (B6, Fig. 21) as an input source of ZmGRP5. The ß-ME contained in the Laemmli extracts was lowered from 10% to 1% by dilution in Laemmli Buffer-NR. Attempts were also made to remove ß-ME completely using Centricon YM-3 centrifugal filter tubes (Millipore Corp.) and two rounds of buffer exchange with Laemmli Buffer-NR. Varying amounts of ß-ME were reintroduced into aliquots of the above samples to create final SDS-PAGE conditions ranging from non-reducing to fully reducing. However, immunoblot analysis revealed the presence of only the 15 kD monomeric form of ZmGRP5 regardless of the final concentration of ß-ME (Fig 24). Previous results from Fig. 21 showed that the input silk extract B6 contained mostly 15 kD monomeric ZmGRP5. The subsequent removal or reduction of ß-ME did not result in reshuffling of

Figure 24. Immunoblot analysis of the effect of the reducing agent ß-ME on SDS-PAGE band size mobility of ZmGRP5 extracted from maize silk tissue. Silk was sampled at developmental stage of 0 dpe. Blots are probed with GST-ZmGRP5 antiserum. 10 µL of each protein sample was loaded.

A 1/10 Dilution of silk tissue extract B6 (Fig. 21) followed by re-addition of ß-ME to produce 1%, 2%, 4%, 6%, 8%, and 10% final samples.

B Removal of ß-ME from silk tissue extract B6 (Fig. 21) with Centricon microcentrifugal devices followed by re-addition of ß-ME to produce 0%, 0.08%, 0.15%, 0.3%, 0.6%, 1.25%, 2.5%, 5%, and 10% final samples.

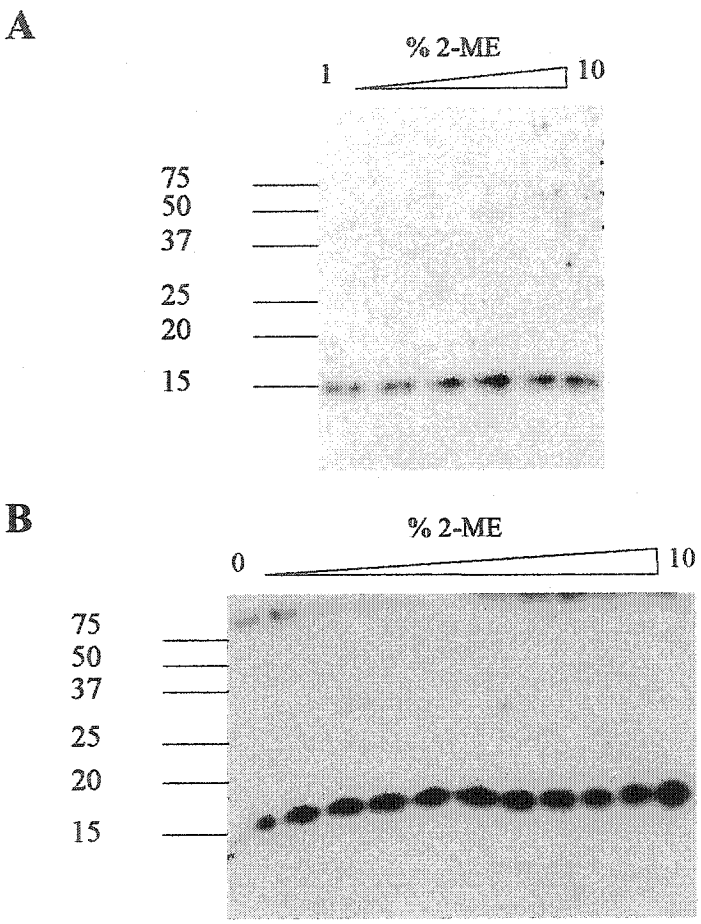
A
% 2-ME
1
10
75
50
37
25
20
15
B
% 2-ME
0
10
75
50
37
25
20
15

disulfide bonds and reformation of a multimeric 60 kD protein complex. As a result, it was not possible to verify the role of reducing agent concentration on the relative abundance of what are suspected to be the monomeric and multimeric forms of ZmGRP5.

3.3.5.3 Partially Reducing 2D SDS-PAGE

Duplicate 2D SDS-PAGE gels were run at a later date using 150 µg of total silk protein. Immunoblot analysis revealed the detection of a single linear smear (Fig. 25B) in the area of the blot where the closely spaced spots *x1, x2, x3* were previously observed (Fig. 25A).The protein spot *x4* remained as a single protein spot in both immunoblots (Fig. 25 A and B). The reproducibility of the above results supports the proposed identity of the spots as isomers of ZmGRP5, and not as artefact spots arising from aberrations in the running of individual gels. In addition, two protein spots with higher molecular weights of approximately 45 kD (*y*) and 35 kD (*z*), both with acidic pI, were also detected. This was repeated once more with the same results (not shown), suggesting that the protein spots y and z are also not artifacts.

The differences in mass and charge between these latter two spots (y, z) and the predicted mass and charge of ZmGRP5 were too great to be a likely result of the previously described post-translational modifications. Instead, the possibility exists that the protein spots of approximately 45 kD (*y*) and 35 kD (*z*) are multi-protein complexes containing ZmGRP5 that are not completely disrupted as was observed in standard SDS-PAGE in section **3.3.5.1**. Similarly, detection of higher molecular weight protein spots representing

Figure 25. Immunblot analysis of silk tissue extracts separated by 2D SDS-PAGE with GST-ZmGRP5 antiserum. Silk was sampled at developmental stage of 0 dpe. Replicates performed on two separate blots from two separate gels loaded with the following:

A. 150 μg total protein (65 mg silk extracted with 250 μL urea buffer). Treatment after IEF with fresh DTT Equilibration Buffer (same as Fig. 22B)

B. 150 μg total protein (125 mg silk extracted with 250 μL urea buffer). Treatment after IEF with DTT Equilibration Buffer stored at 4 °C for 1 month.

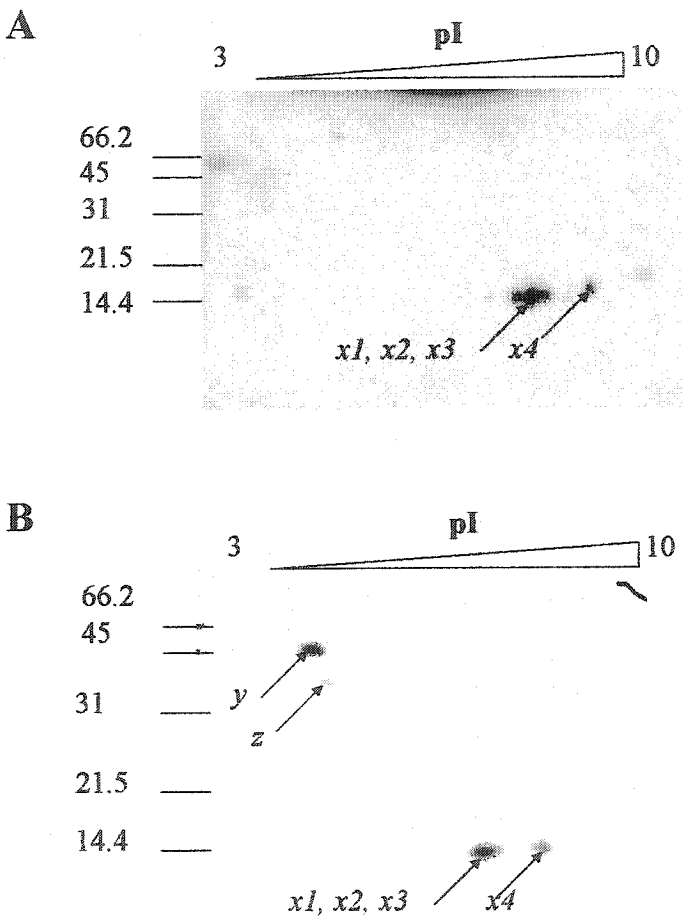
A
pI
3
10
66.2
45
31
21.5
14.4
x1, x2, x3
x4
B
pI
3
10
66.2
45
31
y
z
21.5
14.4
x1, x2, x3
x4

potential multimers was previously observed in five out of ten protein preparations separated by 2D SDS-PAGE (Peng *et al.*, 2003). The duplicate 2D SDS-PAGE gel could have been run under partially reducing conditions. This would explain the detection of both monomeric (*x1, x2, x3, x4*) and multimeric (y, z) forms of ZmGRP5. The possible reasons for the partially reducing conditions in the duplicate gels compared to the fully reducing conditions in the origin 2D SDS-PAGE will be presented in detail in the Discussion.

3.3.6 Immunoprecipitation (IP) of ZmGRP5

IP was attempted as an alternative strategy to 2D SDS-PAGE to isolate the target ZmGRP5 protein from silk extracts for sequence confirmation by LC-MS/MS. IP is a commonly used method to enrich for a specific protein from a complex protein mixture. In addition, IP has also been used in the co-precipitation of protein interaction partners in addition to the target protein. Identification of such protein interaction partners would also greatly clarify the potential functions of ZmGRP5.

The IP method uses specific antibodies, which are added to protein extracts containing the target protein of interest. After incubation, the resulting antibody-antigen complex is then incubated with ProteinA-Sepharose beads. ProteinA is a *Staphylococcus aureus* derived protein that exhibits high binding affinity to the Fc region of IgG. Upon centrifugation, the antigen-antibody-ProteinA complex is recovered in the Sepharose pellet to which the ProteinA is cross-linked. The Sepharose pellet is resuspended, washed

to remove non-specific silk extract contaminants, heated in Laemmli Buffer and run on SDS-PAGE gel. The IgG runs as individual 50 kD heavy chain and 25 kD light chain subunits. Additional protein bands corresponding to the immuno-captured target protein(s) are expected if the IP reaction was successful.

Silk extracted with SDS Buffer was diluted 1/10 in IP buffer to achieve IP compatible levels of SDS. After performing IP, the recovered Sepharose pellet was run on SDS-PAGE and stained with Coomassie Blue. A strongly stained band in the 50 kD range corresponding to the IgG heavy chain was observed, but the 25 kD IgG light chain band was not detectable. This is not unusual, as the light chain is significantly weaker in staining intensity than the heavy chain (Fig. 2, Immunoprecipitation Starter Pack, http://www.jp.amershambiosciences.com/tech_support/tech_material/pdf/18114104.pdf). Most significantly, no visible band was observable at the 15 kD position as was expected for ZmGRP5, suggesting that the IP reaction was either not successful, or not enough ZmGRP5 was isolated to be detected by Coomassie Blue direct protein staining (results not shown).

To check for the presence of the 15 kD target band in amounts that were below the level of detection by Coomassie Blue staining, immunoblot analysis was performed on blots transferred from duplicate SDS-PAGE gels. IgG components from the IP reaction are expected to be directly detected by the secondary antibody (goat anti-rabbit HRPO conjugate), while any target ZmGRP5 captured by the IP reaction will only be detected

by standard immunoblot analysis using the primary GST-ZmGRP5 antiserum followed by the secondary antibody.

Immunoblotting was first performed directly with the secondary antibody only to identify bands resulting from the IgG components of the IP samples. A band of approximately 50-60 kD was detected, supporting its predicted identity as the heavy chain of IgG (Fig. 26A). The 25 kD light chain of IgG was only weakly detectable after extended film exposure times (results not shown).

Standard immunoblot analysis was sequentially performed on the same blot using both primary and secondary antibodies. Once again, only the 50-60 kD band corresponding to the IgG heavy chain was detected, as well as a weak band of approximately 25-30 kD (Fig. 26B), which could possibly be the light chain of IgG. The 15 kD target band corresponding to ZmGRP5 was absent in the IP sample.

The input silk extracts used in the IP experiment were extracted with SDS buffer. The variable solubility of ZmGRP5 in SDS buffer that was observed in section **3.3.2** was not known at the time the IP reactions were performed. Control silk extract samples were run next to the IP reactions and tested positive for the 15 kD ZmGRP5 band. However, these samples were directly extracted with Laemmli Buffer and only control for the presence of the ZmGRP5 target in the silk tissues used, not for the presence of the ZmGRP5 target in the SDS Buffer extracts used in the IP reactions. Therefore, the reasons for the failure of the IP reactions could simply be one of a lack of target ZmGRP5 in the starting silk tissue

Figure 26. Immunoblot analysis of immunoprecipitation (IP) reactions using silk tissue extracts. Silk was sampled at developmental stage of 0 dpe. 10 µL was loaded on gel for both direct Laemmli Buffer tissue extract and ProteinA-Sepharose pellet from IP reaction resuspended in equal volume of Laemmli Buffer.

A. secondary antibody only (goat anti-rabbit HRP conjugate)

B. primary (anti-GST-ZmGRP5 rabbit antiserum) and secondary antibodies.

1. Control silk tissue extracted with Laemmeli Buffer
2. IP reaction using silk tissue extracted with SDS Buffer

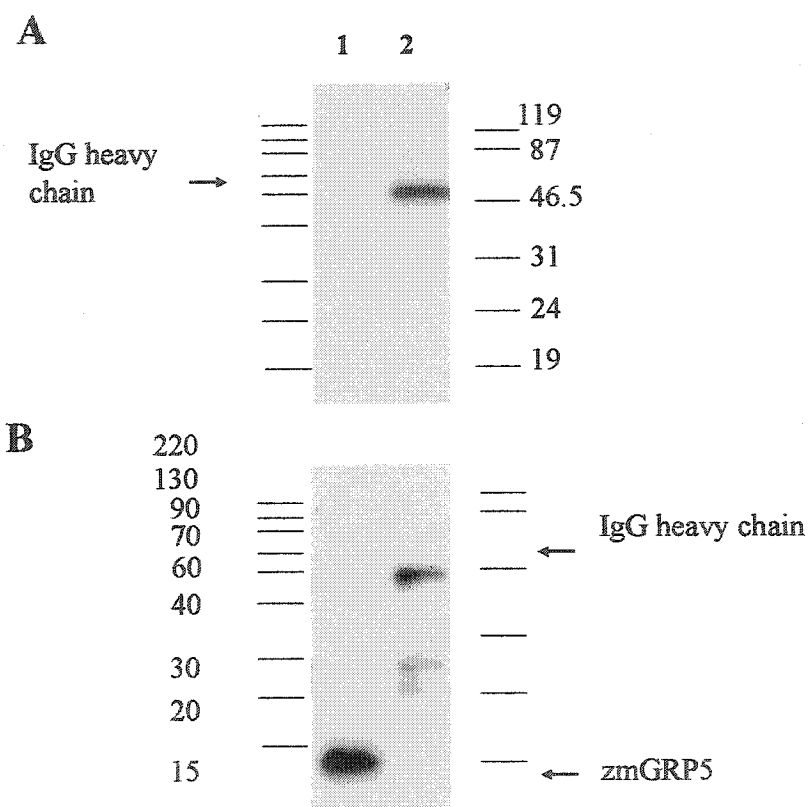
A
1
2
IgG heavy chain
119
87
46.5
31
24
19
B
220
130
90
70
60
40
30
20
15
IgG heavy chain
zmGRP5

SDS extract. Additionally, it is also possible given the solubility problems of the target ZmGRP5 protein that even if it was present in the original 1% SDS extract, subsequent 1/10 dilution in IP Buffer could have caused the ZmGRP5 to aggregate and precipitate out of solution.

In summary, isolation of the native ZmGRP5 protein from maize silk using IP was unsuccessful in this study. The presence of ZmGRP5 in the input silk extract used in the IP reactions was questionable given the variability of ZmGRP5 solubility in SDS buffers. Laemmli Buffer extracts, which consistently solubilized ZmGRP5 from the cell wall, could not be used as a source of input silk protein for IP reactions due to the high ß-ME content. Reduction of disulfide bonds linking the two subunits of light chains and two subunits of heavy chains that make up each IgG molecule by ß-ME would interfere with IgG binding to the ZmGRP5 target protein. Removal of ß-ME from the Laemmli Buffer extracts by filtration devices followed by IP was not attempted in this study due to time constraints, but could be an avenue of exploration in future studies.

4. DISCUSSION

In this study, we have attempted the characterization of ZmGRP5, the predicted protein encoded by a newly isolated maize silk tissue-specific cDNA. ZmGRP5 has a high glycine content of 40%, suggesting possible similarities with other GRPs, a diverse yet poorly understood 'family' of plant proteins. New individual GRP clones are continuously being discovered in ever increasing numbers, especially since the advent of high throughput genomic techniques. Many GRPs are discovered as genes up-regulated by various biotic and abiotic stress treatments, while others exhibit tightly controlled tissue-specific and developmentally defined expression patterns. Despite the abundance and diversity of GRPs, the majority of such proteins remain poorly understood at the functional level.

It has been proposed that the diversity of GRPs should be conceptualised as a disparate collection of modular proteins sharing a glycine-rich domain (Sachetto-Martins *et al.*, 2000). The divergent properties of GRPs are derived from the unique combinations of the glycine-rich domain with other discrete domains found in each particular protein. Bioinformatic analysis has revealed the presence of various putative domains in the ZmGRP5 amino acid sequence. Some of these domains were experimentally investigated in this study to elucidate possible protein function(s). Not surprisingly, the interpretation of experimental results and the determination of possible biological function(s) for ZmGRP5 should also proceed within the context of a modular protein whose unique

properties are derived from the contributing characteristics of each discrete domain (Fig 7A, 7B).

4.1 Summary of Results

Recombinant GST-ZmGRP5 fusion protein was produced and purified from transformed *E. coli* cultures. The purified fusion protein was cut as a gel slice from Coomassie Blue stained SDS-PAGE and was confirmed to be in frame with the correct sequence by LC-MS/MS. Antiserum harvested from rabbits immunized with the above protein was confirmed to be ZmGRP5 specific, reacting only with the ZmGRP5 portion of the fusion protein, and not the GST portion. The GST-ZmGRP5 antiserum was used directly without affinity purification for immunoblot analysis of silk tissue extracts.

ZmGRP5 was experimentally confirmed to be silk tissue specific at the protein level, confirming previous results at the RNA level. Immunoblot analysis detected a protein band of approximately 15 kD corresponding to ZmGRP5 in silk extracts, but not in extracts from other tissues such as leaf, cob, husk, tassel, or pollen. These results support possible fertility related functions as suggested by the bioinformatic detection of a putative domain of ZmGRP5 with homology to an apomictic pistil-specific GRP from buffelgrass.

ZmGRP5 was predicted to contain an amino-terminal signal peptide, which targets proteins to the secretory pathway. Experimental results have localized ZmGRP5 in the

cell wall fraction, and not in the cytosolic fraction. Cell wall fractionation studies using three different methods of crude centrifugation, ultracentrifugation over a sucrose cushion, and Miracloth filtration, have all confirmed the subcellular localization of ZmGRP5. ZmGRP5 was not detected in any other locations along the secretory pathway such as the ER, Golgi apparatus, vacuole, or plasma membrane.

Immobilization of ZmGRP5 to the cell wall matrix was observed to be variable. ZmGRP5 was extracted from freshly harvested silk tissue by buffers containing the anionic detergent SDS. However, silk tissue after extended storage at –80 °C was no longer extractable by SDS buffers, regardless of pH or heat treatment. ZmGRP5 was also resistant to extraction by the non-ionic detergent Triton X-100, and high salt conditions such as 1 M NaCl. In contrast, Laemmli Buffer containing the reducing agent BME consistently solubilized ZmGRP5 from the cell wall. The role of reducing agents in the solubilization of ZmGRP5 suggests that the immobilization of ZmGRP5 could potentially be linked to the redox conditions of the cell wall.

In addition to the solubilization of ZmGRP5 from the cell wall, ß-ME was likely implicated in the disruption of protein bands from putative multimeric protein complexes containing ZmGRP5 subunits into smaller molecular weight monomeric forms. Incomplete disruption of disulfide bonds was suspected to be responsible for the detection of both the ZmGRP5 monomer and multimeric protein complexs containing ZmGRP5 subunit(s) in silk extracts separated by both standard and 2D SDS-PAGE under partially reducing conditions.

Post-translational modifications were implicated in the detection of several isoforms of ZmGRP5 separated by 2D SDS-PAGE. Phosphorylation and glycosylation are two likely forms of modification based on the mass and charge distribution of the ZmGRP5 isoforms and bioinformatic predictions. Phosphorylation suggests potential implications of ZmGRP5 function in protein interactions such as signal transduction, while the addition of oligosaccharides via glycosylation could provide targets for cell surface receptor recognition and/or non-protein based targets for cross-linking to the cell wall matrix.

4.2 Silk Tissue Specificity and Homology to Apomictic Pistil GRP

In this study, we have experimentally confirmed the tissue-specific expression of ZmGRP5 at the protein level in maize silk. Immunoblot analysis of maize tissue extracts with a ZmGRP5 antiserum revealed the detection of the predicted protein band of approximately 15 kD in maize silk, and not in any other maize tissues tested. However, higher molecular weight bands were detected in maize cob tissue.

It is conceivable that antibodies produced against glycine-rich epitopes in the GST-ZmGRP5 fusion protein could cross-react with glycine-rich epitopes in other GRPs that may be found in the maize cob tissue. The cross-reactivity of GRP antibodies to glycine-rich epitopes in other proteins is not uncommon. A peptide derived from GRP1.8, a cell wall glycine-rich protein, was shown to be cross-reactive to antibodies in the serum of

patients with autoimmune disorders and food allergies. The patients' sera were also cross-reactive to human self-antigens containing glycine-rich epitopes such as keratin, collagen, and EBNA-1 (Epstein-Barr Viral Antigen 1) (Lunardi et al., 2000).

MA16, a previously characterized RNA-binding, abscissic acid inducible GRP from embryonic maize endosperm (Gomez *et al.*, 1988) appeared to be a likely candidate for cross-reaction to the antiserum. However, the predicted mass of MA16 is 15.4 kD, and not the higher molecular weight sized bands observed in this experiment. MA16 could be covalently bound in multi-protein or RNA-protein complexes that remain resistant to disruption into monomeric components by ß-ME. The possibility also exists that the protein bands detected in maize cob tissue represent as yet unidentified GRPs.

Alternatively, the higher molecular weight bands could represent multi-protein complexes of ZmGRP5 found in maize cob tissue. This is highly unlikely given the lack of detection of the *zmgrp5* mRNA in cob tissue in previous studies (Figure 5). It is also possible that post-translational protein transport could result in the export of some ZmGRP5 protein from silk tissue to kernel tissue, which is included in the total cob tissue extract sample. The cob tissue sampled could also contain trace amounts of silk tissue that remain at the attachment point to each kernel during tissue processing, as each kernel is joined to a maize silk to form an individual maize pistil.

The detection of the higher molecular weight putative protein complex bands but not the 15 kD ZmGRP5 monomer in cob tissue suggests that the above scenario is unlikely.

However, it is possible that the multi-protein complexes are covalently cross-linked and are resistant to disruption by ß-ME into subunits such as the 15 kD ZmGRP5 monomer. The possibility also exists that the multi-protein complexes are linked by disulfide bonds, but escaped disruption by ß-ME. This is highly unlikely, however, as ß-ME should result in at least partial disruption of disulfide bonds and would have resulted in the detection of at least trace amounts of the 15 kD ZmGRP5 monomer.

Given the higher molecular weight bands detected in maize cob tissue is not 15 kD as expected for ZmGRP5 and the unlikelihood that they are multimers of ZmGRP5, it is reasonable to assume that ZmGRP5 is silk tissue-specific at the translational level. This is consistent with previous experimental results at the transcriptional level using RNA blots probed with radio-labelled ZmGRP5 cDNA (Ouellet *et al.*, 2003).

The tissue specific expression pattern of ZmGRP5 in maize silk, which is functionally equivalent to the stigma and style portions of the pistil, suggests a possible fertility related function. ZmGRP5 also contains a non-glycine-rich region exhibiting limited homology to an apomictic pistil-specific GRP of buffelgrass (Genebank accession# AAK 15500). The related nature of buffelgrass and maize, both in the grass family Poaceae suggest that the two respective proteins may have conserved functions. Additionally, the buffelgrass GRP is very similar to ZmGRP5 in primary amino acid sequence not only in the non-glycine-rich region of homology, but also in the presence of tyrosine and cysteine residues interspersed within the glycine-rich regions.

However, maize reproduces sexually, and apomixis is not known to occur. In addition, sequence similarity between the two GRPs was low, with an E value of only 0.066 using BLASTP 2.2.8. Therefore, the apomictic pistil of buffelgrass is unlikely to be a functional "homologue" of ZmGRP5. The buffelgrass GRP mRNA is differentially expressed in apomictic pistils compared with sexual pistils. It is not known if this differential expression correlates to real functional roles in the process of apomixis. The exact location of the buffelgrass GRP within the apomictic pistil: the stigma, style, or the ovule containing ovary is also not documented in existing publications, and unfortunately cannot be of help in the elucidation of ZmGRP5 function.

Significantly, ZmGRP5 was originally isolated from unfertilized maize silk tissue. The mRNA was developmentally regulated, highest at 0 dpe, and decreasing steadily to barely detectable levels at 8 dpe (Ouellet *et al*, 2003). This expression profile matches the period of pollen receptivity of unfertilized maize silk, which remains viable for up 8 dpe if not fertilized immediately upon emergence. Pollen tube growth proceeds quickly down the length of the silk into the immature kernel, were double fertilization of the ovule and surrounding endosperm takes place (Miller, 1919). Silk senescence proceeds immediately upon fertilization, starting with the collapse of the tissue in the abscission zone at the point of silk entry into the kernel (Heslop-Harrison *et al.*, 1985; Bassetti and Westgate, 1993b). Upon collapse of the abscission zone, the vascular supply is cut off and dessication proceeds rapidly, accompanied by the browning of the senescing silk tissue from oxidation. If ZmGRP5 expression is linked to silk receptivity, even indirectly

related structural functions such as the maintenance of silk osmotic potential could have significant impacts on fertility.

4.3 Signal Peptide and Cell Wall Localization

The detection of a signal peptide at the N-terminus suggests that ZmGRP5 is subcellularly targeted to the secretory pathway. The secretory pathway is distinguished as the site for many post-translational protein modifications such as glycosylation, phosphorylation, multimeric protein complex formation via disulfide bonds, and protein processing via protease digestion. Proteins that enter the secretory pathway are co-translationally inserted from the ribosomes across the ER membrane, where the hydrophobic signal peptides are retained while the mature proteins are cleaved and released into the ER lumen. The mature protein is targeted down the secretory pathway from the ER lumen to the Golgi apparatus, where the proteins are sorted into a range of vesicles for transport onward to the vacuole, plasma membrane, and cell wall (Lippincott-Schwartz *et al.*, 2000).

A major focus of experimental design in this study was the clarification and confirmation of the subcellular localization of ZmGRP5 by the fractionation of silk tissue extracts into subcellular components. ZmGRP5 was localized in the cell wall fraction using each of three fractionation methods employed in this study. The Miracloth filter used in the last method is routinely used to isolate protoplasts from the surrounding cell wall matrix. With a mesh size of 22-25 μm, Miracloth allows intact protoplasts to filter through along

with the smaller-sized organelles such as vacuoles and peroxisomes, disrupted plasma membranes, ER membranes, Golgi apparatus, and vacuolar membranes released from disrupted protoplasts. None of these potential targets along the secretory pathway produced any signal in the "cytosolic" fraction for ZmGRP5 using immunoblot analysis, while the cell wall component exhibited a strong signal.

The lack of detection of any ZmGRP5 in the cytosolic fraction suggests that the amount of ZmGRP5 in transit in the secretory system is very low. The same observations were made in the cell wall fractionation experiments of many other cell wall proteins, including cell wall GRPs (Matsuyama et al, 1999, and Ringli et al, 2001). It is conceivable that higher amounts of ZmGRP5 could be found in transit through the secretory system from maize silk tissue sampled at an earlier developmental stage than the 0 dpe silk used in this study.

Northern blot analysis results from previous studies show that the *zmgrp5* mRNA is also expressed at high levels in pre-emergent maize silk tissue (results not shown). Pre-emergent silk was not used as a source of protein extracts in this study due to the difficulty of sampling at a consistent developmental stage without the silk emergence event as a baseline. However, it is possible that pre-emergent silk tissue sample could contain traces of ZmGRP5 in the cytosolic fraction, representing portions of the protein that are in transit through the secretory system and have not yet reached the cell wall.

Additional confirmation of the fractionation experiments was not performed with antibodies against organelle and cell wall specific markers due to cost and time constraints. Marker specific antibody confirmation was also not commonly performed in fractionation studies of other cell wall proteins in the published literature, including cell wall GRPs (Matsuyama et al, 1999, and Ringli et al, 2001). Therefore, the detection of ZmGRP5 in the cell wall fraction but not in the cytosolic fraction of silk extracts in this study confirms to a reasonable degree that ZmGRP5 is a cell wall protein.

In summary, ZmGRP5 has been experimentally shown to be a cell wall GRP. These proteins have traditionally been assumed to be structural proteins that contribute to cell wall elasticity based on the lack of steric hindrance from glycine residues, which have a lone hydrogen group instead of more complex side chains typical of other amino acids. However, cell walls are also the medium for intercellular signalling between plant cells as well as between the surface plant cells and the environment. Recent advances in murology, the study of cell walls, have revealed that cell walls are dynamic matrices that constantly alter their constituent components, as well as component interactions, to meet the demands of developmental change and environmental stress (Roberts, 2001), such as cold, drought, wounding, and fungal, microbial, and viral elicitor treatments or infections

Cell wall proteins were traditionally divided into structural proteins that serve as substrates for cell wall cross-linking much like that of the non-protein components of the cell wall matrix, or enzymes that modify the matrix components. However, many proteins do not fall so clearly into one category or the other. Cell wall proteins such as

expansins are not structural substrates, but act as regulators of expansive growth by causing 'slippage' of cross-linkages between the matrix constituents via a non-enzymatic mechanism (Li and Cosgrove, 2001). While cell wall GRPs have traditionally been viewed as structural proteins, this view is starting to be challenged by new discoveries such as that of AtGRP3, which is implicated in a pathogen-response signalling pathway (Park *et al.*, 2001).

4.4 Cell Wall Immobilization

The cell wall localization of ZmGRP5 suggests many possible functions, from that of a purely structural polymer protein to that of a protein implicated in a signalling pathway. Given the complexity of cell wall functions, it is necessary to investigate the nature of the interactions of ZmGRP5 with the components of the extracellular matrix that constitute the cell wall. The mechanisms of cell wall immobilization could be divided into three main types: non-covalent interactions, covalent but reversible disulfide bonds, and non-reversible covalent bonds. Non-covalent cell wall immobilization involves ionic bonds, hydrogen bonds, and hydrophobic interactions, all of which could be disrupted by SDS, an anionic detergent. Covalent disulfide bond formation, such as that between the sulfhydryl groups of cysteine residues, occur under oxidative conditions but are reversible upon the addition of reducing agents such as ß-ME. Non-reversible covalent cross-links between tyrosine residues and other potential targets also occur under oxidative conditions but are resistant to disruption by ß-ME.

4.4.1 Non-Covalent Interactions

Cell wall fractionation experiments conducted in this study have consistently confirmed the extracellular targeting of ZmGRP5 to the cell wall. However, inconsistencies in cell wall extractability have been observed with SDS buffer extracts. Matsuyama SDS Buffer had initially been successful in extracting ZmGRP5 from crude cell wall pellets. SDS, an anionic detergent, denatures proteins by disrupting ionic interactions as well as hydrophobic interactions. These interactions could be protein-protein, or between proteins and other components of the cell wall such as pectin, cellulose, and lignin. The initially successful extraction of ZmGRP5 from the cell wall with SDS suggests that our protein of interest is associated with the cell wall matrix by non-covalent interactions.

4.4.2 Reversible Disulfide Bonds

SDS extraction could not be duplicated, however, despite using a series of SDS based buffers with varying pH values. Laemmli Buffer successfully solubilized ZmGRP5 from cell wall samples that were resistant to extraction by SDS. The thiol reducing agent ß-ME is the only component in Laemmli Buffer not found in the various SDS buffers that failed to extract ZmGRP5. This suggests that ZmGRP5 is immobilized to the cell wall through disulfide bonds.

ZmGRP5 has two cysteine residues, C115 and C117. It is conceivable that under oxidizing conditions in the field or during sample storage, ZmGRP5 could become

reversibly cross-linked in the cell wall through disulfide bond formation with other cell wall proteins. Alternatively, ZmGRP5 could form disulfide bonds with non-protein targets, such as sulphated non-proteinaceous cell wall components (Wu *et al.*, 1993), or other unspecified cell wall polymer targets as observed for a potato lectin (Kieliszewski *et al.*, 1994).

The ß-ME mediated solubilization of ZmGRP5 from the cell wall observed in this study suggests that at least one of the cysteine residues of ZmGRP5 is implicated in disulfide bonding *in muro*, and not *in vivo*. Intramolecular protein folding and intermolecular multimer formation via the reduction of cysteine residues occurs inside the controlled redox environment of the ER. In contrast, disulfide bond mediated cross-linking *in muro* is dependent on the redox potential of the cell wall, which is dependant on environmental factors such as ozone (Ranieri *et al.*, 2000), or cell wall peroxidase mediated oxidative burst in response to pathogen infection or wounding (Lamb and Dixon, 1997).

The cause in variation between SDS soluble samples and SDS insoluble samples is not known. It is possible that the silk samples were oxidized during extended storage at -80°C, resulting in the observed variability in extraction. However, no example of disulfide bond cross-linking due to oxidation during cold storage could be found in literature. Alternatively, differences between silk tissue samples collected from the field could also be responsible for the variability in SDS extraction. Although all silk samples were collected at the same developmental stage of 0 dpe, localized field conditions could result in stress factors such as wounding or other oxidative stress that could conceivably

cause the immobilization of ZmGRP5 in one sample and not in another sample not subjected to the same localized stress conditions. Further clarification of the observed insolubilization of ZmGRP5 would be necessary to ascertain if this is an artefact observation in the laboratory, or if the reversible immobilization of ZmGRP5 in the cell wall is a biologically significant feature under field conditions.

4.4.3 Non-Reversible Covalent Bonds

Isodityrosine (Bradley *et al.*, 1992) and di-isodityrosine (Brady and Fry, 1997) cross-link formation in cell wall proteins such as PRPs and HPRGs have been shown to harden the cell wall matrix as a defense response against pathogens. The same mechanism has also been proposed to immobilize cell wall GRPs. Recombinant PvGRP1.8, a cell wall GRP with a high tyrosine content, was cross-linked into aggregates *in vitro* in the presence of peroxidase and peroxide (Ringli *et al.*, 2001a). Additionally, tyrosine residues have also been proposed to be involved in oxidative cross-linking with the aromatic side chains of lignin in the cell wall matrix (Cassab, 1998).

The high tyrosine content of ZmGRP5, at over 8%, suggests that such mechanisms of cross-linking may also be important in addition to disulfide bonds. However, isodityrosine and di-isodityrosine cross-links are covalent and irreversible, rendering the cell wall proteins permanently immobilized to the cell wall matrix. In contrast, ZmGRP5 was freely extractable from the cell wall with Laemmli Buffer containing the reducing agent ß-ME. It is not known if any irreversibly cross-linked ZmGRP5 remain in the cell

wall pellets after extraction with Laemmli Buffer, but such associations are clearly not as evident as disulfide bonds.

4.5 Potential Multimerization of ZmGRP5

Experimental results from silk tissue directly extracted by SDS buffer suggest that ZmGRP5 is likely associated within a multi-protein complex. Immunoblot analysis of silk extracts separated by denaturing SDS-PAGE under fully reducing conditions (Laemmli Buffer) detected a strong 15 kD ZmGRP5 monomeric band and a barely detectable 60 kD band. In contrast, under potentially partial reducing conditions (Ausubel Buffer), strong band intensity was observed for both the 60 kD multimeric band and the 15 kD monomeric band. The potentially partial reducing conditions in the Ausubel Buffer sample are suspected to have resulted from degradation of DTT due to improper storage and the consequent loss of reducing activity.

Partially reducing conditions were also suspected to be responsible for the appearance of 30 kD and 45 kD multimeric isoforms of ZmGRP5 near the acidic end of several gels run a month after the initial 2D SDS-PAGE. To investigate this possibility, the concentration and status of the reducing agent used at all steps in the 2D method was examined in detail. DTT, the reducing agent commonly used in 2D SDS-PAGE, was used at two separate steps in the process. DTT was added at 50 mM in the initial Rehydration Buffer used to extract silk tissue. Subsequently, 2% ([w/v], 250 mM) DTT was added to the

DTT Equilibration Buffer to denature the IPG strip after the completion of IEF and reduce any remaining disulfide bonds.

The detection of higher molecular weight bands in the second immunoblot compared to the first, which did not exhibit any multimeric isoforms, could be a result of differences in handling between the two samples. While the Rehydration Buffer contains low concentrations of 50 mM DTT, the DTT Equilibration Buffer contains a much higher DTT concentration of 2% ([w/v], 250 mM). It is this step that is mainly responsible for the complete reduction of cysteines, which is analogous to boiling samples in Laemmli Buffer prior to standard SDS-PAGE. Most importantly, the two replicates were performed over a month apart using the same DTT Equilibration Buffer, which was stored at 4 °C.

The detection of higher molecular weight "multimers" of ZmGRP5 in 2D immunoblots may be a result of partially reducing SDS-PAGE conditions much like that observed with standard immunoblots. However, the higher molecular weight protein spots detected with the 2D immunblot are approximately 45 kD and 35 kD instead of 60kD as was observed previously with a standard immunoblot. The suspected multimeric identities of the above protein spots and bands have yet to be experimentally verified. However, if the identity of the 45 kD and 35 kD protein spots are multimeric protein complexes containing ZmGRP5, the observed acidic shift in pI suggests that these complexes are hetero-multimers containing other acidic protein subunits rather than homo-multimers of ZmGRP5 all having a pI of 8.7. It is not known if the observed differences in complex

size could be attributed to differences in the tissue extraction buffers used for standard and 2D SDS-PAGE.

Alternatively, the 60 kD band observed with the 1D immunoblot with Ausubel Buffer and the 45 kD and 35 kD spots observed with the 2D immunoblot could result from contamination of the Ausubel Buffer or Rehydration Buffer by bacteria, keratin, or other potential contaminants introduced during preparation of the buffers. Because the immunoblots were detected with crude antiserum instead of affinity purified anti-ZmGRP5, the possibility exists that contaminant antibodies produced in the rabbit antiserum are responsible for the detection of the artefactual band and spots, e.g., anti-*E. coli* antibodies produced as a result of trace amounts of contaminant *E. coli* proteins co-purified with the GST-ZmGRP5 fusion protein used to immunize the rabbit. Trace amounts of keratin contamination could also be introduced during the preparation of the fusion protein or during the immunization step by animal care staff, resulting in the production of anti-keratin. Repetition of the above immunoblots with affinity purified anti-ZmGRP5 would be necessary to clarify the status of the above protein band and spots and confirm the multimeric status of ZmGRP5

4.6 Post-translational Modifications

4.6.1 Phosphorylation

Immunoblot analysis of silk extracts separated by 2D SDS-PAGE identified three separate spots of identical mass (*x1, x2, x3*) that are likely differentially phosphorylated

isoforms of ZmGRP, which is predicted to have ten potential phosphorylation sites. A single phosphorylation event in which a hydroxyl group is replaced by a phosphate group would result in an increase in mass of 80 Daltons (http://www.chemistry.wustl.edu/~msf/damon/post_translation_modifications.html). Such a minimal difference in mass is not readily detectable by SDS-PAGE, as was observed for the protein spots *x1*, *x2*, and *x3*. Phosphorylation results in a net gain of negative charge and a slight acidic shift in the pI of the protein (Duncan *et al.*, 1999). Thus, the three individual protein spots *x1*, *x2*, and *x3* could be viewed as increasingly phosphorylated isoforms with increasingly acidic pI. The protein spot with the most basic pI could possibly be the dephosphorylated isoform, or simply the least phosphorylated isoform. The exact number of phosphorylation events is not known, but is assumed to differ only slightly between the isoforms due to the lack of differences in mass detected between the three protein spots.

The identification of potential phosphorylated isoforms of ZmGRP5 is significant regarding the potential biological functions of the protein. The inducible nature of phosphorylation and the accompanying conformational changes suggest dynamic protein interaction potential. Phosphorylated RNA-binding GRPs have been implicated in seed development (Vilardell *et al.*, 1990) and cold responsive signal transduction (Dunn *et al.*, 1996). No phosphorylated cell wall GRP have been discovered, however, and ZmGRP5 could potentially represent the first documented case.

4.6.2 Glycosylation

The protein spot *x4* has a slightly higher mass and more basic pI than the protein spots *x1, x2, x3*. Cumulative phosphorylation events could be enough to account for the higher mass of *x4*, but not for the more basic pI since phosphorylation should result in an acidic shift in pI. Therefore, *x4* must result from other forms of post-translational modification such as glycosylation, where oligosaccharide side chains are covalently linked to the primary polypeptide backbone at discrete amino acid residues. The composition and length of the oligosaccharide side chains can be highly variable, resulting in considerable mass and charge heterogeneity in differentially glycosylated isoforms of the same primary amino acid sequence (Kieliszewski and Lamport, 1994)

ZmGRP5 was predicted to have two potential N-linked glycosylation sites at amino acid positions N4 and N34. However, N4 is located within the signal peptide and is cleaved from the mature peptide, while the probability for N34 was only marginally above the prediction threshold. Therefore, the validity of such predictions cannot be taken with a high degree of confidence. However, glycoforms have also been resolved that differ in size by as little as 2-4 kDa and differ in pI by less than 0.2 (Wee *et al.*, 1998; Peng *et al.*, 2003). Therefore, it is entirely possible that the protein spot *x4* could be a glycoform of ZmGRP5.

Cell wall proteins such as extensins, AGPs, and other HPRGs are known to be heavily glycosylated. GRPs however, are commonly considered to be unglycosylated (Showalter,

1993; Cassab, 1998). The only experimentally documented example of a glycosylated GRP is from the aleurone layer of soybean seeds (Matsui *et al.*, 1994). ZmGRP5 could potentially be only the second documented case of a glycosylated plant GRP.

4.8 Conclusions

ZmGRP5 has been experimentally proven to be a silk tissue specific protein localized in the cell wall. Interaction with the cell wall matrix is observed to be highly variable and subject to disruption by the addition of the reducing agent ß-ME. The reversible nature of disulfide bond formation under different redox conditions upon the addition of ß-ME *in vivo* suggests that ZmGRP5 could potentially be implicated in the regulation of cell wall structural properties, ie: elasticity and rigidity, in accordance with changing redox conditions *in vivo* in response to environmental and/or developmental changes. The variable immobilization of ZmGRP5 to the cell wall matrix observed in this study could also be a potential mechanism of activation or inactivation of other non-structural functions of ZmGRP5 *in vivo*. The identification of potential post-translational modifications such as phosphorylation and glycosylation suggest additional possibilities for conformational change of ZmGRP5 and additional targets for interactions within the cell wall matrix. The preliminary characterization of ZmGRP5 in this study suggests that the protein's variable extractability and its silk tissue specificity are significantly different from other cell wall GRPs characterized to date, and therefore warrants additional investigation in the future.

4.9 Future Studies

The specificity of expression in maize silk tissue suggests ZmGRP5 could be implicated in fertility related functions. However, to establish a direct link, it would be necessary to localize expression of ZmGRP5 to cell-types of maize silk that line the pollen tube pathway. Cell-type localization was attempted in this study using IHC methods on both paraffin embedded and LR-White (London Resin Co.) embedded maize silk semi-thin cross-sections but was unsuccessful due to high background (results not shown). IHC should be attempted in the future using affinity purified anti-ZmGRP5 instead of raw antiserum to improve signal to noise ratio. Alternative detection methods could be attempted in addition to colloidal gold with silver enhancement. In addition to light microscopy, electron microscopy could also be attempted using ultra-thin LR-White resin cross-sections with colloidal gold detection without silver enhancement to localize ZmGRP5 beyond the cell-type level. Identification of ultrastructural associations such as stress fibres in the middle lamella within the cell wall as that conducted for PvGRP1.8 (Ryser, 2003) would yield additional information regarding potential protein function.

The developmental expression pattern of ZmGRP5 at the protein level has not been tested in this study, which only investigated samples collected at 0 dpe, at the peak of mRNA expression. While it is reasonable to assume that the protein expression profile would match that of the mRNA, this is not necessarily so. Depending on the stability of ZmGRP5, the accumulated protein could persist into senescing silk tissue. The functional availability, and status of cross-linking in the cell wall of ZmGRP5 is worthy of further

characterization at different developmental points. Immunoblots of the developmental expression profile of ZmGRP5 in fertilized silk tissue as well as unfertilized silk tissue could provide additional evidence supporting or refuting fertility-related functions. In addition, the status of ZmGRP5 expression in fertilized silk, at both the mRNA and protein levels, are also worthy of further investigation to discern if ZmGRP5 function is related to silk receptivity.

The redox hypothesis of cell wall immobilization suggested by this study could be tested by immunoblots of the environmental expression profile of ZmGRP5. Silk tissue could be collected at the same developmental stage, such as at 0 dpe, but under different environmental conditions that could potentially create oxidative stress, such as drought, heat, wounding, *Fusarium* infection, and ozone treatment. The cell wall immobilization effects, if any, of these treatments can be compared based on SDS or ß-ME extractability.

The biological implications of the identification of constituent protein subunits in addition to ZmGRP5 in the suspected multimeric complexes could be significant. If SDS solubility of ZmGRP5 can be duplicated using freshly harvested silk tissue, extracts can be separated on non-reducing standard SDS-PAGE gels for isolation and subsequent submission for MS analysis. Alternatively, non-reducing 2D SDS-PAGE could be attempted to isolate multimeric protein spots for excision and MS analysis. Cell wall fractionated samples, and IPG strips with a narrower pI range would have to be used to reduce sample complexity to aid in the picking of specific protein spots.

In addition to isolation of multimeric complexes from non-reducing SDS-PAGE gels, co-immunoprecipitation could be re-attempted using SDS silk extracts containing soluble multimeric forms of ZmGRP5. The identification of the interacting protein subunits in the multimeric protein complex would yield valuable clues regarding the actual function and mechanism of action of the ZmGRP5 protein. Complementing the above strategy, yeast 2-hybrid screening could be performed using a ZmGRP5 bait construct against an expressed maize silk cDNA library to identify potential ligand binding partners in protein-protein interactions.

Phosphorylation and the resulting change in folding conformation of proteins could be associated with biological functions involving dynamic regulation of protein-protein interactions. It is possible that ZmGRP5 could be implicated in a signalling pathway associated with developmental growth of silk tissue, silk osmotic potential regulation, or silk receptivity to fertilization. It is also possible that phosphorylation could simply result in conformational changes that affect the structural properties of ZmGRP5. Future investigations could begin with the verification of the putative phosphorylation isoforms observed in this study. Isoforms detected by immunblotting of 2D SDS-PAGE separated silk extracts with phosphothreonine, phosphotyrosine, and phosphoserine antibodies could be compared with the isoforms detected by the GST-ZmGRP5 antiserum.

The biological implications of potential glycosylation of ZmGRP5 are significant. The addition of sugar moieties to the protein backbone could introduce more complex cross-linking interactions with the cell wall matrix. In addition, the sugar moieties could also

serve as targets for binding and signalling interactions, such as the AGPs of the transmitting tract that are implicated in fertility related functions. Verification of the glycosylation status of ZmGRP5 could be attempted by immunblotting of 2D SDS-PAGE separated silk extracts with glycoprotein detection kits such as the ECL Glycoprotein Detection Module (Amersham Biosciences), which biotinylates carbohydrates and subsequently detects with HRP-conjugated strepavidin. Other carbohydrate moiety detection methods could be attempted using HRP-conjugated ConA (concanavalin-A), a lectin that binds to mannose of N-linked oligosaccharides, or HRP-conjugated WGA (wheat germ agglutinin), which binds to N-acetylglucosamine. Alternatively, deglycosylation of protein extracts could be attempted with PNGaseF (peptide:N-glycosidase F), which enzymatically removes all N-linked sugar subunits, resulting in the elimination of glycosylated protein spots on 2D separated blots.

The putative heme-bind domain was not investigated in this study due to time constraints. Future studies can use metal affinity-Sepharose columns to test the metal-binding potential of recombinant ZmGRP5 protein. Additionally, metal affinity-Sepharose can be used in an attempt to purify ZmGRP5 from silk extracts.

The investigation of ZmGRP5 function via the dual transgenic approaches of over-expression and gene knockout was initiated in this study but was abandoned due to time constraints. This could be re-attempted in future studies. Gene silencing using the non-glycine-rich portion of ZmGRP5, especially the region of homology to the apomictic pistil GRP from buffelgrass, would insure specificity and avoid potential silencing of

other GRPs in maize. The above could be attempted by transformation of maize calli with inverted repeat constructs, or alternatively short double stranded siRNA synthesized *in vitro* using ZmGRP5 inverted repeat DNA template can be injected directly into actively growing maize silk tissue on maize plants in the field. Maize mutants resulting from RescueMu insertional knockouts of ZmGRP5 could also be screened and tested for phenotypic changes to help elucidate ZmGRP5 function.

REFERENCES

Altschul SF, Madden TL, Schäffer AA, Zhang J, Zhang Z, Miller W, and. Lipman DJ. 1997. Gapped BLAST and PSI-BLAST: a new generation of protein database search programs. Nucleic Acids Res 25:3389-3402

Ausubel FM, Brent R, Kingston RE, Moore DD, Smith JA, Seidman JG, Struhl K. 1994. Current protocols in molecular biology. John Wiley & Sons Inc.

Bassetti P, Westgate ME. 1993a. Emergence, elongation, and senescence of maize silks. Crop Sci 33:271-275

Bassetti P, Westgate ME. 1993b. Senescence and receptivity of maize silks. Crop Sci 33:275-278

Bassetti P, Westgate ME. 1993c. Water deficit affects receptivity of maize silks. Crop Sci 33:279-282

Bio-Rad Laboratories Bulletin #2651. 2-D electrophoresis for proteomics: a methods and product manual, p36

Bobek L, Rekosh DM, van Keulen H, LoVerde PT. 1986. Characterization of a female-specific cDNA derived from a developmentally regulated mRNA in the human blood fluke *Schistosoma mansoni*. Proc Natl Acad Sci USA 83:5544-8

Bradley DJ, Kjellbom P, Lamb CJ. 1992. Elicitor- and wound-induced oxidative cross-linking of a proline-rich plant cell wall protein: a novel, rapid defense response. Cell 70:21-30

Brady JD, Fry SC. 1997. Formation of di-isodityrosine and loss of isodityrosine in the cell walls of tomato cell-cuspension cultures treated with fungal elicitors or H2O2. Plant Physiol 115:87-92

Brady KP, Darvill AG, Albersheim P. 1993. Activation of a tobacco glycine-rich protein gene by a fungal glucan preparation. Plant J 4:517-24

Burson BL, Voigt PW, Sherman RA, Dewald CL. 1990. Apomixis and sexuality. I. eastern gamagrass. Crop Sci 30:86-89

Campbell P, Braam J. 1998. Co- and/or post-translational modifications are critical for TCH4 XET activity. Plant J 15:553-61

Carpenter CD, Kreps JA, Simon AE. 1994. Genes encoding glycine-rich *Arabidopsis thaliana* proteins with RNA-binding motifs are influenced by cold treatment and an endogenous circadian rhythm. Plant Physiol 104:1015-25

Carpita NC, Gibeaut DM. 1993. Structural models of primary cell walls in flowering plants: consistency of molecular structure with the physical properties of the walls during growth. Plant J 3:1-30

Cassab GI. 1998. Plant cell wall proteins. Annu Rev Plant Physiol Plant Mol 49:281-309

Chen R, Smith AG. 1993. Nucleotide sequence of a stamen- and tapetum-specific gene from *Lycopersicon esculentum*. Plant Physiol 101:1413

Condit CM. 1993. Developmental expression and localization of petunia glycine-rich protein 1. Plant Cell 5:277-88

Condit CM, Meagher RB. 1987. Expression of a gene encoding a glycine-rich protein in petunia. Mol Cell Biol 7:4273-9

Cosgrove DJ. 2001. Wall structure and wall loosening. A look backwards and forwards. Plant Physiol 125:131-4

Cosgrove DJ. 2000. Loosening of plant cell walls by expansins. Nature 407:321-6

Cosgrove DJ. 1997. Assembly and enlargement of the primary cell wall in plants. Annu Rev Cell Dev Biol 13:171-201

Cretin C, Puigdomenech P. 1990. Glycine-rich RNA-binding proteins from *Sorghum vulgare*. Plant Mol Biol 15:783-5

de Oliveira DE, Seurinck J, Inze D, Van Montagu M, Botterman J. 1990. Differential expression of five *Arabidopsis* genes encoding glycine-rich proteins. Plant Cell 2:427-36

de Oliveira DE, Franco LO, Simoens C, Seurinck J, Coppieters J, Botterman J, Van Montagu M. 1993. Inflorescence-specific genes from *Arabidopsis thaliana* encoding glycine-rich proteins. Plant J 3:495-507

Dellaporta SL, Calderon-Urrea A. 1994. The sex determination process in maize. Science 266:1501-1505

Didierjean L, Frendo P, Burkard G. 1992. Stress responses in maize: sequence analysis of cDNAs encoding glycine-rich proteins. Plant Mol Biol 18:847-9

Doebley J, Goodman MM, Stuber CW. 1984. Isoenzymatic variation in *Zea* (Gramineae). Syst Bot 9:203-218

Duncan RF, Song HJ. 1999. Striking multiplicity of eIF4E-BP1 phosphorylated isoforms identified by 2D gel electrophoresis regulation by heat shock. Eur J Biochem 265:728-43

Dunn MA, Brown K, Lightowlers R, Hughes MA. 1996. A low-temperature-responsive gene from barley encodes a protein with single-stranded nucleic acid-binding activity which is phosphorylated in vitro. Plant Mol Biol 30:947-59

Emanuelsson O, Nielsen H, Brunak S, von Heijne G. 2000. Predicting subcellular localization of proteins based on their N-terminal amino acid sequence. J Mol Biol 300:1005-1016

Esau K. 1967. Plant Anatomy. John Wiley & Sons Inc. 2nd Edition. pp. 375-401

Fang RX, Pang Z, Gao DM, Mang KQ, Chua NH. 1991. cDNA sequence of a virus-inducible, glycine-rich protein gene from rice. Plant Mol Biol 17:1255-7

Ferullo JM, Vezina LP, Rail J, Laberge S, Nadeau P, Castonguay Y. 1997. Differential accumulation of two glycine-rich proteins during cold-acclimation alfalfa. Plant Mol Biol 33:625-33

Frangioni JV, Neel BG. 1993. Solubilization and purification of enzymatically active glutathione S-transferase (pGEX) fusion proteins. Anal Biochem 210:179-87

Furumoto T, Hata S, Izui K. 2000. Isolation and characterization of cDNAs for differentially accumulated transcripts between mesophyll cells and bundle sheath strands of maize leaves. Plant Cell Physiol 41:1200-9

Girault R, His I, Andeme-Onzighi C, Driouich A, Morvan C. 2000. Identification and partial characterization of proteins and proteoglycans encrusting the secondary cell walls of flax fibres. Planta 211:256-64

Goddemeier ML, Wulff D, Feix G. 1998. Root-specific expression of a *Zea mays* gene encoding a novel glycine-rich protein, zmGRP3. Plant Mol Biol 36:799-802

Gomez J, Sanchez-Martinez D, Stiefel V, Rigau J, Puigdomenech P, Pages M. 1988. A gene induced by the plant hormone abscisic acid in response to water stress encodes a glycine-rich protein. Nature 334:262-4

Gosline JM, Guerette, PA, Ortlepp CS, Savage KN. 1999. The mechanical design of spider silks: from fibroin sequence to mechanical function. J Exp Biol 202:3295-3303

Hayashi CY, Lewis RV. 1998. Evidence from flagelliform silk cDNA for the structural basis of elasticity and modular nature of spider silks. J Mol Biol 275:773-784

Hazzard RV, Schultz BB, Groden E, Ngollo ED, Seidlecki E. 2003. Evaluation of oils and microbial pathogens for control of Lepidopteran pests of sweet corn in New England. J Econ Entomol 96:1653-61

Heintzen C, Nater M, Apel K, Staiger D. 1997. AtGRP7, a nuclear RNA-binding protein as a component of a circadian-regulated negative feedback loop in Arabidopsis thaliana.Proc Natl Acad Sci USA 94:8515-20

Heslop-Harrison Y, Reger BJ, Heslop-Harrison J. 1984. The pollen-stigma interaction in the grasses. 5. Tissue organisation and cytochemistry of the stigma ("silk") of *Zea mays* L. Acta botanica Neerl 33:81-99

Heslop-Harrison Y, Heslop-Harrison J, Reger BJ. 1985. The pollen-stigma interaction in the grasses. 7. Pollen-tube guidance and the regulation of tube number in Zea mays L. Acta botanica Neerl. 34:193-211

Hirose T, Sugita M, Sugiura M. 1993. cDNA structure, expression and nucleic acid-binding properties of three RNA-binding proteins in tobacco: occurrence of tissue-specific alternative splicing. Nucleic Acids Res 21:3981-7

Hoffmann MP, Kirkwyland JJ, Gardner J. 2000. Impact of western corn rootworm (Coleoptera: Chrysomelidae) on sweet corn and evaluation of insecticidal and cultural control options. J Econ Entomol 93:805-12

Horvath DP, Olson PA. 1998. Cloning and characterization of cold-regulated glycine-rich RNA-binding protein genes from leafy spurge (*Euphorbia esula* L.) and comparison to heterologous genomic clones. Plant Mol Biol 38:531-8

Jepson I, Lay VJ, Holt DC, Bright SW, Greenland AJ. 1994. Cloning and characterization of maize herbicide safener-induced cDNAs encoding subunits of glutathione S-transferase isoforms I, II and IV. Plant Mol Biol 26:1855-66

Karlson D, Nakaminami K, Toyomasu T, Imai R. 2002. A cold-regulated nucleic acid-binding protein of winter wheat shares a domain with bacterial cold shock proteins. J Biol Chem 277:35248-56

Keller B, Baumgartner C. 1991. Vascular-specific expression of the bean GRP 1.8 gene is negatively regulated. Plant Cell 3:1051-61

Keller B, Sauer N, Lamb CJ. 1988. Glycine-rich cell wall proteins in bean: gene structure and association of the protein with the vascular system. EMBO J 7:3625-33

Kevei Z, Vinardell JM, Kiss GB, Kondorosi A, Kondorosi E. 2002. Glycine-rich proteins encoded by a nodule-specific gene family are implicated in different stages of symbiotic nodule development in *Medicago spp.* Mol Plant Microbe Interact 15:922-31

Kieliszewski MJ, Shpak E. 2001. Synthetic genes for the elucidation of glycosylation codes for arabinogalactan-proteins and other hydroxyproline-rich glycoproteins. Cell Mol Life Sci 58:1386-98

Kieliszewski MJ, Lamport DT. 1994. Extensin: repetitive motifs, functional sites, post-translational codes, and phylogeny. Plant J 5:157-72

Kieliszewski MJ, Showalter AM, Leykam JF. 1994. Potato lectin: a modular protein sharing sequence similarities with the extensin family, the hevein lectin family, and snake venom disintegrins (platelet aggregation inhibitors). Plant J 5:849-61

Koltunow AM, Truettner J, Cox KH, Wallroth M, Goldberg RB. 1990. Different temporal and spatial gene expression patterns occur during anther development. Plant Cell 2:1201-1224

Kroh M, Gorissen MH, Pfahler PL. 1979. Ultrastructural studies on styles and pollen tubes of *Zea mays* L. General survey on pollen tube growth *in vivo*. Acta botanica Neerl 28:513-518

Lamb C, Dixon RA. 1997. The oxidative burst in plant disease resistance. Annu Rev Plant Physiol Plant Mol Biol 48:251-275

Le Provost G, Paiva J, Pot D, Brach J, Plomion C. 2003. Seasonal variation in transcript accumulation in wood-forming tissues of maritime pine (*Pinus pinaster* Ait.) with emphasis on a cell wall glycine-rich protein. Planta 217:820-30

Lei M, Wu R. 1991. A novel glycine-rich cell wall protein gene in rice. Plant Mol Biol 16:187-98

Lewis RV. 1992. Spider silk: the unraveling of a mystery. Acc Chem Res 25:392-398

Li LC, Bedinger PA, Volk C, Jones AD, Cosgrove DJ. 2003. Purification and characterization of four beta-expansins (*Zea* m1 isoforms) from maize pollen. Plant Physiol 132:2073-85

Li LC, Cosgrove DJ. 2001. Grass group I pollen allergens (beta-expansins) lack proteinase activity and do not cause wall loosening via proteolysis. Eur J Biochem 268:4217-26

Lippincott-Schwartz J, Roberts TH, Hirschberg K. 2000. Secretory protein trafficking and organelle dynamics in living cells. Annu Rev Cell Dev Biol 16:557-89

Lodish HF, Berk A, Zipursky SL, Matsudaira P, Baltimore D, Darnell, J. 2000. Post-translational modifications and quality control in the rough ER.17.6, *in* Molecular cell biology.W H Freeman & Co. 4th Edition

Lunardi C, Nanni L, Tiso M, Mingari MC, Bason C, Oliveri M, Keller B, Millo R, De Sandre G, Corrocher R, Puccetti A. 2000. Glycine-rich cell wall proteins act as specific antigen targets in autoimmune and food allergic disorders. International Immunol. 12:647-657

Majewska-Sawka A, Nothnagel EA. 2000. The multiple roles of arabinogalactan proteins in plant development. Plant Physiol 122:3-9

Matsui M, Toyosawa I, Fukuda M. 1994. Novel N-terminal sequence of a glycine-rich protein in the aleurone layer of soybean seeds. Biosci Biotechnol Biochem 58:1920-2

Matsuyama T, Satoh H, Yamada Y, Hashimoto T. 1999. A maize glycine-rich protein is synthesized in the lateral root cap and accumulates in the mucilage.Plant Physiol 120:665-74

McQueen-Mason S, Durachko DM, Cosgrove DJ. 1992. Two endogenous proteins that induce cell wall extension in plants. Plant Cell 4:1425-33

Miller EC. 1919. Development of the pistillate spikelet and fertilization in *Zea mays* L. J Agr Res 18:255-265

Molina A, Mena M, Carbonero P, Garcia-Olmedo F. 1997. Differential expression of pathogen-responsive genes encoding two types of glycine-rich proteins in barley. Plant Mol Biol 33:803-10

Mousavi A, Hiratsuka R, Takase H, Hiratsuka K, Hotta Y. 1999. A novel glycine-rich protein is associated with starch grain accumulation during anther development. Plant Cell Physiol 40:406-16

Mundy J, Chua NH. 1988. Abscisic acid and water-stress induce the expression of a novel rice gene. EMBO J 7:2279-86

Nadeau JA, Zhang XS, Li J, O'Neill SD. 1996. Ovule development: identification of stage-specific and tissue-specific cDNAs. Plant Cell 8:213-39

Naqvi SM, Park KS, Yi SY, Lee HW, Bok SH, Choi D. 1998. A glycine-rich RNA-binding protein gene is differentially expressed during acute hypersensitive response following Tobacco Mosaic Virus infection in tobacco. Plant Mol Biol 37:571-6

Neuteboom LW, Ng JM, Kuyper M, Clijdesdale OR, Hooykaas PJ, van der Zaal BJ. 1999. Isolation and characterization of cDNA clones corresponding with mRNAs that accumulate during auxin-induced lateral root formation. Plant Mol Biol 39:273-87

Nicolas C, Rodriguez D, Poulsen F, Eriksen EN, Nicolas G. 1997. The expression of an abscisic acid-responsive glycine-rich protein coincides with the level of seed dormancy in *Fagus sylvatica*. Plant Cell Physiol 38:1303-10

Nielsen H, Engelbrecht J, Brunak S, von Heijne G. 1997. Identification of prokaryotic and eukaryotic signal peptides and prediction of their cleavage sites. Prot Eng 10:1-6

Ouellet T., Singh J., Tao T., Simmonds J. 2003. Corn silk gene and regulatory region. Patent #US 6,515,204 B1

Ozols J. 1989. Structure of cytochrome b5 and its topology in the microsomal membrane. Biochim Biophys Acta 997:121-30

Park AR, Cho SK, Yun UJ, Jin MY, Lee SH, Sachetto-Martins G, Park OK. 2001. Interaction of the *Arabidopsis* receptor protein kinase Wak1 with a glycine-rich protein, AtGRP-3. J Biol Chem 276:26688-93

Pawlowski K, Twigg P, Dobritsa S, Guan C, Mullin BC. 1997. A nodule-specific gene family from *Alnus glutinosa* encodes glycine- and histidine-rich proteins expressed in the early stages of actinorhizal nodule development. Mol Plant Microbe Interact 10:656-64

Pearson WR, Lipman DJ. 1988. Improved tools for biological sequence comparison. Proc Natl Acad Sci USA 85:2444-8

Pennell R. 1998. Cell walls: structures and signals. Curr Op Plant Biol 1:504-510

Peng Q, McEuen AR, Benyon RC, Walls AF. 2003. The heterogeneity of mast cell tryptase from human lung and skin. Eur J Biochem 270:270-83

Potenza C, Thomas SH, Sengupta-Gopalan C. 2001.Genes induced during early response to *Meloidogyne incognita* in roots of resistant and susceptible alfalfa cultivars. Plant Sci 161:289-299

Ranieri A, Petacco F, Castagna A, Soldatini GF. 2000. Redox state and peroxidase system in sunflower plants exposed to ozone. Plant Sci 159:159-167

Rayle DL, Cleland RE. 1992. The acid growth theory of auxin-induced cell elongation is alive and well. Plant Physiol 99:1271-4

Reid LM, Bolton AT, Hamilton RI, Woldemariam T. 1992. Effect of silk age on resistance of maize to *Fusarium graminearum*. Can J Plant Path 14:293-298

Richard S, Drevet C, Jouanin L, Seguin A. 1999. Isolation and characterization of a cDNA clone encoding a putative white spruce glycine-rich RNA binding protein. Gene 240:379-88

Ringli C, Keller B, Ryser U. 2001. Glycine-rich proteins as structural components of plant cell walls. Cell Mol Life Sci 58:1430-41

Ringli C, Hauf G, Keller B. 2001. Hydrophobic interactions of the structural protein GRP1.8 in the cell wall of protoxylem elements. Plant Physiol 125:673-82

Robert LS, Allard S, Gerster JL, Cass L, Simmonds J. 1994. Molecular analysis of two *Brassica napus* genes expressed in the stigma. Plant Mol Biol 26:1217-22

Roberts K. 2001. How the cell wall acquired a cellular context. Plant Physiol 125:127-130

Robertson D, Mitchell GP, Gilroy JS, Gerrish C, Bolwell GP, Slabas AR. 1997. Differential extraction and protein sequencing reveals major differences in patterns of primary cell wall proteins from plants. J Biol Chem 272:15841-8

Ryser U, Schorderet M, Guyot R, Keller B. 2004. A new structural element containing glycine-rich proteins and rhamnogalacturonan I in the protoxylem of seed plants. J Cell Sci 117:1179-90

Ryser U. 2003. Protoxylem: the deposition of a network containing glycine-rich cell wall proteins starts in the cell corners in close association with the pectins of the middle lamella. Planta 216:854-64

Ryser U, Schorderet M, Zhao GF, Studer D, Ruel K, Hauf G, Keller B. 1997. Structural cell-wall proteins in protoxylem development: evidence for a repair process mediated by a glycine-rich protein. Plant J 12:97-111

Ryser U, Keller B. 1992. Ultrastructural localization of a bean glycine-rich protein in unlignified primary walls of protoxylem cells. Plant Cell 4:773-783

Sachetto-Martins G, Franco LO, de Oliveira DE. 2000. Plant glycine-rich proteins: a family or just proteins with a common motif? Biochim Biophys Acta 1492:1-14

Sakuta C, Satoh S. 2000. Vascular tissue-specific gene expression of xylem sap glycine-rich proteins in root and their localization in the walls of metaxylem vessels in cucumber. Plant Cell Physiol 41:627-38

Sakuta C, Oda A, Yamakawa S, Satoh S. 1998. Root-specific expression of genes for novel glycine-rich proteins cloned by use of an antiserum against xylem sap proteins of cucumber. Plant Cell Physiol 39:1330-6

Salvador RJ. 1997. Maize. 96-7, *in* The encyclopedia of Mexico: history, culture, and society. [ed. Werner MS], Fitzroy Dearborn Publishers

Santino CG, Stanford GL, Conner TW. 1997. Developmental and transgenic analysis of two tomato fruit enhanced genes. Plant Mol Biol 33:405-16

Sato S, Toya T, Kawahara R, Whittier RF, Fukuda H, Komamine A. 1995. Isolation of a carrot gene expressed specifically during early-stage somatic embryogenesis. Plant Mol Biol 28:39-46

Schroder G, Fruhling M, Puhler A, Perlick AM. 1997. The temporal and spatial transcription pattern in root nodules of *Vicia faba* nodulin genes encoding glycine-rich proteins. Plant Mol Biol 33:113-23

Showalter AM. 1993. Structure and function of plant cell wall proteins. Plant Cell 5:9-23

Sigma-Aldrich Canada. 2002-2003 Catalogue: biochemicals and reagents for life science research.

Smart LB, Cameron KD, Bennett AB. 2000. Isolation of genes predominantly expressed in guard cells and epidermal cells of *Nicotiana glauca*. Plant Mol Biol 42:857-69

Steinert PM, Mack JW, Korge BP, Gan SQ, Haynes SR, Steven AC. 1991. Glycine loops in proteins: their occurrence in certain intermediate filament chains, loricrins and single-stranded RNA binding proteins. Int J Biol Macromol 13:130-9

van Kan JA, Cornelissen BJ, Bol JF. 1988. A virus-inducible tobacco gene encoding a glycine-rich protein shares putative regulatory elements with the ribulose bisphosphate carboxylase small subunit gene. Mol Plant Microbe Interact 1:107-12

Vielle-Calzada JP, Nuccio ML, Budiman MA, Thomas TL, Burson BL, Hussey MA, Wing RA. 1996. Comparative gene expression in sexual and apomictic ovaries of *Pennisetum ciliare* (L.) Link. Plant Mol Biol 32:1085-92

Vilardell J, Goday A, Freire MA, Torrent M, Martinez MC, Torne JM, Pages M. 1990. Gene sequence, developmental expression, and protein phosphorylation of RAB-17 in maize. Plant Mol Biol 14:423-32

Waffenschmidt S, Woessner JP, Beer K, Goodenough UW. 1993. Isodityrosine cross-linking mediates insolubilization of cell walls in *Chlamydomonas*. Plant Cell 5:809-20

Wee EG, Sherrier DJ, Prime TA, Dupree P. 1998. Targeting of active sialyltransferase to the plant Golgi apparatus. Plant Cell 10:1759-68

Westgate ME, Boyer JS. 1985. Osmotic adjustment and the inhibition of leaf, root, stem, and silk growth at low water potentials in maize. Planta 164:540-549

Wu HM, Zou J, May B, Gu Q, Cheung AY. 1993. A tobacco gene family for flower cell wall proteins with a proline-rich domain and a cysteine-rich domain. Proc Natl Acad Sci USA 90:6829-33

Xu M, Lewis RV. 1990. Structure of a protein superfiber: spider dragline silk. Proc Natl Acad Sci USA 87:7120-4

Yang EJ, Oh YA, Lee ES, Park AR, Cho SK, Yoo YJ, Park OK. 2003. Oxygen-evolving enhancer protein 2 is phosphorylated by glycine-rich protein3/wall-associated kinase 1 in *Arabidopsis*. Biochem Biophys Res Commun 305:862-8

Yasuda E, Ebinuma H, Wabiko H. 1997. A novel glycine-rich/hydrophobic 16 kDa polypeptide gene from tobacco: similarity to proline-rich protein genes and its wound-inducible and developmentally regulated expression. Plant Mol Biol 33:667-78

Yu LX, Chamberland H, Lafontaine JG, Tabaeizadeh Z. 1996. Negative regulation of gene expression of a novel proline-, threonine-, and glycine-rich protein by water stress in *Lycopersicon chilense*. Genome 39:1185-93

Zhang Y, Sederoff RR, Allona I. 2000. Differential expression of genes encoding cell wall proteins in vascular tissues from vertical and bent loblolly pine trees. Tree Physiol 20:457-466

List of Appendices

A1 Molecular Weight Prediction and Composition Analysis of Preprotein of ZmGRP5

Analysis	Whole Protein
Molecular Weight	17446.53 m.w.
Length	187
1 microgram =	57.321 pMoles
Molar Extinction coefficient	25130±5 %
1 A(280) =	0.69 mg/ml
Isoelectric Point	8.71
Charge at pH 7	3.51

Whole Protein Composition Analysis

Amino Acid(s)	Number count	% by weight	% by frequency
Charged (RKHYCDE)	40	32.68	21.39
Acidic (DE)	8	5.60	4.28
Basic (KR)	11	8.72	5.88
Polar (NCQSTY)	49	34.85	26.20
Hydrophobic (AILFWV)	29	16.97	15.51
A Ala	8	3.26	4.28
C Cys	2	1.18	1.07
D Asp	4	2.64	2.14
E Glu	4	2.96	2.14
F Phe	2	1.69	1.07
G Gly	76	24.85	40.64
H His	4	3.14	2.14
I Ile	0	0.00	0.00
K Lys	7	5.14	3.74
L Leu	9	5.84	4.81
M Met	1	0.75	0.53
N Asn	13	8.50	6.95
P Pro	9	5.01	4.81
Q Gln	6	4.41	3.21
R Arg	4	3.58	2.14
S Ser	10	4.99	5.35
T Thr	3	1.74	1.60
V Val	9	5.11	4.81
W Trp	1	1.07	0.53
Y Tyr	15	14.03	8.02
B Asx	0	0.00	0.00
Z Glx	0	0.00	0.00
X Xxx	0	0.00	0.00
. Ter	0	0.00	0.00

A2 NetPhos 2.0 Prediction Results for Phosphorylation of ZmGRP5

Technical University of Denmark

---

187 Sequence

MGVNKSAVLLGVVLVSVLLGFLDVVYARELTEANGSGLKNNVKPAGEPGLKDEKWFGGRYKHG

GGYGNNQPGYGGGGNSQ 80

PGYGGGGNSQPGYGGGYKRHHPGGGYGSGQGGPGCGCGGGYGGGNGSPGYGDDNGGGS

GTGGGNGNAGGYGGGGGGGYGG 160

GYGSGSGTAPGGGYHGGGGAQRYAGQN 240

.....T.....Y.....Y..... 80

..Y.....Y...Y.....S..Y.....S..... 160

...S..... 240

Phosphorylation sites predicted: Ser: 3 Thr: 1 Tyr: 6

Serine predictions

Name	Pos	Context	Score	Pred
Sequence	6	GVNKSAVLL	0.011	.
Sequence	16	VVLVSVLLG	0.024	.
Sequence	36	EANGSGLKN	0.033	.
Sequence	79	GGGNSQPGY	0.025	.
Sequence	89	GGGNSQPGY	0.025	.
Sequence	108	GGYGSGQGG	0.088	.
Sequence	127	GGNGSPGYG	0.724	*S*
Sequence	138	NGGGSGTGG	0.736	*S*
Sequence	164	GGYGSGSGT	0.580	*S*
Sequence	166	YGSGSGTAP	0.476	.

Threonine predictions

Name	Pos	Context	Score	Pred
Sequence	31	ARELTEANG	0.528	*T*
Sequence	140	GGSGTGGGN	0.089	.
Sequence	168	SGSGTAPGG	0.052	.

Tyrosine predictions

Name	Pos	Context	Score	Pred
Sequence	26	LDVVYAREL	0.070	.
Sequence	60	FGGRYKHGG	0.454	.
Sequence	66	HGGGYGNNQ	0.821	*Y*
Sequence	73	NQPGYGGGG	0.648	*Y*
Sequence	83	SQPGYGGGG	0.838	*Y*
Sequence	93	SQPGYGGGY	0.686	*Y*
Sequence	97	YGGGYKRHH	0.638	*Y*
Sequence	106	PGGGYGSGQ	0.462	.
Sequence	121	CGGGYGGGN	0.268	.
Sequence	130	GSPGYGDDN	0.898	*Y*
Sequence	150	NAGGYGGGG	0.337	.
Sequence	158	GGGGYGGGY	0.069	.
Sequence	162	YGGGYGSGS	0.412	.
Sequence	174	PGGGYHGGG	0.361	.
Sequence	183	GAQRYAGQN	0.052	.

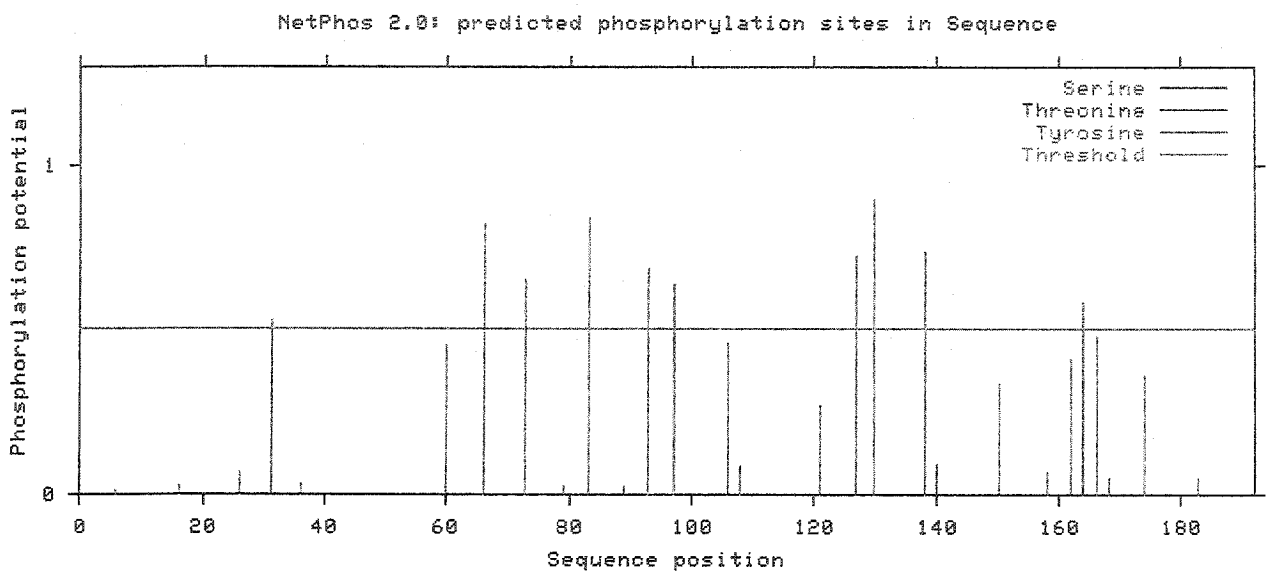

Explain the output. Go back.

A3 NetOGlyc 3.0 Prediction Results for O-linked Glycosylation of ZmGRP5

Technical University of Denmark

Name: Sequence Length: 187

MGVNKSAVLLGVVLVSVLLGFLDVVYARELTEANGSLKNNVKPAGEPGLKDEKWFGGRYKHG
GGYGNNQPGYGGGGNSQ
PGYGGGGNSQPGYGGGYKRHHPGGGYGSGQGGPGCGCGGGYGGGNGSPGYGDDNGGGS
GTGGGNGNAGGYGGGGGGGYGG
GYGSGSGTAPGGGYHGGGGAQRYAGQN

.....

.....

.....

Name	S/T	Pos	Score	Y/N	Comment
Sequence	S	6	0.229	.	-
Sequence	S	16	0.111	.	-
Sequence	T	31	0.271	.	-
Sequence	S	36	0.236	.	-
Sequence	S	79	0.307	.	-
Sequence	S	89	0.313	.	-
Sequence	S	108	0.257	.	-
Sequence	S	127	0.320	.	-
Sequence	S	138	0.309	.	-
Sequence	T	140	0.404	.	-
Sequence	S	164	0.335	.	-
Sequence	S	166	0.343	.	-
Sequence	T	168	0.403	.	-

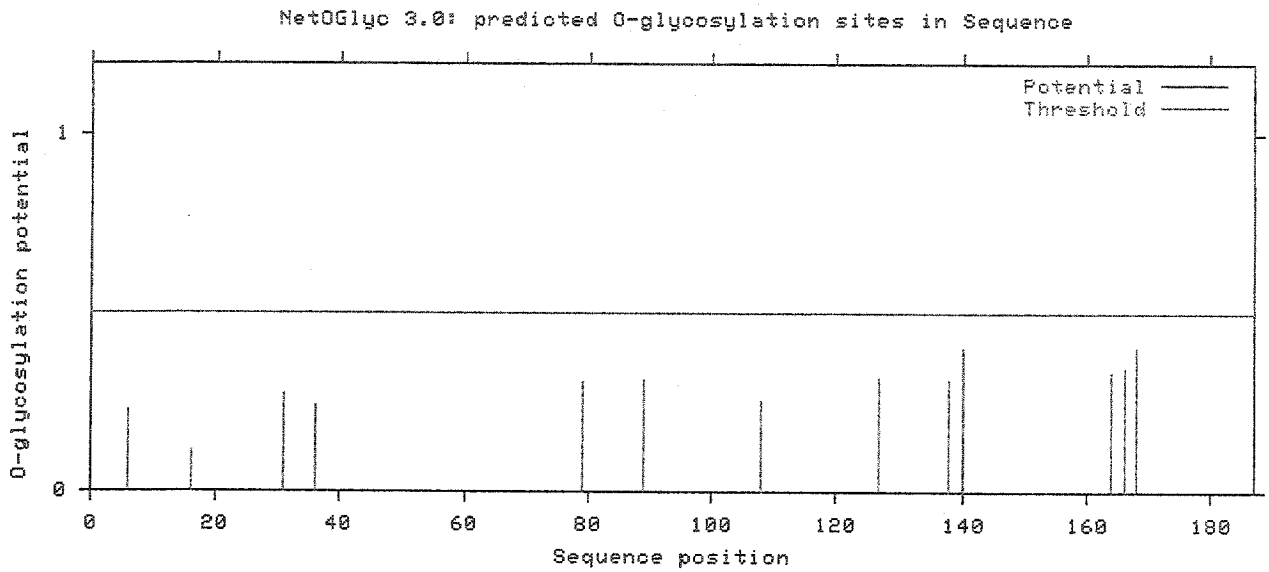

Graphics in PostScript

Explain the output. Go back.

A4 DictyOGlyc 1.1 Prediction Results for O-linked Glycosylation of ZmGRP5

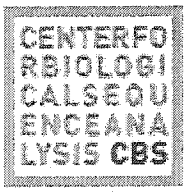

Technical University of Denmark

Name: Sequence Length: 187

MGVNKSAVLLGVVLVSVLLGFLDVVYARELTEANGSGLKNNVKPAGEPGLKDEKWFGGRYKHG

GGYGNNQPGYGGGGNSQ 80

PGYGGGGNSQPGYGGGYKRHHPGGGYGSGQGGPGCGCGGGYGGGNGSPGYGDDNGGGS

GTGGGNGNAGGYGGGGGGGYGG 160

GYGSGSGTAPGGGYHGGGGAQRYAGQN

..... 80

..... 160

.....

Name	Residue	Number	Potential	Threshold	Assignment
Sequence	Ser	0006	0.0415	0.6065	.
Sequence	Ser	0016	0.0429	0.8523	.
Sequence	Thr	0031	0.0184	0.4866	.
Sequence	Ser	0036	0.0452	0.4726	.
Sequence	Ser	0079	0.2398	0.4936	.
Sequence	Ser	0089	0.2456	0.4926	.
Sequence	Ser	0108	0.0143	0.5176	.
Sequence	Ser	0127	0.2805	0.4906	.
Sequence	Ser	0138	0.4180	0.4866	.
Sequence	Thr	0140	0.0122	0.5006	.
Sequence	Ser	0164	0.0163	0.5456	.
Sequence	Ser	0166	0.0430	0.5376	.
Sequence	Thr	0168	0.0144	0.5086	.

A5 NetNGlyc 1.0 Prediction Results for N-linked Glycosylation of ZmGRP5

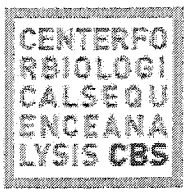

Technical University of Denmark

Asn-Xaa-Ser/Thr sequons in the sequence output below are highlighted in blue. Asparagines predicted to be N-glycosylated are highlighted in red. For further details on the output format, click here.

Predictions for N-Glycosylation sites in 1 sequence

Name: Sequence Length: 187

MGVNKSAVLLGVVLVSVLLGFLDVVYARELTEANGSGLKNNVKPAGEPGLKDEKWFGGRYKHG

GGYGNNQPGYGGGGNSQ 80

PGYGGGGNSQPGYGGGYKRHHPGGGYGSGQGGPGCGCGGGYGGGNGSPGYGDDNGGGS

GTGGGNGNAGGYGGGGGGGYGG 160

GYGSGSGTAPGGGYHGGGGAQRYAGQN

...N.....N..... 80

..... 160

.....

(Threshold=0.5)

SeqName	Position	Potential	Jury agreement	NGlyc result
Sequence	4 NKSA	0.7229	(9/9)	++
Sequence	34 NGSG	0.5021	(5/9)	+
Sequence	125 NGSP	0.2041	(9/9)	---

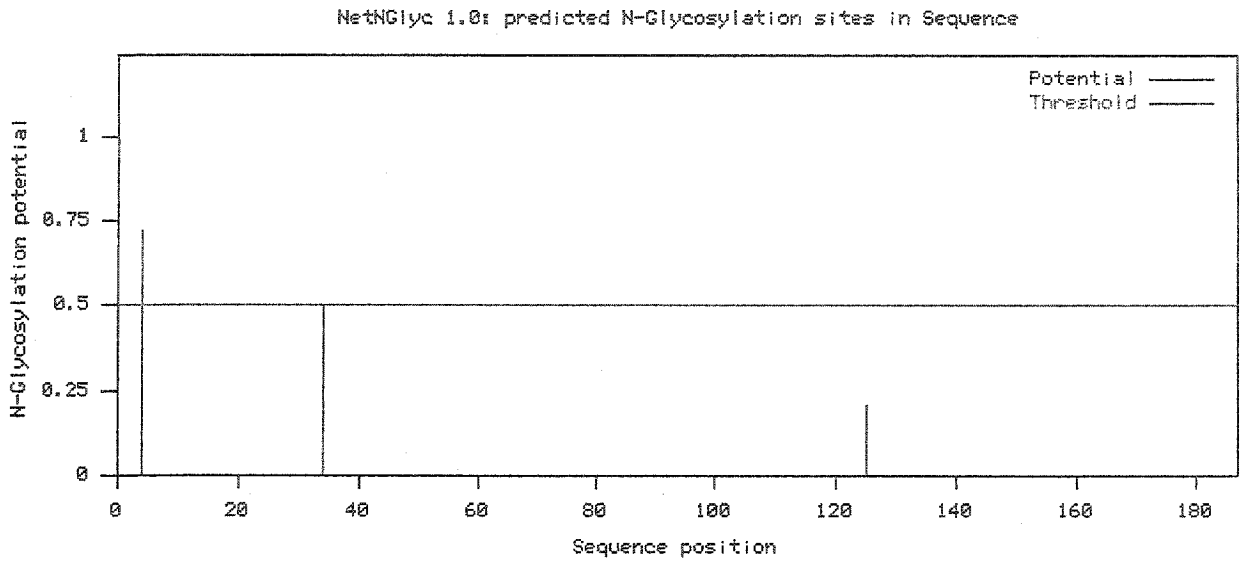

Graphics in PostScript

A6 TargetP V1.0 Prediction Results of Subcellular Targeting of ZmGRP5

```
# Number of input sequences: 1
# Cleavage site predictions included.
# Using PLANT networks.

#              Name   Length          cTP   mTP    SP other  Loc.  RC    TPlen
#----------------------------------------------------------------------------
             Sequence      187      0.004 0.033 0.994 0.036  S     1       27
#----------------------------------------------------------------------------
# cutoff                      0.00  0.00  0.00  0.00
```

Interpretation of TargetP output

COLUMNS:

Name
Sequence name as annotated in fasta file (without initial ">") or on TargetP input page. The name may be of any length, but only 30 characters will be preserved throughout the prediction.

Length
Sequence length. Only the 130 N-terminal amino acids are used in the prediction; submitting sequences longer than 130 residues does not improve the prediction (but it does slow down the prediction).

cTP/mTP/SP/other
The neural network output score for each of the possible categories. If non-plant version is chosen, cTP is not included as a possible location. The scores are NOT probabilities, and they do NOT necessarily add to one (1). However, the location with the highest score is the most likely one according to TargetP, and the relation between the scores may be an indication of how certain the prediction is (see column RC).

Loc.
The subcellular localization predicted by TargetP:
C : Chloroplast, *i.e. the sequence contains a chloroplast transit peptide, cTP*
M : Mitochondrion, *i.e. the sequence contains a mitochondrial targeting peptide, mTP*
S : Secretory pathway, *i.e. the sequence contains a signal peptide, SP*
_ : any other location
* : "don't know". This character appears if cutoff restrictions were demanded and the

winning network output score for a sequence was BELOW the requested cutoff for that category. The asterisk shows that no prediction was done by TargetP (although the output scores and RCs are presented also for these sequences).

RC
Reliability Class: a measure of the size of the difference (diff) between the highest (winning) and the second highest output scores. There are 5 reliability classes, defined as follow:
RC 1: diff > 0.800
RC 2: 0.800 > diff > 0.600
RC 3: 0.600 > diff > 0.400
RC 4: 0.400 > diff > 0.200
RC 5: 0.200 > diff

TPlen
For sequences predicted to contain a cTP/mTP/SP, this is the predicted *length* of the presequence. For SPs, SignalP is used in this prediction, and for cTPs, ChloroP is used.

A7 PSORT Prediction Results for Subcellular Targeting of ZmGRP5

PSORT --- Prediction of Protein Localization Sites
version 6.4(WWW)

ORIGIN plant
BEGIN
>MYSEQ
MGVNKSAVLL GVVLVSVLLG FLDVVYAREL TEANGSGLKN NVKPAGEPGL
KDEKWFGGRY KHGGGYGNNQ PGYGGGGNSQ PGYGGGGNSQ PGYGGGYKRH
HPGGGYGSGQ GGPGCGCGGG YGGGNGSPGY GDDNGGGSGT GGGNGNAGGY
GGGGGGGYGG GYGSGSGTAP GGGYHGGGGA QRYAGQN

MYSEQ 187 Residues
Species classification: 5

*** Reasoning Step: 1

Preliminary Calculation of ALOM (threshold: 0.5)
count: 1
Position of the most N-terminal TMS: 6 at i=1
MTOP: membrane topology (Hartmann et al.)
i(middle): 13 Charge diffirence(C-N): -4.0
McG: Examining signal sequence (McGeoch)
Length of UR: 17
Peak Value of UR: 3.48
Net Charge of CR: 1
Discriminant Score: 11.94
GvH: Examining signal sequence (von Heijne)
Signal Score (-3.5): 5.39
Possible cleavage site: 27
>>> Seems to have a cleavable N-term signal seq.
Amino Acid Composition of Predicted Mature Form:
calculated from 28

ALOM new cnt: 1 ** thrshld changed to -2

Cleavable signal was detected in ALOM?: 1B

ALOM: finding transmembrane regions (Klein et al.)

count: 0 value: 17.67 threshold: -2.0

PERIPHERAL Likelihood = 17.67

modified ALOM score: -4.43

Rule: vesicular pathway

Rule: vesicular pathway

Rule: vesicular pathway

(22) or uncleavable?

Gavel: Examining the boundary of mitochondrial targeting seq.

motif at: 22

Uncleavable? Ipos set to: 32

Discrimination of mitochondrial target seq.:

notclr (0.24)

Hydrophobic moment analysis for chloroplast proteins

Hmax: 7.29 at (32)

Disc.Score from Amino Acid Composition (chloroplast)

score from the 3-11 region: 0.00

score from the 1-31 region: 5.04

Chloroplast protein? Status: negative (-7.63)

Rule: vesicular pathway

Rule: vesicular pathway

*** Reasoning Step: 2

KDEL Count: 0

Number of Potential N-glycosylation Sites: 2

Out: score 0.800

Checking apolar signal for intramitochondrial sorting

(Gavel position 32) from: 7 to: 22 Score: 13.5

>>> Seems to have an intramitochondrial signal

Checking apolar signal for intrachloroplastic sorting

Howe: Checking the consensus for intrachloropl.sorting

SKL motif (signal for peroxisomal protein):

pos: -1(187), count: 0

Amino Acid Composition Tendency for Peroxisome: 8.68

AAC not from the N-term., score modified

Peroxisomal proteins? Status: notclr

AAC score (peroxisome): 0.320

Amino acid composition tendency for vacuolar proteins

Score: 6.36 Status: positive

Checking the amount of Basic Residues (nucleus)

Checking the 4 residue pattern for Nuclear Targeting

Checking the 7 residue pattern for Nuclear Targeting

Checking the Robbins & Dingwall consensus (nucleus)

Checking the RNA binding motif (nucleus or cytoplasm)

Nuclear Signal Status: negative (0.00)

Checking CaaX motif..

Checking N-myristoylation..

>>> Seems to be N-myristoylated (0.10)

Checking CaaX motif..

----- Final Results -----

vacuole --- Certainty= 0.900(Affirmative) < succ>

outside --- Certainty= 0.820(Affirmative) < succ>

microbody (peroxisome) --- Certainty= 0.320(Affirmative) < succ>

plasma membrane --- Certainty= 0.190(Affirmative) < succ>

----- The End -----

A8 Molecular Weight Prediction and Composition Analysis of Mature Protein of ZmGRP5

Analysis	Whole Protein
Molecular Weight	14887.12 m.w.
Length	160
1 microgram =	68.087 pMoles
Molar Extinction coefficient	23850±5 %
1 A(280) =	0.62 mg/ml
Isoelectric Point	8.74
Charge at pH 7	3.51

Whole Protein Composition Analysis

Amino Acid(s)	Number count	% by weight	% by frequency
Charged (RKHYCDE)	37	36.05	23.12
Acidic (DE)	7	5.87	4.38
Basic (KR)	10	9.49	6.25
Polar (NCQSTY)	45	38.32	28.12
Hydrophobic (AILFWV)	12	8.16	7.50
A Ala	6	2.90	3.75
C Cys	2	1.40	1.25
D Asp	3	2.35	1.88
E Glu	4	3.52	2.50
F Phe	1	1.00	0.62
G Gly	73	28.36	45.62
H His	4	3.74	2.50
I Ile	0	0.00	0.00
K Lys	6	5.24	3.75
L Leu	3	2.31	1.88
M Met	0	0.00	0.00
N Asn	12	9.32	7.50
P Pro	9	5.95	5.62
Q Gln	6	5.23	3.75
R Arg	4	4.25	2.50
S Ser	8	4.74	5.00
T Thr	3	2.07	1.88
V Val	1	0.67	0.62
W Trp	1	1.27	0.62
Y Tyr	14	15.55	8.75
B Asx	0	0.00	0.00
Z Glx	0	0.00	0.00
X Xxx	0	0.00	0.00
. Ter	0	0.00	0.00

A9 Lasergene Protean Structural Prediction Results for ZmGRP5

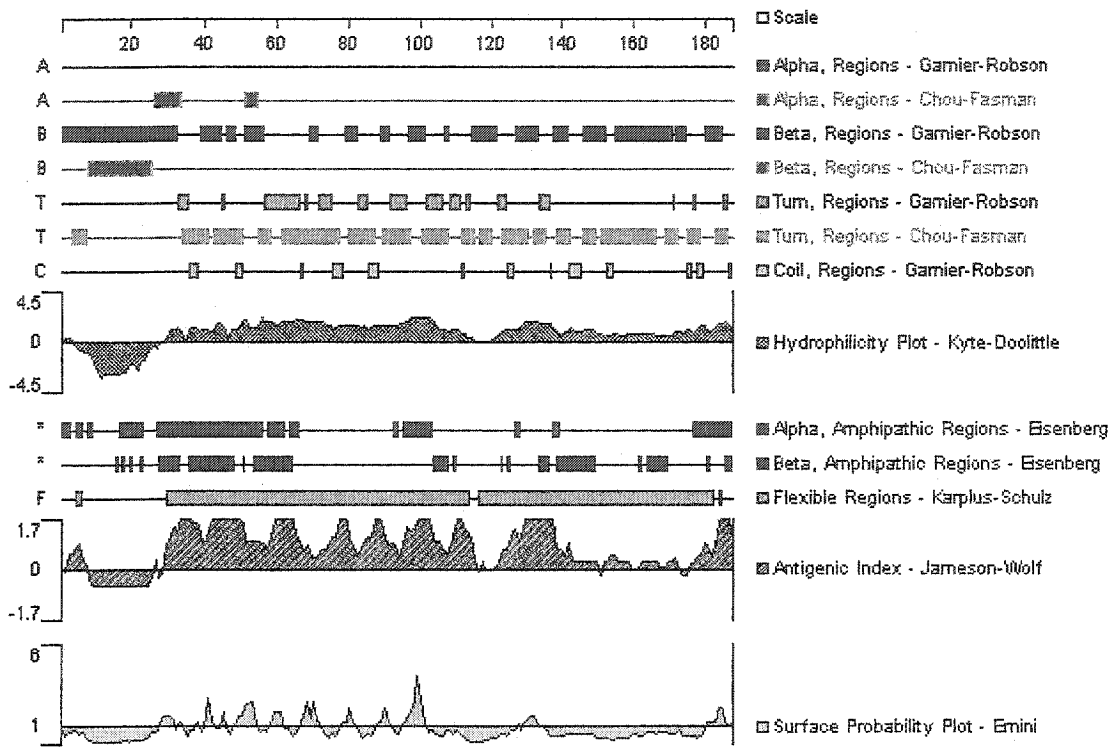

A10 PROSITE Domain Search Results for ZmGRP5

http://us.expasy.org/cgi-bin/scanprosite

Search a sequence against PROSITE

Sequence:

```
MGVNKSAVLL GVVLVSVLLG FLDVVYAREL TEANGSGLKN NVKPAGEPGL KDEKWFGGRY
KHGGGYGNNQ PGYGGGGNSQ PGYGGGGNSQ PGYGGGYKRH HPGGGYGSGQ GGPGCGCGGG
YGGGNGSPGY GDDNGGGSGT GGGNGNAGGY GGGGGGGYGG GYGSGSGTAP GGGYHGGGGA
QRYAGQN
```

PROSITE Release 18.5, of 30-Aug-2003

>PDOC00001 PS00001 **ASN_GLYCOSYLATION** N-glycosylation site [pattern] [Warning: pattern with a high probability of occurrence].

```
  4 -  7  NKSA
 34 - 37  NGSG
```

>PDOC00008 PS00008 **MYRISTYL** N-myristoylation site [pattern] [Warning: pattern with a high probability of occurrence].

```
  2 -  7  GVnkSA
 37 - 42  GLknNV
 63 - 68  GGgyGN
 64 - 69  GGygNN
 74 - 79  GGggNS
 75 - 80  GGgnSQ
 84 - 89  GGggNS
 85 - 90  GGgnSQ
103 - 108 GGgyGS
104 - 109 GGygSG
107 - 112 GSgqGG
111 - 116 GGpgCG
114 - 119 GCgcGG
116 - 121 GCggGY
118 - 123 GGgyGG
119 - 124 GGygGG
122 - 127 GGgnGS
135 - 140 GGgsGT
136 - 141 GGsgTG
137 - 142 GSgtGG
139 - 144 GTggGN
141 - 146 GGgnGN
142 - 147 GGngNA
143 - 148 GNgnAG
145 - 150 GNagGY
148 - 153 GGygGG
151 - 156 GGggGG
152 - 157 GGggGG
153 - 158 GGggGY
155 - 160 GGgyGG
156 - 161 GGygGG
159 - 164 GGgyGS
```

```
160 - 165  GGygSG
163 - 168  GSgsGT
167 - 172  GTapGG
172 - 177  GGyhGG
176 - 181  GGggAQ
```

>PDOC00170 PS00191 **CYTOCHROME_B5_1** Cytochrome b5 family, heme-binding domain signature [pattern].

```
97 - 104  YKrhHPGG
```

>PDOC50099 PS50315 **GLY_RICH** Glycine-rich region [profile].

```
35 - 179
Gsglknnvkpagepglkdekwfggrykhgggygnnqpgyggggnsqpgyggggnsqpgyg

ggykrhhpgggygsgqggpgcgcgggyggggngspgygddngggsgtgggngnaggyggggg
                gggyggggygsgsgtapgggyhgggG
```

NiceSite View of PROSITE: PDOC00170 (documentation)

Cytochrome b5 family, heme-binding domain signature and profile

PROSITE cross-reference(s)

PS00191; CYTOCHROME_B5_1
PS50255; CYTOCHROME_B5_2

Documentation

```
Cytochrome b5 is a membrane-bound hemoprotein which acts as an
electron
carrier for several membrane-bound oxygenases [1]. There are two
homologous
forms of b5, one found in microsomes and one found in the outer
membrane of
mitochondria. Two conserved histidine residues serve as axial ligands
for the
heme group. The structure of a number of oxidoreductases consists
of the
juxtaposition of a heme-binding domain homologous to that of b5 and
either a
flavodehydrogenase or a molybdopterin domain. These enzymes are:

 - Lactate dehydrogenase (EC 1.1.2.3) [2], an enzyme that consists
of a
   flavodehydrogenase domain and a heme-binding domain called
cytochrome b2.
 - Nitrate reductase (EC 1.7.1.-), a key enzyme involved in the first
step of
   nitrate assimilation in plants, fungi and bacteria [3,4].
Consists of a
   molybdopterin domain (see <PDOC00484>), a heme binding domain
called
   cytochrome b557, as well as a cytochrome reductase domain.
 - Sulfite oxidase (EC 1.8.3.1) [5], which catalyzes the terminal
reaction in
```

the oxidative degradation of sulfur-containing amino acids. Also consists
of a molybdopterin domain and a heme-binding domain.
- Yeast acyl-CoA desaturase 1 (EC 1.14.19.1) (gene OLE1). This enzyme
contains a C-termainal heme-binding domain.

This family of proteins also includes:

- TU-36B, a Drosophila muscle protein of unknown function [6].
- Fission yeast hypothetical protein SpAC1F12.10c.
- Yeast hypothetical protein YMR073c.
- Yeast hypothetical protein YMR272c.

We used a segment which includes the first of the two histidine heme ligands,
as a signature pattern for the heme-binding domain of cytochrome b5 family.

Description of pattern(s) and/or profile(s)

Consensus pattern	[FY]-[LIVMK]-x(2)-H-P-[GA]-G [H is a heme axial ligand]
Sequences known to belong to this class detected by the pattern	ALL.
Other sequence(s) detected in Swiss-Prot	7.
Sequences known to belong to this class detected by the profile	ALL.
Other sequence(s) detected in Swiss-Prot	NONE.
Note	this documentation entry is linked to both a signature pattern and a profile. As the profile is much more sensitive than the pattern, you should use it if you have access to the necessary software tools to do so.

Expert(s) to contact by email

Rouze P.	pierre.rouze@gengenp.rug.ac.be

Last update

December 2001 / Text revised; profile added.

References

[1]
Ozols J.
Biochim. Biophys. Acta 997:121-130(1989).

[2]
Guiard B.
EMBO J. 4:3265-3272(1985).

[3]
Calza R., Huttner E., Vincentz M., Rouze P., Galangau F., Vaucheret H., Cherel I., Meyer C., Kronenberger J., Caboche M.
Mol. Gen. Genet. 209:552-562(1987).

[4]
Crawford N.M., Smith M., Bellissimo D., Davis R.W.
Proc. Natl. Acad. Sci. U.S.A. 85:5006-5010(1988).

[5]
Guiard B., Lederer F.
Eur. J. Biochem. 100:441-453(1979).

[6]
Levin R.J., Boychuk P.L., Croniger C.M., Kazzaz J.A., Rozek C.E.
Nucleic Acids Res. 17:6349-6367(1989).

Copyright

View entry in original PROSITE document format

View entry in raw text format (no links)

A11 BLASTP-2.2.8 Homology Search Results for ZmGRP5

[Jan-05-2004]

Reference:
Altschul, Stephen F., Thomas L. Madden, Alejandro A. Schäffer, Jinghui Zhang, Zheng Zhang, Webb Miller, and David J. Lipman (1997), "Gapped BLAST and PSI-BLAST: a new generation of protein database search programs", Nucleic Acids Res. 25:3389-3402.

RID: 1082660509-7670-60920303036.BLASTQ3

Query= gi|20372712|gb|AAM16281.1| glycine-rich protein GRP5

[Zea mays] (187 letters)

Database: All non-redundant GenBank CDS

translations+PDB+SwissProt+PIR+PRF

2,768,312 sequences; 778,115,222 total letters

If you have any problems or questions with the results of this search please refer to the **BLAST FAQs**

Taxonomy reports

Distribution of 2 Blast Hits on the Query Sequence

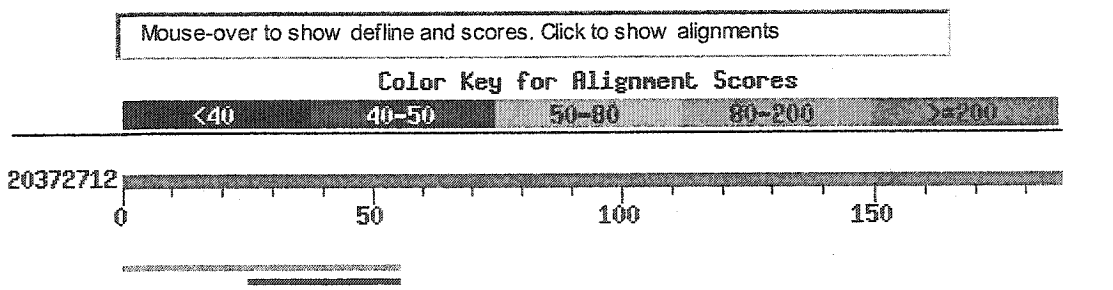

Sequences producing significant alignments:		Score (bits)	E Value
gi|20372712|gb|AAM16281.1|	glycine-rich protein GRP5 [Zea m...	57	2e-07
gi|13194670|gb|AAK15500.1|	glycine rich protein [Pennisetum...	39	0.066

Alignments

>gi|20372712|gb|AAM16281.1| glycine-rich protein GRP5 [Zea mays]

Length = 187

Score = 57.0 bits (136), Expect = 2e-07
Identities = 56/56 (100%), Positives = 56/56 (100%)

```
Query: 1  MGVNKSAVLLGVVLVSVLLGFLDVVYARELTEANGSGLKNNVKPAGEPGLKDEKWF 56
          MGVNKSAVLLGVVLVSVLLGFLDVVYARELTEANGSGLKNNVKPAGEPGLKDEKWF
Sbjct: 1  MGVNKSAVLLGVVLVSVLLGFLDVVYARELTEANGSGLKNNVKPAGEPGLKDEKWF 56
```

>gi|13194670|gb|AAK15500.1| glycine rich protein [Pennisetum ciliare]

Length = 197

Score = 38.9 bits (89), Expect = 0.066
Identities = 20/31 (64%), Positives = 22/31 (70%), Gaps = 2/31 (6%)

```
Query: 26 YARELTEANGSGLKNNVKPAGEPGLKDEKWF 56
          YARELTEANG   + +VK AG PG KD KW
Sbjct: 25 YARELTEANGP--EGSVKLAGGPGFKDVKWL 53
```

Database: All non-redundant GenBank CDS translations+PDB+SwissProt+PIR+PRF
Posted date: Apr 19, 2004 3:24 AM
Number of letters in database: 778,115,222
Number of sequences in database: 2,768,312

Lambda	K	H
0.306	0.128	0.371

Gapped

Lambda	K	H
0.267	0.0410	0.140

Matrix: BLOSUM62
Gap Penalties: Existence: 11, Extension: 1
Number of Hits to DB: 7,481,441
Number of Sequences: 2768312
Number of extensions: 133401
Number of successful extensions: 87
Number of sequences better than 10.0: 1
Number of HSP's better than 10.0 without gapping: 0
Number of HSP's successfully gapped in prelim test: 1
Number of HSP's that attempted gapping in prelim test: 86
Number of HSP's gapped (non-prelim): 1
length of query: 187
length of database: 778,115,222
effective HSP length: 119
effective length of query: 68
effective length of database: 448,686,094
effective search space: 30510654392
effective search space used: 30510654392
T: 11

A12 Apomictic Buffelgrass GRP: Genebank Accession

1: AAK15500. glycine rich prot...[gi:13194670]

```
LOCUS       AAK15500                 197 aa            linear   PLN 04-
MAR-2001
DEFINITION  glycine rich protein [Pennisetum ciliare].
ACCESSION   AAK15500
VERSION     AAK15500.1  GI:13194670
DBSOURCE    locus AF325718 accession AF325718.1
KEYWORDS    .
SOURCE      Pennisetum ciliare (buffelgrass)
  ORGANISM  Pennisetum ciliare
            Eukaryota; Viridiplantae; Streptophyta; Embryophyta;
Tracheophyta;
            Spermatophyta; Magnoliophyta; Liliopsida; Poales; Poaceae;
PACCAD
            clade; Panicoideae; Paniceae; Pennisetum.
REFERENCE   1  (residues 1 to 197)
  AUTHORS   Li,Z., Burson,B.L., Zhang,F. and Hussey,M.A.
  TITLE     Isolation and Characterization of Genes Differentially
Expressed in
            the Pistils of Apomictic Buffelgrass (Pennisetum ciliare
[L.] Link)
  JOURNAL   Unpublished
REFERENCE   2  (residues 1 to 197)
  AUTHORS   Li,Z., Burson,B.L. and Hussey,M.A.
  TITLE     Direct Submission
  JOURNAL   Submitted (04-DEC-2000) Soil and Crop Sciences, Texas A&M
            University, College Station, TX 77843-2474, USA
COMMENT     Method: conceptual translation supplied by author.
FEATURES             Location/Qualifiers
     source          1..197
                     /organism="Pennisetum ciliare"
                     /db_xref="taxon:35520"
                     /clone="2"
                     /tissue_type="pistil"
     Protein         1..197
                     /product="glycine rich protein"
     CDS             1..197
                     /coded_by="AF325718.1:6..599"
                     /note="Pcp2"
ORIGIN
        1 mkvksavllc vvlaslllat qdatyarelt eangpegsvk laggpgfkdv
kwllgghkhg
       61 ggygneggyg ggygnnggyg ggndppsygg gsgpgyggpg ygtggryggp
gfgrsykhhv
      121 hgggggygpgy gggygpgygg gnscppcgsg nagpgygggy gggngggygs
gsgsgsgngg
      181 gggggygggy gssgisp
//
```

A13 FASTA 3.4t21 Homology Search Results for ZmGRP5

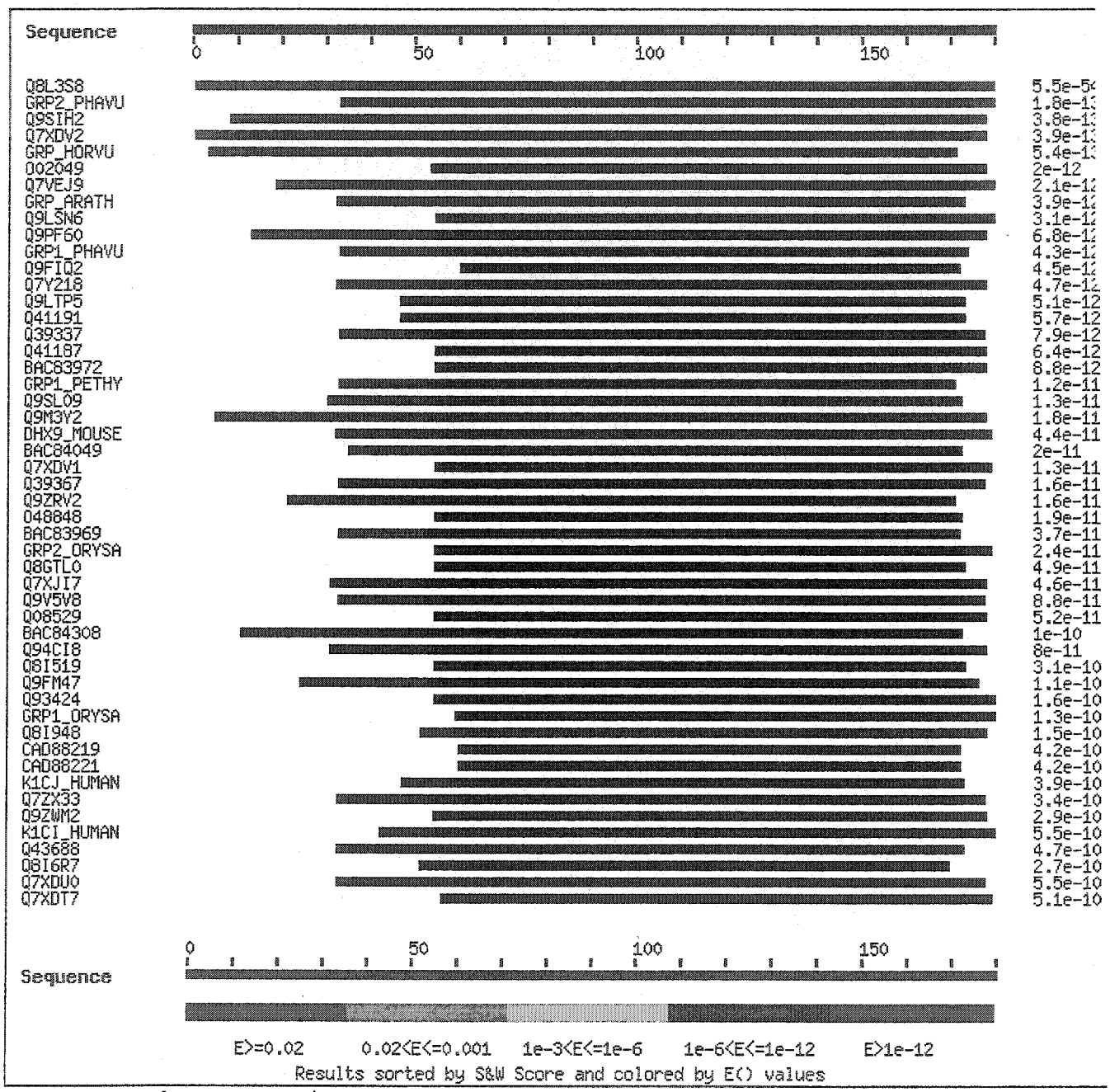


```
 FASTA searches a protein or DNA sequence data bank
 version 3.4t21 May 14, 2003
Please cite:
 W.R. Pearson & D.J. Lipman PNAS (1988) 85:2444-2448

  1>>>Sequence - 187 aa
 vs  UniProt library
searching /ebi/services/idata/v761/fastadb/uniprot library

454171735 residues in 1422690 sequences
 statistics extrapolated from 60000 to 1416395 sequences
```

Expectation_n fit: rho(ln(x))= 6.3390+/-0.000233; mu= 1.5031+/- 0.013
mean_var=159.4749+/-31.886, 0's: 164 Z-trim: 431 B-trim: 34 in 1/64
Lambda= 0.101561

FASTA (3.45 Mar 2002) function [optimized, BL50 matrix (15:-5)] ktup: 2
join: 36, opt: 24, open/ext: -10/-2, width: 16
Scan time: 15.980

The best scores are:		opt	bits	E(1422690)
UNIPROT:Q8L3S8 Q8L3S8 Glycine-rich protein GRP5.	(187)	1376	212.5	5.5e-54
UNIPROT:GRP2_PHAVU P10496 Glycine-rich cell wall	(465)	463	79.2	1.8e-13
UNIPROT:Q9SIH2 Q9SIH2 At2g36120 protein (Hypothet	(255)	452	77.2	3.8e-13
UNIPROT:Q7XDV2 Q7XDV2 Putative glycine-rich prote	(222)	451	77.0	3.9e-13
UNIPROT:GRP_HORVU P17816 Glycine-rich cell wall s	(200)	447	76.4	5.4e-13
UNIPROT:O02049 O02049 T20B6.3 protein.	(259)	436	74.9	2e-12
UNIPROT:Q7VEJ9 Q7VEJ9 RNA-binding protein, RRM do	(252)	435	74.7	2.1e-12
UNIPROT:Q9LSN6 Q9LSN6 Genomic DNA, chromosome 3,	(175)	429	73.7	3.1e-12
UNIPROT:GRP_ARATH P27483 Glycine-rich cell wall s	(349)	431	74.3	3.9e-12
UNIPROT:GRP1_PHAVU P10495 Glycine-rich cell wall	(252)	428	73.7	4.3e-12
UNIPROT:Q9FIQ2 Q9FIQ2 Genomic DNA, chromosome 5,	(268)	428	73.7	4.5e-12
UNIPROT:Q7Y218 Q7Y218 Hypothetical protein At5g46	(290)	428	73.8	4.7e-12
UNIPROT:Q9LTP5 Q9LTP5 Genomic DNA, chromosome 3,	(174)	424	72.9	5.1e-12
UNIPROT:Q41191 Q41191 Glycine-rich protein (Fragm	(173)	423	72.8	5.7e-12
UNIPROT:Q41187 Q41187 Glycine-rich protein (Fragm	(210)	423	72.9	6.4e-12
UNIPROT:Q9PF60 Q9PF60 Endo-1,4-beta-glucanase.	(592)	429	74.3	6.8e-12
UNIPROT:Q39337 Q39337 Glycine-rich_protein_(aa1-2	(291)	423	73.1	7.9e-12
UNIPROT:BAC83972 BAC83972 Putative glycine-rich c	(296)	422	72.9	8.8e-12
UNIPROT:GRP1_PETHY P09789 Glycine-rich cell wall	(384)	421	72.9	1.2e-11
UNIPROT:Q7XDV1 Q7XDV1 Putative glycine-rich prote	(185)	415	71.6	1.3e-11
UNIPROT:Q9SL09 Q9SL09 At2g05580 protein.	(302)	418	72.3	1.3e-11
UNIPROT:Q9ZRV2 Q9ZRV2 Glycine-rich protein 2 (Fra	(208)	414	71.6	1.6e-11
UNIPROT:Q39367 Q39367 Glycine-rich protein (Fragm	(220)	414	71.6	1.6e-11

UNIPROT:Q9M3Y2 Q9M3Y2 Glycine-rich protein precur (390) 417 72.3 1.8e-11
UNIPROT:O48848 O48848 At2g32690 protein. (201) 412 71.3 1.9e-11
UNIPROT:BAC84049 BAC84049 Putative glycine-rich c (356) 415 72.0 2e-11
UNIPROT:GRP2_ORYSA P29834 Glycine-rich cell wall (183) 409 70.8 2.4e-11
UNIPROT:BAC83969 BAC83969 Putative glycine-rich c (359) 409 71.1 3.7e-11
UNIPROT:DHX9_MOUSE O70133 ATP-dependent RNA helic (1380) 416 72.8 4.4e-11
UNIPROT:Q7XJI7 Q7XJI7 Glycine-rich protein TomR2. (304) 406 70.6 4.6e-11
UNIPROT:Q8GTL0 Q8GTL0 Putative glycine-rich cell (400) 407 70.9 4.9e-11
UNIPROT:Q08529 Q08529 Glycine-rich protein. (271) 404 70.2 5.2e-11
UNIPROT:Q94CI8 Q94CI8 Glycine-rich protein LeGRP1 (284) 400 69.7 8e-11
UNIPROT:Q9V5V8 Q9V5V8 CG13214 protein. (610) 404 70.7 8.8e-11
UNIPROT:BAC84308 BAC84308 Putative glycin-rich pr (422) 400 69.9 1e-10
UNIPROT:Q9FM47 Q9FM47 Similarity to RNA binding p (423) 399 69.7 1.1e-10
UNIPROT:GRP1_ORYSA P25074 Glycine-rich cell wall (165) 392 68.2 1.3e-10
UNIPROT:Q8I948 Q8I948 Acanthoscurrin 1 precursor. (156) 390 67.9 1.5e-10
UNIPROT:Q93424 Q93424 Hypothetical glycine-rich 3 (385) 395 69.1 1.6e-10
UNIPROT:Q8I6R7 Q8I6R7 Acanthoscurrin 2 precursor (131) 383 66.8 2.7e-10
UNIPROT:Q9ZWM2 Q9ZWM2 Glycine-rich protein-2 (Fra (261) 387 67.7 2.9e-10
UNIPROT:Q8I519 Q8I519 Erythrocyte membrane protei (2359) 400 70.8 3.1e-10
UNIPROT:Q7ZX33 Q7ZX33 Similar to heterogeneous ri (399) 388 68.1 3.4e-10
UNIPROT:K1CJ_HUMAN P13645 Keratin, type I cytoske (593) 389 68.4 3.9e-10
UNIPROT:CAD88219 CAD88219 C. elegans GRL-25 prote (774) 390 68.7 4.2e-10
UNIPROT:CAD88221 CAD88221 C. elegans GRL-25 prote (774) 390 68.7 4.2e-10
UNIPROT:Q43688 Q43688 Glycin-rich protein (Fragme (408) 385 67.7 4.7e-10
UNIPROT:Q7XDT7 Q7XDT7 Putative glycine-rich prote (185) 379 66.4 5.1e-10
UNIPROT:Q7XDU0 Q7XDU0 Putative glycine-rich prote (280) 381 66.9 5.5e-10
UNIPROT:K1CI_HUMAN P35527 Keratin, type I cytoske (622) 386 68.0 5.5e-10

```
>>UNIPROT:Q8L3S8 Q8L3S8 Glycine-rich protein GRP5.          (187 aa)
 initn: 1376 init1: 1376 opt: 1376  Z-score: 1112.2  bits: 212.5 E():
5.5e-54
Smith-Waterman score: 1376;  100.000% identity (100.000% ungapped) in
187 aa overlap (1-187:1-187)

               10        20        30        40        50        60
Sequen MGVNKSAVLLGVVLVSVLLGFLDVVYARELTEANGSGLKNNVKPAGEPGLKDEKWFGGRY
       ::::::::::::::::::::::::::::::::::::::::::::::::::::::::::::
UNIPRO MGVNKSAVLLGVVLVSVLLGFLDVVYARELTEANGSGLKNNVKPAGEPGLKDEKWFGGRY
               10        20        30        40        50        60

               70        80        90       100       110       120
Sequen KHGGGYGNNQPGYGGGGNSQPGYGGGGNSQPGYGGGYKRHHPGGGYGSGQGGPGCGCGGG
       ::::::::::::::::::::::::::::::::::::::::::::::::::::::::::::
UNIPRO KHGGGYGNNQPGYGGGGNSQPGYGGGGNSQPGYGGGYKRHHPGGGYGSGQGGPGCGCGGG
               70        80        90       100       110       120

              130       140       150       160       170       180
Sequen YGGGNGSPGYGDDNGGGSGTGGGNGNAGGYGGGGGGGYGGGYGSGSGTAPGGGYHGGGGA
       ::::::::::::::::::::::::::::::::::::::::::::::::::::::::::::
UNIPRO YGGGNGSPGYGDDNGGGSGTGGGNGNAGGYGGGGGGGYGGGYGSGSGTAPGGGYHGGGGA
              130       140       150       160       170       180


Sequen QRYAGQN
       :::::::
UNIPRO QRYAGQN


>>UNIPROT:GRP2_PHAVU P10496 Glycine-rich cell wall struc  (465 aa)
 initn: 375 init1: 375 opt: 463  Z-score: 384.6  bits: 79.2 E(): 1.8e-
13
Smith-Waterman score: 463;  48.148% identity (52.349% ungapped) in 162
aa overlap (35-187:306-463)

           10        20        30        40        50        60
Sequen KSAVLLGVVLVSVLLGFLDVVYARELTEANGSGLKNNVKPAGEPGLKDEKWFGGRY----
                                     :.:   . . .:  :  .    :: :
UNIPRO GGGQGGGAGGGYGAGGEHGGGAGGGQGGGAGGGYGAGGEHGGGGGGGQGGGAGGGYAAVG
         280       290       300       310       320       330

               70              80        90       100       110
Sequen KHGGGYGNNQPG-----YGGGGNSQPGYGGGGNSQPGYGGGYKRHHPGGGYGSGQGGPGC
       .::::::..: :     :: ::.   ::::: ..  : : :   .: ::::.:::: :
UNIPRO EHGGGYGGGQGGGDGGGYGTGGEHGGGYGGGQGGGAGGGYGTGGEH-GGGYGGGQGGGG-
         340       350       360       370       380       390

         120       130       140       150       160       170
Sequen GCGGGYGGGNGSPGYGDDNGGGSGTGGGNGNAGGYGGGGGGGYGGGYGSGSGTAPGGGYH
         : : :: .:. :::  .::::.:.::: :..:..::: ::: ::: : :.: : ::::
UNIPRO --GYGAGGDHGAAGYGGGEGGGGGSGGGYGDGGAHGGGYGGGAGGGGGYGAGGAHGGGYG
             400       410       420       430       440       450

         180
Sequen GGGGAQRYAGQN
       ::::     : :
```

```
UNIPRO GGGGIGGGHGGNVP
              460

>>UNIPROT:Q9SIH2 Q9SIH2 At2g36120 protein (Hypothetical    (255 aa)
 initn: 1071 init1: 417 opt: 452  Z-score: 378.9  bits: 77.2 E(): 3.8e-
13
Smith-Waterman score: 457;  45.641% identity (50.857% ungapped) in 195
aa overlap (9-185:13-205)

                     10        20        30          40          50
Sequen      MGVNKSAVLLGVVLVSVLLGFLDVVYARELTEANG--SGLKN--NVKPAGEPGLKD
                    :.:. : :.  ..:.   ..  . : :  :::.   .:  .: ::
UNIPRO MANHKNLFFLCFLIGLGLCSARRALLSSSESEAEVAAYGVNSGLSAGLGVGIGGGPG-GG
                10        20        30        40        50

              60          70        80        90         100
Sequen EKWFGGRYKHG--GGYGNNQPGYGGGGNSQPGYGGGGNSQP--GYGGGYKRHHPGGGYGS
         . ::   . :  ::.:... : ::::.   : :::::. :  :::::  . .  :.::::.
UNIPRO SGYGGGSGEGGGAGGHGEGHIGGGGGGGHGGGAGGGGGGGPGGGYGGG-SGEGGGAGYGG
      60         70         80         90        100         110

      110             120         130       140       150       160
Sequen GQ-----GGPGCGCGGGYGGGNGSPG--YGDDNGGGSGTGGGNGNAGGYGGGGGGGYGGG
       :.     :: : : ::: :::.:. :  ::  .:.:.: : :.:.:::.:::::::: :::
UNIPRO GEAGGHGGGGGGGAGGGGGGGGGAHGGGYGGGQGAGAGGGYGGGGAGGHGGGGGGGNGGG
      120       130       140       150       160       170

               170       180
Sequen YGSGSGT--APGGGYHGGGGA-QRYAGQN
        :.:::   : :::: .:::: . :.:
UNIPRO GGGGSGEGGAHGGGYGAGGGAGEGYGGGAGAGGHGGGGGGGGGSGGGGGGGGGYAAASGY
      180       190       200       210       220       230

>>UNIPROT:Q7XDV2 Q7XDV2 Putative glycine-rich protein.     (222 aa)
 initn: 642 init1: 426 opt: 451  Z-score: 378.8  bits: 77.0 E(): 3.9e-
13
Smith-Waterman score: 451;  45.408% identity (51.149% ungapped) in 196
aa overlap (1-185:1-185)

                10        20        30                40        50
Sequen MGVNKSAVLLGVVLVSVLLGFLDVVYARELT------EANGSGLKNNVKPAGEPGLKDEK
       :...:  ::: ..:: . .:.  .. :: :       :..:.:  ..   .:  : .
UNIPRO MATTKHFVLL-IILVLLSIGM--TTSARTLLGYGIGGEGGGGGGGGGSGGGGGYGGSGYG
               10          20          30        40        50

           60        70        80        90       100       110
Sequen WFGGRYKHGGGYGNNQPGYGGGGNSQPGYGGGGNSQPGYGGGYKRHHPGGGYGSGQ-GGP
        :. : .::: : .  :.::::..  : ::::.:  ::::.:   .  :.::::::  :.
UNIPRO -SGSGYGEGGGAGAGGYGHGGGGGGGGGEGGGSGS--GYGSG---QGSGSGYGSGAFGAG
         60        70        80        90             100       110

           120       130           140       150       160
Sequen GCGCGGGYGGGNGSPGYGDDNG-G---GSGTGGGNGNAGGYGGGGGGGYGGGYGSGSGTA
       : : ::: :::... :::. .: :   :::.:::..:.::.:::::::: ::::::::: .
UNIPRO GYGSGGGGGGGGAGSGYGSGEGYGSGYGSGAGGASGGGGGHGGGGGGGQGGGYGSGSGYG
             120       130       140       150       160       170
```

A14 Molecular Weight Prediction and Composition Analysis of GST-ZmGRP5 (pB1)

Analysis	Whole Protein
Molecular Weight	35255.20 m.w.
Length	313
1 microgram =	28.365 pMoles
Molar Extinction coefficient	54630±5%
1 A(280) =	0.65 mg/ml
Isoelectric Point	7.43
Charge at pH 7	1.30

Whole Protein Composition Analysis

Amino Acid(s)	Number count	% by weight	% by frequency
Charged (RKHYCDE)	115	44.13	36.74
Acidic (DE)	41	14.18	13.10
Basic (KR)	41	16.02	13.10
Polar (NCQSTY)	66	22.89	21.09
Hydrophobic (AILFWV)	86	27.75	27.48
A Ala	12	2.42	3.83
C Cys	4	1.17	1.28
D Asp	21	6.86	6.71
E Glu	20	7.32	6.39
F Phe	11	4.59	3.51
G Gly	40	6.47	12.78
H His	9	3.50	2.88
I Ile	15	4.81	4.79
K Lys	27	9.82	8.63
L Leu	30	9.63	9.58
M Met	9	3.35	2.88
N Asn	11	3.56	3.51
P Pro	21	5.78	6.71
Q Gln	8	2.91	2.56
R Arg	14	6.20	4.47
S Ser	15	3.70	4.79
T Thr	8	2.29	2.56
V Val	13	3.86	4.15
W Trp	5	2.64	1.60
Y Tyr	20	9.26	6.39
B Asx	0	0.00	0.00
Z Glx	0	0.00	0.00
X Xxx	0	0.00	0.00
. Ter	1	0.00	0.32

A15 Prediction Results for Trypsin Digestion of GST-ZmGRP5 (pB1)

Trypsin - 40 cuts						
1	9	1093.32	8.86	>20h	22.95	MSPILGYWK
10	2	258.33	9.00	30m	5.04	IK
12	7	788.89	10.04	>20h	12.35	GLVQPTR
19	9	1148.33	4.15	3m	21.98	LLLEYLEEK
28	8	1137.19	4.70	10m	17.80	YEEHLYER
36	5	561.52	3.78	3m	0.49	DEGDK
41	2	359.40	10.04	?	10.38	WR
43	2	259.27	9.00	?	0.00	NK
45	1	146.17	9.00	3m	0.00	K
46	19	2228.50	3.69	3m	67.18	FELGLEFPNLPYYIDGDVK
65	9	1031.26	10.04	3m	19.42	LTQSMAIIR
74	5	607.67	5.95	10m	11.43	YIADK
79	9	955.14	8.24	?	11.98	HNMLGGCPK
88	2	302.30	6.24	30m	0.00	ER
90	14	1515.77	3.96	>20h	23.19	AEISMLEGAVLDIR
104	5	579.63	9.04	10m	9.07	YGVSR
109	5	579.66	8.85	30m	11.71	IAYSK
114	6	750.82	4.18	3m	13.68	DFETLK
120	6	706.81	5.97	>20h	14.18	VDFLSK
126	6	728.92	6.22	3m	15.72	LPEMLK
132	5	695.77	4.17	>20h	12.44	MFEDR
137	4	498.62	8.24	3m	6.62	LCHK
141	35	4060.68	3.84	>20h	73.54	TYLNGDHVT...PMCLDAFPK
176	5	607.78	8.23	3m	13.35	LVCFK
181	1	146.17	9.00	3m	0.00	K
182	1	173.19	10.04	2m	0.00	R
183	9	1025.18	4.18	30m	18.48	IEAIPQIDK
192	3	421.51	8.85	10m	10.46	YLK
195	3	319.33	9.00	>20h	0.00	SSK
198	21	2325.58	7.14	10m	67.85	YIAWPLQGWQATFGGGDHPPK
219	6	684.77	6.01	>20h	10.90	SDLVPR
225	16	1602.73	4.44	>20h	57.73	GSIPEFPTEANGSGLK
241	12	1222.37	8.83	?	10.83	NNVKPAGEPGLK
253	3	389.38	4.18	3m	0.00	DEK
256	5	620.68	10.04	?	16.75	WFGGR
261	2	308.35	8.85	10m	4.17	YK
263	37	3431.44	8.62	?	63.12	HGGGYGNNQ...QPGYGGGYK
300	1	173.19	10.04	2m	0.00	R
301	3	447.47	9.96	?	1.97	HHR
304	6	618.62	6.01	>20h	4.41	VDSSGR
310	5	446.49	3.45	30m	7.81	IVTD.

Thrombin protease digestion site

A16 LC-MS/MS Results for GST-ZmGRP5 (pB1)

ingel1514.RAW

Reference: GST-fusion
Database: ecoli.fasta
Number of Amino Acids: 313 Average Mass: 35256.9 pI: 7.11

Protein:

MSPILGYWKI KGLVQPTRLL LEYLEEKYEE HLYERDEGDK WRNKKFELGL EFPNLPYYID GDVKLTQSMA IIRYIADKHN MLGGCPKERA EISMLEGAVL
DIRYGVSRIA YSKDFETLKV DFLSKLPEML KMFEDRLCHK TYLNGDHVTH PDFMLYDALD VVLYMDPMCL DAFPKLVCFK KRIEAIPQID KYLKSSKYIA
WPLQGWQATF GGGDHPPKSD LVPRGSIPEF PTEANGSGLK NNVKPAGEPG LKDEKWFGGR YKHGGGYGNN QPGYGGGGNS QPGYGGGGNS QPGYGGGYKR
HHEVDSSGRI VTD

1+ 3431.4
2+ 1716.2
3+ 1144.5

Protein Coverage:

Sequence	MH+	% Mass	AA	% AA
MSPILGYWK	1095.34	3.11	1 - 9	2.88
MSPILGYWK	1095.34	3.11	1 - 9	2.88
MSPILGYWK	1095.34	3.11	1 - 9	2.88
MSPILGYWK	1095.34	3.11	1 - 9	2.88
MSPILGYWK	1095.34	3.11	1 - 9	2.88
MSPILGYWK	1095.34	3.11	1 - 9	2.88
MSPILGYWK	1095.34	3.11	1 - 9	2.88
MSPILGYWK	1095.34	3.11	1 - 9	2.88
MSPILGYWK	1095.34	3.11	1 - 9	2.88
MSPILGYWKIKGLVQPTR	2088.55	5.92	1 - 18	5.75
IKGLVQPTR	1012.23	2.87	10 - 18	2.88
LLEYLEEK	1150.35	3.26	19 - 27	2.88
YEEHLYERDEGDKWR	2026.11	5.75	28 - 42	4.79
LTQSMAIIR	1033.27	2.93	65 - 73	2.88
YIADKHNMLGGCPK	1547.83	4.39	74 - 87	4.47
ERAEISMLEGAVLDIR	1803.07	5.11	88 - 103	5.11
AEISMLEGAVLDIR	1517.77	4.30	90 - 103	4.47
YGVSR	581.64	1.65	104 - 108	1.60
IAYSKDFETLK	1315.50	3.73	109 - 119	3.51
DFETLKVDFLSK	1442.64	4.09	114 - 125	3.83
VDFLSKLPEMLK	1420.74	4.03	120 - 131	3.83
LPEMLKMFEDR	1409.70	4.00	126 - 136	3.51
MFEDRLCHK	1179.40	3.35	132 - 140	2.88
KRIEAIPQIDK	1311.56	3.72	181 - 191	3.51
KRIEAIPQIDK	1311.56	3.72	181 - 191	3.51
RIEAIPQIDK	1183.38	3.36	182 - 191	3.19
RIEAIPQIDKYLK	1587.89	4.50	182 - 194	4.15
IEAIPQIDK	1027.20	2.91	183 - 191	2.88
IEAIPQIDKYLK	1431.70	4.06	183 - 194	3.83
GSIPEFPTEANGSGLK	1604.74	4.55	225 - 240	5.11
GSIPEFPTEANGSGLKNNVK	2060.25	5.84	225 - 244	6.39
NNVKPAGEPGLKDEK	1596.77	4.53	241 - 255	4.79
Totals:	16695.39	47.35	143	45.69

A17 Molecular Weight Prediction and Composition Analysis of GST after Thrombin Digestion of GST-ZmGRP5 (pB1)

Analysis	Whole Protein
Molecular Weight	26186.48 m.w.
Length	224
1 microgram =	38.218 pMoles
Molar Extinction coefficient	41160±5 %
1 A(280) =	0.64 mg/ml
Isoelectric Point	6.35
Charge at pH 7	-2.20

Whole Protein Composition Analysis

Amino Acid(s)	Number count	% by weight	% by frequency
Charged (RKHYCDE)	89	45.52	39.73
Acidic (DE)	34	15.81	15.18
Basic (KR)	31	16.26	13.84
Polar (NCQSTY)	42	19.81	18.75
Hydrophobic (AILFWV)	74	32.15	33.04
A Ala	10	2.72	4.46
C Cys	4	1.58	1.79
D Asp	18	7.92	8.04
E Glu	16	7.90	7.14
F Phe	9	5.06	4.02
G Gly	14	3.05	6.25
H His	6	3.14	2.68
I Ile	13	5.62	5.80
K Lys	21	10.29	9.38
L Leu	28	12.11	12.50
M Met	9	4.51	4.02
N Asn	4	1.74	1.79
P Pro	14	5.20	6.25
Q Gln	5	2.46	2.23
R Arg	10	5.97	4.46
S Ser	9	3.00	4.02
T Thr	6	2.32	2.68
V Val	10	3.79	4.46
W Trp	4	2.85	1.79
Y Tyr	14	8.73	6.25
B Asx	0	0.00	0.00
Z Glx	0	0.00	0.00
X Xxx	0	0.00	0.00
. Ter	0	0.00	0.00

A18 Molecular Weight Prediction and Composition Analysis of ZmGRP5 after Thrombin Digestion of GST-ZmGRP5 (pB1)

Analysis	Whole Protein
Molecular Weight	9106.72 m.w.
Length	89
1 microgram =	109.809 pMoles
Molar Extinction coefficient	13370±5%
1 A(280) =	0.68 mg/ml
Isoelectric Point	9.36
Charge at pH 7	3.41

Whole Protein Composition Analysis

Amino Acid(s)	Number count	% by weight	% by frequency
Charged (RKHYCDE)	26	40.04	29.21
Acidic (DE)	7	9.46	7.87
Basic (KR)	10	15.30	11.24
Polar (NCQSTY)	24	31.70	26.97
Hydrophobic (AILFWV)	12	15.07	13.48
A Ala	2	1.56	2.25
C Cys	0	0.00	0.00
D Asp	3	3.79	3.37
E Glu	4	5.67	4.49
F Phe	2	3.23	2.25
G Gly	26	16.29	29.21
H His	3	4.52	3.37
I Ile	2	2.49	2.25
K Lys	6	8.44	6.74
L Leu	2	2.49	2.25
M Met	0	0.00	0.00
N Asn	7	8.77	7.87
P Pro	7	7.47	7.87
Q Gln	3	4.22	3.37
R Arg	4	6.86	4.49
S Ser	6	5.74	6.74
T Thr	2	2.22	2.25
V Val	3	3.27	3.37
W Trp	1	2.04	1.12
Y Tyr	6	10.75	6.74
B Asx	0	0.00	0.00
Z Glx	0	0.00	0.00
X Xxx	0	0.00	0.00
. Ter	1	0.00	1.12

A19 Schematic Illustration of Purification Strategy and Thrombin Digestion of GST-ZmGRP5 (pB1)

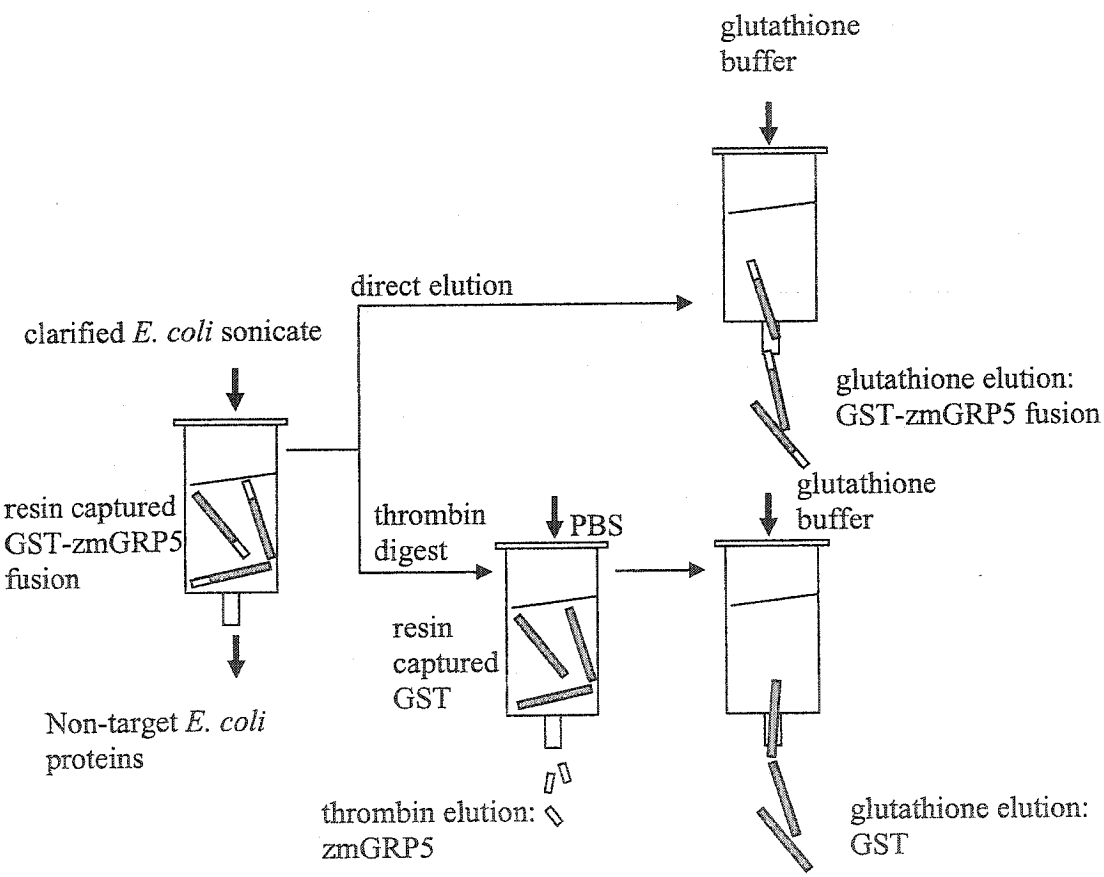

A20 LC-MS/MS Results for Prothrombin Contaminant

Sample: Bourassa, S. INGEL1515 TTAOC3 Reference: gi|135806

Directory: sbourassaingel1515 C3 Database: F:/database/nr.fasta

Send To: PepCut | PepStat | Gap | MuQuest | Sequence | Abstract | Blast

Header: gi|135806|sp|P00735|THRB_BOVIN Prothrombin precursor gi|625233|pir||TBBO thrombin (EC 3.4.21.5) precursor - bovine

Avg Mass: 70505.5 Coverage: 32/625 = 5.1% by amino acid count, 3338.7/70505.5 = 4.7% by mass

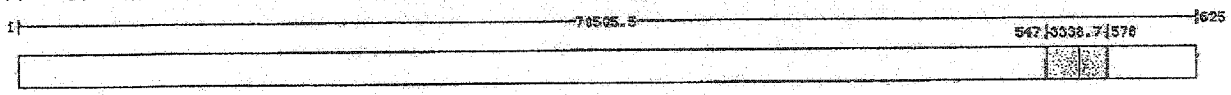

MARVRGPRLP GCLALAALFS LVRSQHVFLA HQQASSLLQR ARRANKGFLE EVRKGNLERE CLEEPCSREE AFEALESLSA TDAFWAKYTA
CESARNPREK LNECLEGNCA EGVGMNYRGN VSVTRSGIEC QLWRSRYPHK PEINSTTHPG ADLRENFCRN PDGSITGPWC YTTSPTLRRE
ECSVPVCGQD RVTVEVIPRS GGSTTSQSPL LETCVPDRGR EYRGRLAVTT SGSRCLAWSS EQAKALSKDQ DFNPAVPLAE NFCRNPDGDE
EGAWCYVADQ PGDFEYCDLN YCEEPVDGDL GDRLGEDPDP DAAIEGRTSE DHFQPFFNEK TFGAGEADCG LRPLFEKKQV QDQTEKELFE
SYIEGRIVEG QDAEVGLSPW QVMLFRKSPQ ELLCGASLIS DRWVLTAAHC LLYPPWDKNF TVDDLLVRIG KHSRTRYERK VEKISMLDKI
YIHPRYNWKE NLDRDIALLK LKRPIELSDY IHPVCLPDKQ TAAKLLHAGF KGRVTGWGNR RETWTTSVAE VQPSVLQVVN LPLVERPVCK
ASTRIRITDN MFCAGYKPGE GKRGDACEGD SGGPFVMKSP YNNRWYQMGI VSWGEGCDRD GKYGFYTHVF RLKKWIQKVI DRLGS

Sort by:	Sequence	Position
PepStat	GDACEGDSGGPFVMK	564 - 578
PepStat	ITDNMFCAGYKPGEGK	547 - 562
PepStat	ITDNMFCAGYKPGEGKR	547 - 563
PepStat	RGDACEGDSGGPFVMK	563 - 578